Universidade do Minho
Escola de Engenharia

Pedro Moreira Montenegro da Silva

Modulating bacterial cellulose production through the pool of c-di-GMP in *Komagataeibacter sucrofermentans*

July, 2026

Modulating bacterial cellulose production through the pool of c-di-GMP in *Komagataeibacter sucrofermentans*

Pedro Montenegro-Silva

UMinho | 2026

Universidade do Minho
Escola de Engenharia

Pedro Moreira Montenegro da Silva

Modulating bacterial cellulose production through the pool of c-di-GMP in *Komagataeibacter sucrofermentans*

Doctorate Thesis
Doctorate in Chemical and Biological Engineering

Work developed under the supervision of:

Lucília Maria Ribeiro Alves Domingues
Francisco Miguel Portela da Gama

July, 2026

DIREITOS DE AUTOR E CONDIÇÕES DE UTILIZAÇÃO DO TRABALHO POR TERCEIROS

Este é um trabalho académico que pode ser utilizado por terceiros desde que respeitadas as regras e boas práticas internacionalmente aceites, no que concerne aos direitos de autor e direitos conexos.

Assim, o presente trabalho pode ser utilizado nos termos previstos na licença abaixo indicada.

Caso o utilizador necessite de permissão para poder fazer um uso do trabalho em condições não previstas no licenciamento indicado, deverá contactar o autor, através do RepositoriUM da Universidade do Minho.

License granted to the users of this work



Creative Commons Attribution-NonCommercial-ShareAlike 4.0 International

CC BY-NC-SA 4.0

https://creativecommons.org/licenses/by-nc-sa/4.0/deed.en

Acknowledgements

Sinto que nada do que eu diga pode expressar a gratidão que tenho por todas as pessoas que, de uma forma ou de outra, contribuíram para que este percurso chegasse até aqui.

Não posso deixar de começar pelos meus orientadores, Prof.ª Lucília e Prof. Miguel, a quem agradeço a oportunidade de trabalhar neste projeto. A vossa orientação, paciência e incentivo foram fundamentais para o meu crescimento académico e pessoal. Deixo também um agradecimento ao Prof. Fernando Dourado e à Dr.ª Ana Cristina que contribuíram significativamente com o seu conhecimento e experiência.

Agradeço igualmente ao Prof. Tom Ellis, do Imperial College London, por me ter recebido no seu laboratório e partilhado o KTK, e ao Dr. Kenneth Walker pela mentoria. Não posso deixar de agradecer também à Maria e ao Henry por todos os momentos que partilhámos em Londres.

Foram muitas as pessoas que passaram pelo LBM nos últimos anos, e lamento não poder dirigir palavras a cada uma individualmente. Em muitos momentos, vocês foram a razão para sair da cama. Estes que passo a mencionar em particular mereciam um capítulo dedicado a eles. Agradeço à Diana pela presença constante, nos melhores e piores momentos. Obrigado por me "adoptares" ao almoço e pela amizade que construímos. Fica um enorme sentimento de carinho, respeito, admiração e gratidão. Ao Luís, obrigado pela confidência e por uma amizade que me orgulha e certamente levarei para a vida. À Clara, ao Miguel F. e ao Eduardo, é um previlégio, hoje, chamar-vos amigos. À Tatiana, agradeço tudo o que me ensinaste, a amizade, e o carinho. Marcaste de forma permanente a forma como penso ciência, e por isso te sou profundamente grato. Aos restantes (Miguel P., Lígia, João M., Carlos, João C., Joana, David, e Catarinas), obrigado pelo companheirismo, por todas as vezes que nos rimos juntos, e uns dos outros.

Agradeço a todos os meus queridos amigos e camaradas, em particular ao Tiago, Joana C., António, Eduardo, Couto, Nádia, Renata, Rainha, Joana G., Quiqui, Carlota, Tó, Tinoco, Filho, Migas, Coutinho e Torcato. Mudámos e crescemos muito, e é notável que continuemos tão próximos. Um agradecimento especial à Beatriz, por tudo o que cresci e aprendi contigo, e por me inspirares a retomar o meu caminho quando mais estive perdido. Obrigado a todos vocês por todo o carinho, pelas incontáveis aventuras e loucuras e, acima de tudo, por vos poder chamar de família. Sem vocês não tinha conseguido chegar ao final.

Por fim, mas não menos importante, agradeço aos meus pais, irmão, e Tia Lau pelo apoio incondicional. São a minha base, e tudo o que sou devo-vos. Espero poder retribuir, ao longo da vida, o amor e o apoio que sempre me deram.

Obrigado à FCT por financiar a minha bolsa de doutoramento (2021.07153.BD), ao BC BOOST (COMPETE2030-FEDER-00715800 - https://sciproj.ptcris.pt/177623PRJ), ao CEB/DEB e à direção do Programa Doutoral em Engenharia Química e Biológica por me terem acolhido e apoiado ao longo destes anos.

STATEMENT OF INTEGRITY

I hereby declare having conducted this academic work with integrity. I confirm that I have not used plagiarism or any form of undue use of information or falsification of results along the process leading to its elaboration.

I further declare that I have fully acknowledged the Code of Ethical Conduct of the Universidade do Minho.

_____, _____

(Place) (Date)

_____

(Pedro Moreira Montenegro da Silva)

DECLARATION ON THE USE OF ARTIFICIAL INTELLIGENCE (AI) TOOLS

I hereby declare having acted this academic work with integrity and confirm that I have not resorted to any form of undue use of AI tools, nor to the falsification or omission of information, sources, data, results or processes in any of the stages leading to its elaboration.

I further declare that any use of AI tools was done in a transparent and responsible manner, being duly noted in the work, and that I critically verified the accuracy of the content produced with their support, assuming full responsibility for what I submit.

I further declare that I have fully acknowledged the Code of Ethical Conduct of the University of Minho, as well as the applicable standards of academic integrity and data protection.

Resumo

Modulação da produção de celulose bacteriana através da regulação dos níveis de c-di-GMP em Komagataeibacter sucrofermentans

A celulose bacteriana (CB), um biopolímero nanoestruturado de elevada pureza produzido por espécies de *Komagataeibacter*, apresenta notável potencial em aplicações biomédicas, alimentares e em materiais avançados; contudo, a produção economicamente viável permanece limitada pelo metabolismo oxidativo das bactérias acéticas, que desvia a glucose para ácido glucónico em detrimento da biossíntese de celulose, e pela escassa disponibilidade de ferramentas genéticas avançadas.

O Capítulo II caraterizou as quatro desidrogenases de membrana dependentes de pirroloquinolina quinona (PQQ-mDHs). O knockout da PQQ-GDH (KS003) eliminou a acumulação de ácido glucónico e aumentou a produção de CB 5,77 vezes em relação ao tipo selvagem, confirmando a oxidação periplásmica da glucose como o principal constrangimento metabólico; a PQQ-ADH foi ainda identificada como mediadora do efeito estimulante do etanol na produção de CB. O Capítulo IV testou módulos heterólogos transportador–cinase (*GLF–GLK* e *GALP3–GLK*) na KS003 para superar o estrangulamento na captação intracelular de glucose; embora a disrupção da mGDH se mantivesse como o determinante dominante da partição do carbono, os módulos produziram apenas ganhos modestos, implicando o peso dos plasmídeos e a capacidade metabólica a jusante como fatores limitantes residuais.

O Capítulo III examinou a edição genómica mediada por CRISPR–Cas9 em *K. sucrofermentans*: todas as construções falharam na geração de transformantes, independentemente da arquitetura do promotor ou das condições de eletroporação, demonstrando que a expressão basal de Cas9 é intrinsecamente letal neste hospedeiro. Uma análise comparativa inter-géneros identificou princípios de design fundamentais para orientar o desenvolvimento de novas plataformas de edição genómica em *Komagataeibacter*.

Em conjunto, esta tese estabelece uma compreensão mecanística da hierarquia de alocação de carbono em *Komagataeibacter* produtor de CB, demonstra o impacto transformador da disrupção da PQQ-GDH no rendimento de CB, e estabelece as bases para estratégias de edição genómica sem marcador que permitam a reprogramação metabólica precisa de estirpes produtoras de CB.

Palavras-chave: Celulose Bacteriana · CRISPR–Cas9 · *Komagataeibacter* · Engenharia Metabólica · Desidrogenases dependentes de PQQ

Objetivos de Desenvolvimento Sustentável (ODS):



Abstract

Modulating bacterial cellulose production through the pool of c-di-GMP in *Komagataeibacter sucrofermentans*

Bacterial cellulose (BC), a high-purity nanostructured biopolymer produced by *Komagataeibacter* species, holds outstanding promise across biomedical, food, and advanced materials applications; yet cost-effective production is constrained by the oxidative metabolism of acetic acid bacteria (AAB), which diverts glucose toward gluconic acid rather than cellulose biosynthesis, and by the limited availability of advanced genetic tools.

This thesis addresses these bottlenecks through metabolic engineering of *K. sucrofermentans* ATCC 700178 carbon metabolism and development of genome editing tools.

Chapter II systematically characterised the four pyrroloquinoline quinone (PQQ)-dependent membrane dehydrogenases (PQQ-mDHs). Knockout of PQQ-GDH (strain KS003) eliminated gluconic acid accumulation and raised BC production 5.77-fold over the wild type, establishing periplasmic glucose oxidation as the primary metabolic constraint; PQQ-ADH was further identified as the mediator of ethanol-driven BC enhancement. Chapter IV tested heterologous transporter–kinase modules (*GLF–GLK* and *GALP3–GLK*) in KS003 to overcome the resulting cytoplasmic glucose uptake bottleneck; while mGDH disruption remained the dominant determinant of carbon partitioning, the modules yielded only modest gains, implicating plasmid burden and downstream metabolic capacity as residual limiting factors.

Chapter III examined CRISPR–Cas9 genome editing in *K. sucrofermentans*: all nuclease-active Cas9 constructs failed to yield transformants regardless of promoter architecture or electroporation conditions, demonstrating that basal Cas9 expression is intrinsically lethal in this host. Cross-genera analysis identified key design principles, including tightly regulated dual-plasmid systems and temporally separated nuclease activation, to guide development of markerless editing platforms for *Komagataeibacter*.

Collectively, this thesis establishes a mechanistic understanding of the carbon allocation hierarchy in BC-producing *Komagataeibacter*, demonstrates the transformative yield impact of PQQ-GDH disruption, and lays the groundwork for markerless genome editing strategies enabling precise metabolic rewiring of BC-producing strains.

Keywords: Bacterial Cellulose · CRISPR–Cas9 · *Komagataeibacter* · Metabolic Engineering · PQQ-dependent dehydrogenases ·

Sustainable Development Goals (SDG):



Contents

Resumo **v**

Abstract **vi**

Contents **vii**

List of Figures **x**

List of Tables **xiii**

Thesis Outline **3**

1 Introduction **5**

1.1 Abstract 5

1.2 Introduction 5

1.3 Bacterial Cellulose Biosynthesis 7

1.4 Synthetic Biology and Genetic Engineering of BC-Producing Strains 9

1.4.1 Overview of synthetic biology tools (e.g., plasmids, CRISPR, gene circuits, promoters) 9

1.4.2 Key genetic approaches to enhance BC yield 12

1.4.3 Key genetic approaches to modulate and functionalize BC 14

1.5 Conclusions 18

1.6 Objectives 20

1.7 References 20

2 Impact of Different PQQ-Dependent Dehydrogenase Knockouts and Ethanol Supplementation in BC production **28**

2.1 Abstract 28

2.2 Introduction 28

2.3 Materials and Methods 31

2.3.1 Bacterial strains and growth conditions 31

2.3.2 Gene disruption of PQQ-mDHs 31

2.3.3 Analytical procedures 33

2.3.4 BC preparation 33

2.3.5 Statistics and data analysis 34

2.4 Results 34

2.4.1 CFR77_05025 and CFR77_00430 are responsible for the periplasmic oxidation of glucose and ethanol, respectively. 34

2.4.2 The strain KS003 shows improved BC production in static culture 36

2.4.3 Ethanol concentration modulates BC production and metabolic responses in *Komagataeibacter* strains . . . 38
2.5 Discussion . . . 42
2.6 Conclusions . . . 46
2.7 References . . . 47

3 Engineering cytoplasmic glucose uptake in *Komagataeibacter sucrofermentans* ATCC 700178 lacking membrane glucose dehydrogenase 51
3.1 Abstract . . . 51
3.2 Introduction . . . 52
3.3 Materials and Methods . . . 54
3.3.1 Strains and culture conditions . . . 54
3.3.2 DNA assembly . . . 56
3.3.3 Transformation of *K. sucrofermentans* . . . 59
3.3.4 Metabolite analysis and BC quantification . . . 59
3.3.5 Data analysis . . . 60
3.4 Results and Discussion . . . 60
3.5 Conclusion . . . 63
3.6 References . . . 64

4 Design Considerations for Implementing CRISPR–Cas9 Genome Editing in *Komagataeibacter sucrofermentans* ATCC 700178 67
4.1 Abstract . . . 67
4.2 Introduction . . . 68
4.3 Materials and Methods . . . 69
4.3.1 Strains, plasmids, media and culture conditions . . . 69
4.3.2 Construction of plasmids . . . 71
4.3.3 Electroporation . . . 74
4.4 Results . . . 76
4.4.1 Electroporation optimization . . . 78
4.5 Understanding the logic behind CRISPR implementation in recalcitrant bacteria . . . 81
4.5.1 Plasmids, Transformation, and Curing . . . 81
4.5.2 Cas9 Expression Strategies . . . 87
4.5.3 Recombinase Modules and Donor DNA . . . 91
4.5.4 sgRNA Architecture and Promoters . . . 99
4.5.5 Multiplex editing . . . 102
4.6 Design rules for new CRISPR systems . . . 104
4.6.1 Rule 1 – Delivery feasibility defines everything downstream . . . 104

4.6.2 Rule 2 — Treat Cas9 as a Conditional Toxin: Inducibility, Timing, and Leakage Define Success . . . 105
4.6.3 Rule 3 — Match Donor DNA Architecture to Edit Type, Recombination Capacity, and Repair Pathways . . . 107
4.6.4 Rule 4 — Assume Endogenous Repair Is Insufficient . . . 109
4.6.5 Rule 5 — Treat the PAM as a Spatial Constraint, Not a Reason to Change the System . . . 110
4.6.6 Rule 6 — Multiplexing Scales Biological Risk Faster Than Technical Capability 111
4.6.7 Rule 7 — Markerless strains are not optional in applied workflows . . . 112
4.7 Chapter outlook . . . 113
4.8 References . . . 114

5 General conclusions and future perspectives 123

List of Figures

I.1 Proposed organization of the Type I BCS complex [44, 49, 50]. b) Type I Bacterial cellulose operon [49] (figure and legend from Römling and Galperin [49]). 8

I.2 Diagram shows the molecular strategies and techniques for Komagataeibacter strains development (figure from Malcı et al. [15], ACS Synthetic Biology, used under CC-BY 4.0 license). 10

I.3 SynBio and computational tools for engineering BC producers. The genetic toolkits developed for *Komagataeibacter*. The first toolkit is based on Biobrick assembly with constitutive and inducible promoters and a small RNA (sRNA) targeting UGPase mRNA. The second version of the Biobrick-based toolkit, offering a wide array of promoters, RBSs, coding sequences (CDSs), terminators, and protein tags, tested and characterized in *K. xylinus*, *K. hansenii*, and *K. rhaeticus*. The Golden Gate-based *Komagataeibacter* SynBio toolkit (KTK) enables the hierarchical assembly of transcription units and multicassette plasmids, available as a cost-effective 96-well plate on Addgene (figure adapted from Malcı et al. [15], ACS Synthetic Biology, used under CC-BY 4.0 license). 10

II.1 Overview of the key metabolic steps and pathways involved in BC production and energy generation in the presence of glucose and ethanol. The periplasmic oxidation of the sugars, alcohols, and sugar alcohols is linked to the electron transport chain (ETC) – the dehydrogenases transfer the reducing equivalents to ubiquinone (UQ – dark green) converting it to its reduced form, ubiquinol (UQ – light green). UQ can be further re-oxidized by terminal oxidases in a process coupled with oxygen (O_2) reduction to water (H_20) and the generation of a proton (H^+) gradient. Then, F_1F_0 ATPase facilitates H^+ translocation, owing to the H^+ gradient, in a process coupled with adenosine triphosphate (ATP) generation. 29

II.2 Time-course growth and metabolic profiles of agitated cultures in HS-glucose medium for five K. sucrofermentans strains - A: KS001; B: KS002; C: KS003; D: KS004; E: KS005. For each strain: The left panel shows OD_{600nm} monitoring; the middle panel depicts glucose concentration (g/L); the right panel represents gluconic acid concentration (g/L). In all panels, Replicate 1 (orange lines with dot markers) and Replicate 2 (blue lines with cross markers) are shown. 35

II.3 pH variation during fermentations of K. sucrofermentans strains in different media – A: pH measurements for strains KS001 to KS005 over time in HS-glucose medium; B: pH values for the same strains in HS-ethanol medium. 36

II.4 Time-course growth and metabolic profiles of agitated cultures in HS-ethanol medium for five K. sucrofermentans strains - A: KS001; B: KS002; C: KS003; D: KS004; E: KS005. For each strain: The left panel shows OD_{600nm} monitoring; the middle panel depicts ethanol concentration (g/L); the Right panel represents acetic acid concentration (g/L). In all panels, Replicate 1 (orange lines with dot markers) and Replicate 2 (blue lines with cross markers) are shown. 37

II.5 BC production (g/L) of K. sucrofermentans strains KS001 to KS005 grown in HS-glucose (black bars) and HS-ethanol (white bars) media, in static culture. Error bars denote standard deviations.* Statistically significant difference in BC concentration compared to the KS001 strain for the corresponding carbon source (N=2; p<0.05). 38

II.6 Comparative Analysis of Bacterial Cellulose Production Efficiency in K. sucrofermentans strains in HS-glucose-ethanol media in a range of ethanol concentrations, in static culture - A: KS001; B: KS003; C: KS004. The top panel (VPE) represents Volumetric Production Efficiency (g/L), the second panel (BPCG) shows Bacterial Cellulose Production Per Consumed Glucose (g/mol), the third panel (BPCE) denotes Bacterial Cellulose Production Per Consumed Ethanol (g/mol), and the bottom panel (BPCC) illustrates Bacterial Cellulose Production Per Consumed Carbon (g/mol). Red bars represent data at 7 days, while green bars denote data at 14 days. Error bars indicate the standard deviation. * Significance against strain KS001 for the same condition and timepoint (N= 2; p<0.1). ** Significance when comparing 14 days to 7 days for a given condition (N=2; p<0.1). 39

II.7 Metabolic profiles of K. sucrofermentans strains in HS-glucose-ethanol media. Each panel shows the residual concentration of (from top to bottom) glucose, gluconic acid, ethanol, and acetic acid (all in g/L) for strains KS001 (A), KS003 (B), and KS004 (C). Red and green bars indicate measurements at 7 and 14 days, respectively; error bars represent standard deviation; the horizontal blue dashed line represents the initial glucose concentration (g/L). * Significant differences from strain KS001 under identical conditions (N=2; p<0.1). ** Significant differences between the time points for each strain (N=2; p<0.1). 41

III.1 Effects of heterologous glucose uptake modules on bacterial cellulose production and metabolite formation in K. sucrofermentans. Strains derived from the wild-type (KS001) K. sucrofermentans ATCC 700178 and from the ΔmGDH mutant KS003 were transformed with either no plasmid (“none”), an empty vector control, or plasmids encoding the glucose facilitator–glucokinase module (*Zm*GLF–*Ks*GLK) or the galactose permease–glucokinase module (GAL–GLK). (A) Final BC (BC) concentration (g L^{-1}). (B) BC yield relative to consumed glucose (mg mg^{-1}). (C) Total glucose consumed during cultivation (g L^{-1}). The dashed line indicates the initial glucose concentration (20 g L^{-1}). (D) Gluconic acid produced (g L^{-1}). (E) Residual acetic acid concentration (g L^{-1}). Bars represent mean values of biological replicates (n = 2–3) and error bars indicate standard deviation. Statistical significance between selected conditions was evaluated using Welch’s t-test; p values are indicated above brackets. Significance levels are denoted as $p \leq 0.001$, $p \leq 0.01$, $p \leq 0.05$*, † $p \leq 0.10$, and ns (not significant). The vertical dotted line separates KS003-derived strains from KS001-derived strains. The glucose consumption profiles further illustrate the metabolic divergence between the two strains. All wild-type derivatives consumed essentially all available glucose (20 g L^{-1}) during cultivation, whereas KS003 strains consumed only approximately half of the available glucose. . . . 62

IV.1 Transformation outcomes across Cas9 architectures. Promoter strength, regulatory logic, and replication origin were varied independently; every assembled active-Cas9 construct yielded no transformants (0 CFU μg^{-1}), whereas a catalytically dead dCas9 control was recovered. Electroporation was tuned by a central-composite design (validated optimum 1.24×10^6 CFU μg^{-1}; N=3), confirming that DNA delivery is not the limiting factor. 78
IV.2 Response surface analysis of electroporation efficiency in *K. sucrofermentans* ATCC 700178. Three-dimensional response surfaces generated from the fitted quadratic model illustrating the effects of: **A)** harvest OD_{600} (X_1) and OD_{600} after concentration (X_2); **B)** harvest OD_{600} (X_1) and DNA concentration (X_3); and **C)** OD_{600} after concentration (X_2) and DNA concentration (X_3) on transformation efficiency (CFU μg^{-1} DNA). In each panel, the non-plotted factor was held at its central coded value (0). 80
IV.3 Decision framework for CRISPR–Cas system design in non-model Gram-negative bacteria. 106

List of Tables

II.1 List of primers used for construction of suicide plasmids for knockout of the genes coding for PQQ-mDHs. Overhangs for assembly with InFusion® Cloning HD are represented in lower case letters, while template specific bases are in upper case letters. 32

III.1 Strains used in this study. 55
III.2 Plasmids used in this study. 55
III.3 Primers used in this study. 57

IV.1 Strains used in this study. 69
IV.1 Strains used in this study. 70
IV.2 Plasmids used in this study. 70
IV.2 Plasmids used in this study. 71
IV.3 Primers used in this study. 73
IV.3 Primers used in this study. 74
IV.4 Statistical Surface Optimization conditions. 75
IV.4 Statistical Surface Optimization conditions. 76
IV.5 Transformation efficiency of Cas9-encoding plasmids in *K. sucrofermentans* before and after electroporation optimization. 77
IV.5 Transformation efficiency of Cas9-encoding plasmids in *K. sucrofermentans* before and after electroporation optimization. 78
IV.6 Electroporation efficiency values obtained for each central composite design run. 79
IV.7 Replication origins, delivery routes, and curing strategies. 82
IV.8 Cas9 expression strategies by host. 88
IV.9 Recombinase + donor compatibility. 91
IV.10 sgRNA regulation and assembly. 100

Scientific output

According to the 2nd paragraph of article 8 of the Portuguese Decree-Law no. 388/70, the scientific outputs of this thesis are listed below. The results presented in this thesis have been partially published elsewhere.

Peer-reviewed journal articles:

- **Montenegro-Silva, P.**, Ellis, T., Dourado, F., Gama, M., & Domingues, L. (2024). Enhanced bacterial cellulose production in *Komagataeibacter sucrofermentans*: impact of different PQQ-dependent dehydrogenase knockouts and ethanol supplementation. *Biotechnology for Biofuels and Bioproducts*, 17(1):35. doi: 10.1186/s13068-024-02482-9.

Book chapters:

- Pacheco, M., **Montenegro-Silva, P.**, Dourado, F., Gama, M., Domingues, L., & Dias, Ó. (Forthcoming). Bacterial cellulose production from non-conventional strains. In F. Dourado, M. Gama, F. Hong, R. Banerjee, & M. Das (Eds.), *Advances in bacterial nanocellulose: Towards sustainable production and emerging applications*. Springer Nature.
- **Montenegro-Silva, P.**, Pacheco, M., Dias, Ó., Dourado, F., Gama, M., & Domingues, L. (Forthcoming). Synthetic biology as a paradigm shift in bacterial cellulose-based material design and production. In F. Dourado, M. Gama, F. Hong, R. Banerjee, & M. Das (Eds.), *Advances in bacterial nanocellulose: Towards sustainable production and emerging applications*. Springer Nature.

Oral communications in conferences:

- Microbiotec'25 – Congress of Microbiology and Biotechnology (Faro, Portugal). **Montenegro-Silva, P.**, Ellis, T., Dourado, F., Gama, M., & Domingues, L. Modular engineering of substrate oxidation and electron flow for enhanced bacterial cellulose biosynthesis in *Komagataeibacter*. [Oral, OP1.22]
- ISBNC2024 – 6th International Symposium on Bacterial Nanocellulose (Shanghai, China). **Montenegro-Silva, P.**, Ellis, T., Dourado, F., Gama, M., & Domingues, L. Combining ethanol supplementation and genetic engineering for high-yield bacterial cellulose production. [Oral]

Posters in conferences:

- ISBNC2024 – 6th International Symposium on Bacterial Nanocellulose (Shanghai, China). Rodrigues, A.C., Martins, D., **Montenegro-Silva, P.**, Duarte, S.M., Silva-Carvalho, R., Marques, S., Cavaleiro, A.J., Dourado, F., & Gama, M. Optimizing bacterial nanocellulose production from *Eucalyptus* biomass: a circular approach to wastewater management and resource recovery. [Poster]

- Microbiotec'23 – Congress of Microbiology and Biotechnology (Covilhã, Portugal). **Montenegro-Silva, P.**, Ellis, T., Dourado, F., Gama, M., & Domingues, L. Optimizing bacterial cellulose production in *Komagataeibacter spp.* through metabolic engineering. [Poster]

Thesis Outline

The research activities described in this doctoral thesis were developed at CEB – Centre of Biological Engineering, University of Minho (Braga, Portugal), under the supervision of Professor Lucília Domingues and Professor Francisco Gama. Part of this work was developed in close collaboration with the Department of Bioengineering at Imperial College London (London, United Kingdom), under the supervision of Professor Tom Ellis, whose tools and expertise underpinned the experimental work described throughout this thesis.

This doctoral thesis is divided into five chapters, three of them describing experimental research published or in preparation for submission to international peer-reviewed journals.

Chapter I (*Introduction: Bacterial Cellulose and Synthetic Biology*) encompasses a comprehensive review of the production, properties, and applications of bacterial cellulose (BC), with particular focus on the synthetic biology tools and strategies available for engineering BC-producing microorganisms of the genus *Komagataeibacter*. This chapter introduces the key metabolic and regulatory features governing BC biosynthesis and critically reviews the expanding genetic toolkit available for this non-model bacterial host, including modular cloning systems and CRISPR-based approaches. The challenges and opportunities of applying these tools to improve BC yields and broaden its material properties are discussed, framing the experimental work that follows. This chapter is adapted from an original book chapter (*in press*).

Chapter II (*Impact of different PQQ-dependent dehydrogenase knockouts and ethanol supplementation in BC production*) describes the construction and phenotypic characterisation of knockout mutants targeting four pyrroloquinoline quinone (PQQ)-dependent membrane dehydrogenases (PQQ-mDH) in *K. sucrofermentans* ATCC 700178. Disruption of the gene encoding the membrane glucose dehydrogenase (mGDH) yielded a 5.77-fold increase in BC production, accompanied by elimination of gluconic acid accumulation, establishing periplasmic glucose oxidation as the dominant metabolic bottleneck. Ethanol supplementation is further demonstrated as a practical strategy to enhance BC yields through metabolic rerouting. This chapter is published as:

> Montenegro-Silva P, Ellis T, Dourado F, Gama M, Domingues L. Enhanced bacterial cellulose production in *Komagataeibacter sucrofermentans*: impact of different PQQ-dependent dehydrogenase knockouts and ethanol supplementation. *Biotechnol Biofuels Bioprod.* 2024;17(1):35. doi: 10.1186/s13068-024-02482-9.

Chapter III (*Engineering cytoplasmic glucose uptake in Komagataeibacter sucrofermentans ATCC 700178 lacking membrane glucose dehydrogenase*) builds on the mGDH-deficient strain KS003 (described in Chapter II), investigating whether the introduction of heterologous cytoplasmic glucose transport modules can further improve BC production. Two transporter–kinase modules were assembled using the *Komagataeibacter* Tool Kit (KTK) modular cloning system and introduced into both wild-type and KS003 backgrounds: a *Zymomonas mobilis* glucose facilitator–glucokinase (GLF-GLK) module and a native galactose permease homologue–glucokinase (GALP3-GLK) module. Whereas both modules were expressed, their contribution to BC yields beyond the improvements already conferred by mGDH disruption was

modest, pointing to downstream metabolic capacity as the next-order constraint. This chapter requires additional experimental characterisation before submission as a research article to an international peer-reviewed journal.

Chapter IV (*Design considerations for implementing CRISPR–Cas9 genome editing in* Komagataeibacter sucrofermentans *ATCC 700178*) provides a systematic analysis of the challenges encountered when attempting to establish CRISPR–Cas9-based genome editing in *K. sucrofermentans*. Through the construction and evaluation of multiple plasmid architectures differing in promoter logic, induction strategy, and replication origin, we demonstrate that even sub-threshold Cas9 expression is lethal in this host, irrespective of the delivery route used. In contrast, the catalytically dead dCas9 variant was stably maintained, validating CRISPR interference (CRISPRi) as a deployable alternative for gene repression. These findings are synthesised into a cross-species framework of design principles for CRISPR–Cas9 implementation in non-model Gram-negative bacteria. This chapter is in preparation for submission as a literature review article to an international peer-reviewed journal.

Chapter V presents the major conclusions drawn from this doctoral project, highlights the key contributions to the understanding of BC metabolism and the genetic engineering of *Komagataeibacter*, and sets out the most promising directions for future research, with emphasis on the prospects for functional CRISPR–Cas9 editing, chromosomal strain improvement, and scale-up of BC production.

1 Introduction

1.1 Abstract

Bacterial cellulose (BC) is a high-performance biomaterial characterized by exceptional properties; however, its production is subject to certain limitations. The emergence of synthetic biology has progressively facilitated the precise control over BC-producing microorganisms, which is beneficial not only for enhancing yields but also for broadening its properties and applications. Innovations such as Clustered Regularly Interspaced Short Palindromic Repeats (CRISPRi) interference, quorum sensing circuits, and modular expression systems are augmenting BC biosynthesis and functionalization. Co-culture strategies, particularly with organisms more amenable to genetic modification, can enhance the incorporation of biosensing, enzymatic activity, and self-patterning, thereby paving the way for next-generation materials. The future integration of multi-omics, computational modelling, and automation is expected to refine BC bioengineering. As synthetic biology progresses, BC is evolving from a natural polymer to a programmable material with extensive industrial, environmental, and biomedical potential.

1.2 Introduction

The most notable Bacterial cellulose (BC) producers are bacterial within the *Komagataeibacter* genus, widely known as remarkable producers [1, 2]. BC is a natural biopolymer that, unlike plant-derived cellulose, is produced in a highly pure form due to the absence of hemicellulose and lignin, eliminating the need for energy-intensive downstream processing. The physicochemical properties of BC make it an exceptional biodegradable material with high water absorption capacity, crystallinity, and mechanical strength [3–5]. The material's properties make it exceptional for the use of BC in various advanced applications, across several industries [6–9].BC is composed of glucan chains of glucose units, linked by β-1,4-glycosidic bonds, which can be arranged into cellulose I (native; crystalline), or cellulose II (reconstituted; crystalline) [10]. BC can form composites with other materials, and be impregnated with functional agents, further expanding its utility to fields as bioelectronics, environmental technologies, and acoustics [11–13].

Both the BC production process and the modulation of its' properties have been mostly achieved through process optimization and in-situ or ex-situ modifications, respectively [13]. However, the continuous progress made in synthetic biology and systems biology are enabling the development of novel microbial strains and co-culture systems with superior yields and novel material functionalities (e.g. antibacterial, electric conductivity), [14–16] thus allowing BC to stand out as a versatile platform for generate novel advanced materials with application across diverse industries [6, 14–18].The biotechnological field of BC production and functionalization has been largely transformed by synthetic biology. The emerging interdisciplinary field applies principles such as modularity, standardization and programmable DNA design, facilitated the development of engineered BC producers with improved traits [15, 19–21]. The adoption

of BC has been hindered by high costs associated with synthetic culture media, which has been mitigated through the utilization of industrial by-products and fermentation optimization techniques, achieving yields as high as 10 g L^{-1} and productivity rates up to 0.4 g L^{-1} h^{-1} [18, 22–24].

Beyond its material properties, BC has attracted growing commercial interest: the global BC market was valued at approximately USD 410–610 million in 2024 and is projected to grow at a compound annual growth rate of roughly 12–13% over the following decade, driven by demand in the biomedical, food, cosmetic, and packaging sectors [25, 26]. BC already occupies high-value, specialised niches in which its purity and nanofibrillar structure justify a premium over plant-derived cellulose [3].

Nevertheless, widespread industrial adoption of BC remains constrained by its high production cost. Techno-economic analyses estimate selling prices of around USD 25/kg for BC produced with conventional synthetic media and substantial capital investment, whereas the valorisation of low-cost agro-industrial residues has been proposed to lower production costs to as little as USD 1.63/kg [25]. These figures underscore that improving strain productivity and substrate utilisation, rather than economic viability alone, remains the central bottleneck for cost-competitive, large-scale BC production [3, 24].

Despite the embryonic stage of the synthetic biology tools for *Komagataeibacter*, when compared with other organisms, the availability of genetic tools has increased considerably (e.g. plasmid backbones, promoters, terminators, CRISPR interference (Clustered Regularly Interspaced Repeats; CRISPRi)), enabling targeted modifications for yield improvements, by-product reduction, and modulation of the material's properties [27, 28].

The development of BC-based composites through co-culture systems and material incorporation was a critical innovation in BC functionality [14, 16, 29]. The relevance lies in the utilization of more tractable organisms for the production of functional components such as alginate, collagen or gelatin, whose incorporation into BC matrices, can enhance properties like mechanical strength and antimicrobial activity [14, 29–33]. Engineered Living Materials (ELMs) are responsive, multifunctional composites for diverse applications, including medicine, architecture and electronics [34–36]. ELMs can even be programmed with easy-to-assemble modular genetic circuits for enhanced functionality, specificity, and spaciotemporal control [15, 19–21, 37–41], BC research is currently aiming at enabling the cost-effective production tailor-made BC products, which requires optimization of microbial strains and bioprocesses, and can be revolutionized by multidisciplinary advances in bioreactor design, co-culture strategies, and synthetic biology [4, 5, 10, 12, 14, 15, 21, 28, 38, 42, 43]. Such advances are gradually driving the research field to meet the demand for improved materials in industries ranging from biomedical engineering to green electronics [1–5, 16, 22, 23].

The genus *Komagataeibacter*, formerly classified within the genera *Gluconacetobacter* and *Acetobacter*, belongs to the acetic acid bacteria (AAB) – a group of obligately aerobic α-Proteobacteria of the family *Acetobacteraceae* characterised by the incomplete oxidation of sugars and alcohols [44]. The strain used throughout this work, *K. sucrofermentans* ATCC 700178, was originally isolated from a cherry as the strain BPR 2001 and described as a potent cellulose producer under agitated cultures, initially leading to the proposal of *Acetobacter xylinum* subsp. *sucrofermentans* [45].

The genome of *K. sucrofermentans* ATCC 700178 (DSM 15973) comprises approximately 3.44 Mbp organised into five closed replicons – a single chromosome and four plasmids – with a G+C content of about 62% (GenBank assembly GCF_040581405.1) [46]. This compact, multi-replicon genome is characteristic of *Komagataeibacter* and encodes the cellulose synthase (*bcs*) machinery responsible for BC biosynthesis, providing the genetic context for the metabolic and engineering strategies explored in this thesis.

This chapter explores the impact of synthetic biology in the development of high yield BC-producing strains, and BC-based materials with increased functionality. It starts by briefly introducing the most relevant biosynthetic pathways, and the advances in genetic and metabolic engineering as innovation driving forces.Key questions addressed include: How can synthetic biology tools and approaches be leveraged to improve BC yield and properties? What strategies are most effective for tailoring BC to meet the requirements of advanced applications, such as biomedical devices and smart materials? By addressing these questions, this chapter highlights the paradigm shift in material design and production enabled by synthetic biology, paving the way for next-generation BC-based materials.

1.3 Bacterial Cellulose Biosynthesis

Komagataeibacter species synthesize BC in a highly efficient process that polymerizes glucose into nanostructured cellulose materials with unique mechanical and functional properties. The first committal step in BC biosynthesis is the conversion of glucose-6-phosphate to glucose-1-phosphate by phosphoglucomutase. The phosphorylated sugar is further converted to uridine diphosphate (UDP)-glucose, by UDP-glucose pyrophosphorylase, which is the substrate of the bacterial cellulose synthase (BCS) complex - the transmembrane heteromeric complex responsible for the simultaneous polymerization of UDP-glucose monomers into β-1,4-glucan chains, and respective extrusion to the extracellular environment [13, 38, 47–50].

The genetic composition of the *bcs* operon varies across bacterial taxa and, while maintaining the core biosynthetic mechanism, such variation translates into substantial differences in terms of strain productivity and physicochemical properties. Within the *Komagataeibacter* genus, the *bcsABCD* operon encodes the key subunits responsible for cellulose biosynthesis [49]. BcsA forms a channel that spans across the inner membrane, contains the catalytic glycosyltransferase domain and a PilZ-like domain, which binds cyclic diguanylic acid (c-di-GMP), an essential allosteric activator [49, 51–53]. BcsB acts as a chaperone, stabilizing BcsA activity and aiding glucan chain translocation through the inner membrane. BcsC forms an outer membrane pore to guide the nascent glucan chain outside the cell, while BcsD organizes glucan chains into crystalline fibrils, enhancing structural alignment and overall cellulose production efficiency [13, 38, 44, 49, 50, 54] (**Figure I. 1a**).

Regulation of cellulose biosynthesis involves both genetic and environmental factors. The levels of c-di-GMP are modulated by diguanylate cyclases (DGCs) and phosphodiesterases (PDEs), encoded by several operons such as *cdg1*, *cdg2*, and *cdg3*. This layer of regulation allows the bacteria to precisely adjust the

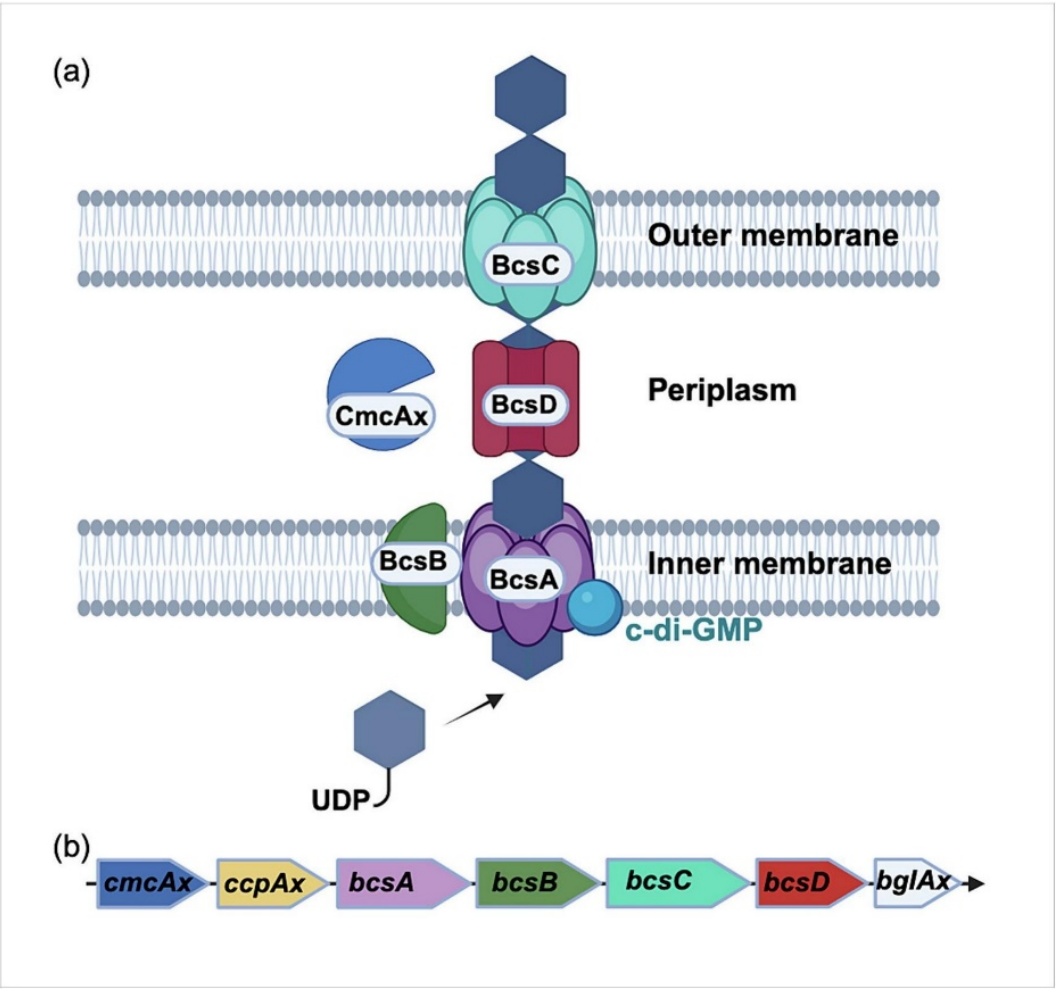


Figure I.1: Proposed organization of the Type I BCS complex [44, 49, 50]. b) Type I Bacterial cellulose operon [49] (figure and legend from Römling and Galperin [49]).

activity of the BCS complex in response to environmental cues (e.g. oxygen availability) [49, 52, 53, 55, 56]. The *bcsABCD* operon contains accessory genes that, while not being essential, are important for the cellulose's structural integrity and/or the strains' maximum productivity [13, 38, 49, 50, 52, 53, 56].

The fine coordination between the simulataneous polymerization and secretion processes is a major factor affecting the maximum BC productivity, and the material's properties. During this process, the nascent glucan chains are gradually assembled into protofibrils and further into larger microfibrils, and further into hydrogen-bonded cellulose ribbons. The delicately assembled nanostructure is responsible for the distinctive mechanical strength, water retention capacity, and biocompatibility of BC [3, 4, 14, 22, 24, 57, 58].

Despite the remarkable efficiency of natural BC synthesis in *Komagataeibacter* species, several challenges hinder its optimization for industrial applications. By-product formation is one of the major bottlenecks (e.g. gluconic acid, exopolysaccharide (EPS)) due to reduction of the process' cost-efficiency [42, 59–64]. Additionally, *Komagataeibacter* strains are highly sensitive to environmental factors (e.g.

oxygen availability, pH, temperature) which potentially affects the intracellular concentration of regulatory molecules such as c-di-GMP [4, 13, 38, 50, 52]. Another challenge lies in the high energy and precursor demands of BC production, which can strain cellular resources, particularly under suboptimal growth conditions [3, 13, 38]. These challenges pose an opportunity to leverage synthetic biology and genetic engineering for targeted strategies to suppress by-product formation, optimize metabolic fluxes and improve the robustness of the production process [14, 15, 21, 38].

1.4 Synthetic Biology and Genetic Engineering of BC-Producing Strains

Advances in genetic engineering and synthetic biology have revolutionized the engineering of BC producers (**Figure I. 2**). Traditional genetic engineering focuses on manipulating individual genes, while metabolic engineering focuses on the optimization metabolic flows and networks. Synthetic biology, on the other hand, applies engineering principles, through a modular and programmable approach that enables precise control over cellular behaviour thus facilitating the generation of organisms with tailormade traits [39–41]. A cornerstone of synthetic biology in this context is the use of ELMs — biomaterials that integrate functional properties during the growth process of living organisms like BC-producing bacteria [41]. ELMs offer a unique advantage by combining biological self-assembly with engineered functionalities, allowing researchers to design BC with customizable mechanical, chemical, or sensory properties during its biosynthesis [14, 15, 21, 41].

Moreover, ELMs can also be generated through co-culture strategies that pair BC-producing bacteria with engineered model organisms such as the bacteria *Escherichia coli*, or the yeast *Saccharomyces cerevisiae* [29, 65]. The tractability of model organisms can be leveraged to add functionality (e.g. production of cross-linking agents, dyes) and further expand the versatility of BC-based products [14, 15, 21, 29, 66].

This section will focus on the synthetic biology and genetic/metabolic engineering tools that are driving innovations in BC production, and also explore key engineering approaches to enhance BC yield, customize its properties, and co-culture strategies to create multifunctional BC-based ELMs for advanced applications.

1.4.1 Overview of synthetic biology tools (e.g., plasmids, CRISPR, gene circuits, promoters)

Synthetic biology has had a large impact in the field of BC production due to the introduction of flexible, modular, and programmable tools to engineer *Komagataeibacter* species [28, 43, 67]. The novel tools accelerated the assembly of standardized parts into plasmid backbones (e.g. transcription units, gene circuits, CRISPRi), which can be used to generate productive strains that are able to synthesize BC with tuneable properties [28, 43, 67, 68] (**Figure I. 3**).

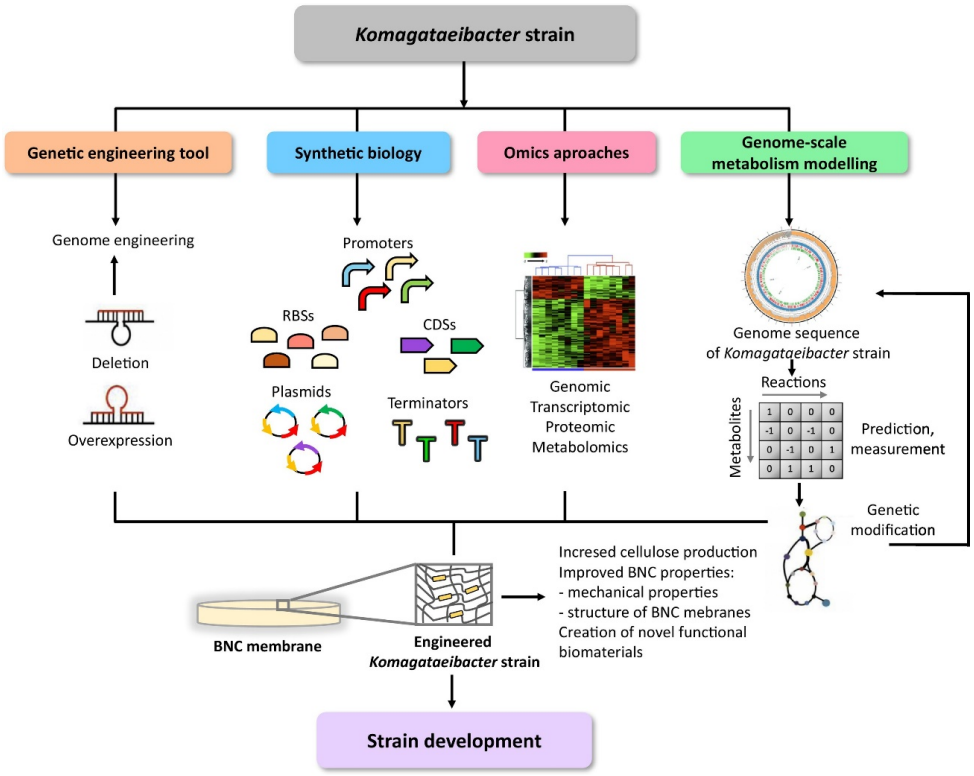


Figure I.2: Diagram shows the molecular strategies and techniques for Komagataeibacter strains development (figure from Malcı et al. [15], ACS Synthetic Biology, used under CC-BY 4.0 license).

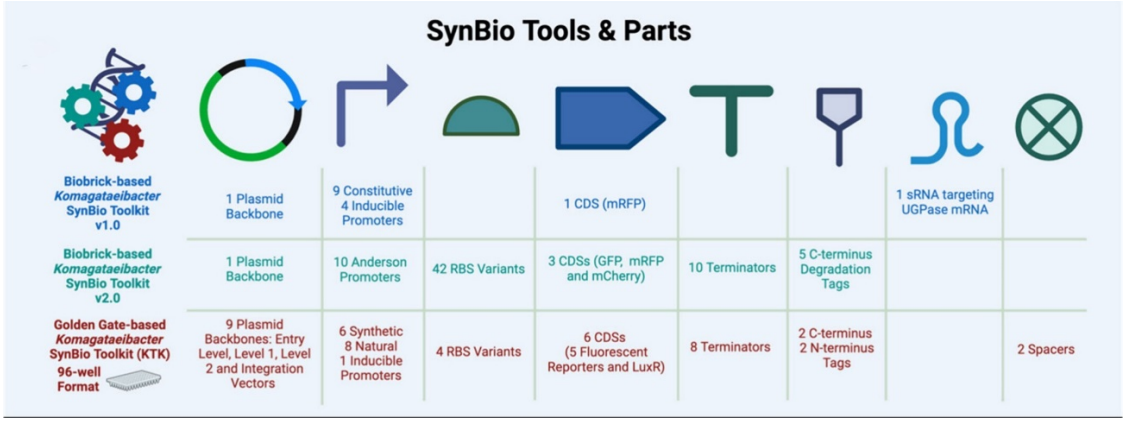


Figure I.3: SynBio and computational tools for engineering BC producers. The genetic toolkits developed for *Komagataeibacter*. The first toolkit is based on Biobrick assembly with constitutive and inducible promoters and a small RNA (sRNA) targeting UGPase mRNA. The second version of the Biobrick-based toolkit, offering a wide array of promoters, RBSs, coding sequences (CDSs), terminators, and protein tags, tested and characterized in *K. xylinus*, *K. hansenii*, and *K. rhaeticus*. The Golden Gate-based *Komagataeibacter* SynBio toolkit (KTK) enables the hierarchical assembly of transcription units and multicassette plasmids, available as a cost-effective 96-well plate on Addgene (figure adapted from Malcı et al. [15], ACS Synthetic Biology, used under CC-BY 4.0 license).

For more than a decade, the targeted genetic modification of *Komagataeibacter* species was relatively rare and primarily relied on two expression vector backbones: pSA and pBBR122 [69–72]. More recently, the plasmid repertoire has been expanded with the plasmids pTI99, pTSa and pSEVA331Bb. These vectors have been employed for both endogenous and heterologous gene expression [68, 73–75]. Gene disruption was typically achieved through homologous recombination using non-replicating plasmid-based disruption cassette carriers such as pUC18/pUC19, pT7Blue, pET14, or pHSG399 [59, 60, 64, 74, 76].

In 2016, Florea *et al.* has made the first effort to bring modularization and standardization of genetic constructs to the field. The researchers started by engineering the plasmids pSEVA321 and pSEVA331 to make them compatible with BioBrick standard, and proceeded with the characterization of 9 constitutive promoters, 2 inducible promoters (P_{Lux} and P_{Tet}), and 3 fluorescent proteins. Additionally, a small RNA tool for genetic knockdowns was also developed and used for translational modulation of UDP glucose pyrophosphorylase transcripts, allowing control over BC production levels [68] (**Figure I. 3**).

Three years later, the tool repertoire for *Komagataibacter* was further expanded by Teh *et al.* with libraries consisting of several constitutive and inducible synthetic promoters, 10 terminators, 42 ribosome-binding sites (RBSs) and 5 degradation tags to fine-tune transcription and translation levels. The inducible promoters P_{BAD} and P_{Lux} were comparatively characterized with the first showing lower induction levels, but also less leakiness. Additionally, RBS characterization allowed the identification of important sequence features that could facilitate the design of novel RBSs with desired strengths. The parts were characterized in different species, namely *K. rhaeticus* iGEM, *K. sucrofermentans* ATCC 700178 and *Novacetimonas hansenii* ATCC 53582, showing that the toolkit is applicable in multiple BC producers, although some parts might behave differently across species [28, 68].

In 2020, Hur & Choi *et al.* aimed at balancing the translation strengths of the gene products of *pgm* (phosphoglucomutase), *galU* (UDP-glucose pyrophosphorylase) and *ndp* (nucleoside diphosphate kinase) by generating several engineered RBSs with varying translation strengths. These enzymes are involved in the biosynthesis of the direct precursor of BC, UDP-glucose. The systematic evaluation of the impact of different RBS strengths allowed to increase BC production by balancing protein expression levels in *K. xylinus* DSM 2325 [77].

In 2021, Goosens *et al.* developed a Golden Gate-based system, named KTK, designed for standardized, modular, and hierarchical assembly of diverse genetic parts [43]. The KTK features an user-friendly and expandable plasmid library of genetic parts, which includes promoters, RBSs, terminators, fusion tags and reporter proteins, along with replicating plasmids. Using one-pot Golden Gate reactions, researchers can rapidly assemble these parts into transcriptional units and further combine them into complex multi-gene constructs [43] (**Figure I. 3**). Due to its standardized and modular nature, KTK can be a driving force in BC research by facilitating collaboration between research groups and improving data reproducibility.

The development of CRISPRi, has simultaneously added a new layer of precision to gene regulation, and enabled the easy and reprogrammable knock down of essential genes, which is useful due to the lethality associated with eliminating such targets [78–80]. CRISPRi uses a catalytically inactive Cas9 (dCas9) protein to repress transcription without introducing double-strand breaks [78–80]. This technique

has been employed to downregulate key genes like *acsAB* and *galU* in *K. xylinus* CGMCC 2955 and *N. hansenii* ATCC 53582, respectively, resulting in tailored alterations in BC production and material properties [28, 67]. As an example, transcriptomic data hints that galU is critical for controlling the carbon flux between BC biosynthesis and the pentose phosphate pathway, thus influencing the rate of BC biosynthesis. By using CRISPRi to control the galU expression levels, Huang et al. [67] was able to understand its relationship with porosity and crystallinity [67].

Gene circuits and quorum-sensing systems have also been explored to expand the toolkit for BC engineering. In 2016, Florea et al. [68] adapted an acyl-homoserine lactone (AHL)-based system for inter-strain communication and regulation of BC biosynthesis [68]. Building on this, another tool was developed specifically for co-culture systems, where "sender" cells produce AHL to trigger a response in "receiver" cells, enabling spatial patterning and underlining the versatility of synthetic biology to develop intelligent biomaterials [81].

Overall, the integration of synthetic biology tools such as plasmids, CRISPR systems and gene circuits has revolutionized the genetic engineering of BC-producing bacteria. These tools not only enhance BC yields but also allow for the customization of its structural and functional properties, paving the way for novel applications in material science and biomanufacturing. As these technologies continue to evolve, their application across various *Komagataeibacter* species is expected to unlock even greater potential for sustainable and high-performance BC production.

1.4.2 Key genetic approaches to enhance BC yield

Broadening the range of substrates for BC production enhances both cost-effectiveness and versatility by allowing the use of diverse carbon sources and feedstocks. For example, overexpressing sucrose synthase enables the efficient conversion of sucrose into UDP-glucose. This process, coupled with UDP recycling, sustains cellulose biosynthesis and prevents the accumulation of metabolic intermediates [70]. Similarly, modifying the mannose catabolic pathway of *K. xylinus* ATCC 23770, by expressing mannose kinase and phosphomannose isomerase, has improved the utilization of mannose-rich biomass. These modifications resulted in an 84% increase in BC yield and enhanced mechanical properties, including greater tensile strength and elongation [82]. Furthermore, introducing the *lacZ* gene in *K. xylinus* ITz3 enables lactose metabolism, allowing the use of lactose-rich substrates such as whey, leading to a 28-fold increase in BC production [83]. There have also been efforts to improve glucose utilization through heterologous expression of the glucose facilitator protein from *Zymomonas mobilis* and the phosphoenolpyruvate-dependent glucose phosphotransferase system (PTS_{Glc}), with the latter being more efficient [42, 61]. Restoring the PTS_{Glc} system in *K. xylinus* CGMCC 2955 required the balanced expression of one operon and one additional gene, while restoring glycolysis required pfkA overexpression [61]. These genetic improvements demonstrate the potential for leveraging diverse and economically viable carbon sources to enhance BC yields and industrial scalability [61, 70, 82, 83].

In addition to optimizing substrate utilization, environmental and operational conditions play a crucial role in enhancing BC production (e.g. oxygen availability, static/agitated culture). The expression of the

Vitreoscilla hemoglobin in *K. xylinus* BCRC 12334 has been shown to increase BC synthesis by up to 70%. This effect is particularly pronounced under oxygen-limited conditions, likely due to improved adenosine triphosphate (ATP) generation, which redirects carbon flux toward BC biosynthesis. Furthermore, lowering oxygen tension in sealed cultures reduces the oxygen-intensive incomplete oxidation of glucose. While this process contributes to ATP generation via the electron transport chain, it also leads to the extracellular accumulation of gluconic acids, which in turn lowers the culture's pH [71]. This incomplete oxidation process is inherently linked to oxygen availability, as oxygen serves as the final electron acceptor in the periplasmic oxidation of sugars and sugar alcohols.

However, this oxygen-dependent periplasmic oxidation is a double-edged sword. While it provides an ecological advantage for the genus, it also reduces carbon availability for BC synthesis and contributes to acidification, which forces BCS to function under suboptimal conditions. That is the case for the supra-mentioned partial oxidation of glucose, which competes with BC production. To address this inefficiency, several studies report significant improvements in BC production following the knockout of the *gcd* gene, in various *Komagataeibacter* strains, which encodes a pyrroloquinoline quinone (PQQ)-dependent glucose dehydrogenase, thus preventing the oxidation of glucose into gluconic acid [42, 59, 60, 62].

In sharp contrast, ethanol supplementation is a recurring strategy to boost BC production across the literature [27, 62, 84]. Unlike glucose oxidation, ethanol oxidation produces acetic acid, which is further metabolized in the tricarboxylic acid cycle without a pH drop as drastic as in the former example [27, 62]. *In K. sucrofermentans* ATCC 700178, knocking out the gene encoding the PQQ-dependent alcohol dehydrogenase produces a strain that retains the ability to metabolize ethanol. However, BC production no longer benefits from ethanol supplementation. The mutant also differs from the parental strain in its non-diauxic growth in the presence of ethanol and extracellular accumulation of only insignificant amounts of acetic acid [62].

Addressing the occurrence of non-producing (Cel-) mutants, often caused by insertion sequences disrupting the *bcsA* gene, is also key for maintaining high BC productivity. Genetic modifications to stabilize the *bcs* operon have reduced IS element insertion events, increasing BC yield by 1.7-fold [85]. Additionally, the spontaneous conversion of *Cel+* to *Cel-* phenotypes, frequently observed in cellulose-producing species, has been linked to stress factors like increased oxygen concentration, agitation speed and temperature [86, 87]. Furthermore, transcriptomic analysis has demonstrated that ethanol supplementation downregulates genes encoding transposases of the IS110 family, contributing to greater genomic stability in *K. xylinus* E25 [27]. Both genetic and supplementation approaches result in higher BC production and are useful to increase the process' reliability due to increased genetic stability [85].

Systems biology and multi-omics have an important role in guiding metabolic engineering strategies. For example, the genome-scale metabolic model (GEM) KxyMBEL1810, for *K. xylinus* DSM 2325 has identified key overexpression targets, including *pgi* (glucose-6-phosphate isomerase) and *gnd* (phospho-gluconate dehydrogenase) [88]. These enzymes, selected based on random sampling and correlation analysis, play crucial roles in glycolysis and the pentose phosphate pathway, respectively. Overexpression of either *pgi* or *gnd* genes resulted in improved BC production, with the former leading to a 115.8%

increase [88].

In another study, another GEM of *K. xylinus* DSM 2325 was reconstructed through genome sequencing and analysis, identifying the introduction of the *pfkA* gene, under control of the tac promoter, as a critical factor for improving BC yield since it restores the Embden-Meyerhof-Parnas pathway, which is commonly absent in bacteria within the genus [75]. Simulated flux balance analysis revealed that expressing *pfkA* not only increased ATP flux but also enhanced other central metabolic fluxes. Further improvement was achieved by incorporating the catabolite repressor protein (CRP) regulator, which was expected to modulate the expression of carbon metabolism-related genes and coincided with a reduction in gluconic acid accumulation [75]. To further optimize production, computational fluid dynamics (CFD) was employed to refine fermentation parameters, including impeller configuration, pH and oxygen levels — adjustments that also correlated with an increase in BC yield. Consequently, BC yield improved from 9.5% to 28.4% in the resulting S.Koma-pfkA/crp strain, reaching up to 31.5% under optimized fermentation conditions (g BC per g glucose). These findings underscore the potential of rational metabolic engineering, coupled with fermentation optimization, to significantly enhance BC production for industrial applications [75].

Genetic engineering has significantly improved BC yield by optimizing metabolic pathways, substrate utilization and fermentation conditions. Future advances in synthetic biology and multi-omics may help further refining these strategies, or discovering novel ones, potentially enabling scalable and sustainable BC production.

1.4.3 Key genetic approaches to modulate and functionalize BC

Traditional *ex-situ* methods for functionalizing BC involve dissolving or disintegrating its matrix to blend it with functional molecules, or additives, such as polymers, nanoparticles, or enzymes. While this approach allows precise control over the material's composition, it disrupts BC's nanostructure, reducing its mechanical integrity and biocompatibility. A less invasive modification route consists in immersing the BC pelicles in solutions containing additives, but this route typically results in less uniform materials. These limitations were major drivers toward *in-situ* and *in-vivo* strategies that homogeneously incorporate additives during BC biosynthesis to preserve its structural properties [14, 89]. *In-situ* approaches involve adding functional molecules directly to the culture medium during BC production, thus allowing bacteria to incorporate the molecules into the cellulose matrix as it forms, minimizing disruptions to the nanostructure. However, this method is often limited by the high cost of purified additives, which may be lost, to some extent, during the BC washing/purification. A more recent advancement, *in-vivo* biomanufacturing, leverages genetically engineered co-culture systems. For example, certain *Komagataeibacter* species have been co-cultured with engineered *E. coli* to produce composites with enhanced molecular sequestration and probiotic functionality [65, 90]. These systems can potentially reduce costs and allow greater control over composite properties, by adjusting parameters such as inoculation ratios and carbon source feed rates. The production of composites can be achieved also by genetically modifying the BC-producing

strains.

1.4.3.1 Modulation and functionalization of BC by engineering BC producers

An interesting case of mechanic properties' modulation through genetic engineering consisted in the overexpression of *motA* and *motB* in *N. hansenii* ATCC 23769, which resulted in elongated cells with increased motility and productivity [74, 91]. The resulting structure, with thicker fibers and larger pores, suggests that ribbon formation is affected by cell elongation, possibly due to life cycle-related fibre rearrangement. Additionally, the upregulation of genes related to stress response, translation, and biofilm formation was also observed, which further supports the role of *motA* and *motB* in regulating both cellular functions and BC architecture [74, 91].

To improve biodegradation, an engineered strain of *K. xylinus* ATCC 10245 was modified to incorporate N-acetylglucosamine (GlcNAc) residues into its BC matrix, creating a BC-chitin composite. This was achieved by introducing and expressing a synthetic operon from *C. albicans* containing the *AGM1*, *UAP1* and *NAG5* genes, which drive the biosynthesis of UDP-GlcNAc. The BCS complex was able to efficiently utilize this activated sugar precursor during cellulose synthesis, leading to the formation of a hybrid polymer with a disrupted crystalline structure. The modified BC exhibited improved susceptibility to enzymatic degradation by lysozyme and cellulase, facilitating potential applications in the biomedical fields [72]. Another example is a BC/Curdlan nanocomposite produced by a genetically modified *N. hansenii* ATCC 23769 strain able to co-synthesize these two biopolymers in vivo, due to the heterologous expression of the crdS gene from *Agrobacterium sp.* ATCC 31749, responsible for curdlan biosynthesis. The engineered strain simultaneously produced cellulose nanofibers and β-1,3-glucan without additional secretion machinery, producing a less water-permeable composite with altered surface morphology that preserves the integrity of the BC matrix [73]. Another good example is the fabrication of nanocomposite materials through the simultaneous production of BC and hyaluronan (HA) in a genetically engineered *N. hansenii* ATCC 23769 strain. The approach required the introduction of key genes, including *PmHAS* from *Pasteurella multocida* and UDP-glucose dehydrogenase from *Sinorhizobium meliloti*, which are essential for HA biosynthesis. Fluorescence microscopy analysis suggested that HA is co-secreted with BC through the bacterium's native cellulose secretion machinery, aligning with the previous findings where *N. hansenii* ATCC 23769 was engineered to produce curdlan-based nanocomposites, reinforcing the hypothesis that its transmembrane channels facilitate the secretion of heterologous polysaccharides. Notably, the HA/BC nanocomposites exhibited enhanced structural and biofunctional properties compared to conventional *in situ* nanocomposites, demonstrating improved surface morphology, stability, and adhesion between HA and BC. These advancements highlight the potential of *N. hansenii* ATCC 23769 as a versatile microbial platform for the biosynthesis of innovative biomaterials with applications in biomedicine [92].

The production of dyed BC by synthetic biology was elegantly presented by Walker *et al.*. This approach potentially represents an alternative to conventional dyeing processes, which often rely on chemical-intensive methods, by engineering a BC producer to produce self-pigmented materials [93]. The authors

modified the *K. rhaeticus* iGEM strain to synthesize eumelanin through the expression of an heterologous tyrosinase. Due to the stability and low solubility in water of the black pigment, the resulting BC membranes retained their coloration after autoclaving, posing as a demonstration of the pigmentation robustness. Additionally, the researchers were able to scale-up the production process in order to prototype fashion products such as wallets and shoe uppers. Given the stability of eumelanin and its additional properties, including UV protection and heat resistance, melanated BC holds potential as a sustainable textile material [93]. The current method involves a two-step process requiring a development buffer, awaiting future optimizations that could streamline pigment synthesis under the naturally acidic conditions of *K. rhaeticus* iGEM, reducing water consumption and enhancing sustainability. Further exploration of acid-tolerant tyrosinases and alternative melanin biosynthesis pathways could improve efficiency and facilitate industrial-scale implementation [93]. The researchers further explored spatial control over pigment deposition by implementing a blue-light sensitive T7 RNA polymerase system, which enabled patterned gene expression on the cellulose pellicle [93, 94]. Although the patterning approach faced challenges such as elevated background pigmentation, this work lays the foundation for creating advanced BC-based biofabricated textiles with customizable designs.

Even though this chapter enumerates several toolkits and strategies to engineer BC-producing bacteria, other microorganisms can be easier and more flexible to genetically engineer or be better chassis for the desired phenotype. For that reason, sometimes it is easier to co-culture BC producers with microorganisms that have more tools available and/or are more amenable to genetic modification. For instance, *Komagataeibacter spp.* are not as proficient as yeast at secreting recombinant proteins. A co-culture of *K. rhaeticus* iGEM with *S. cerevisiae* yCelMix, an engineered yeast strain that secretes a cellulose-degrading enzyme cocktail, has been used as a strategy for modulation of the mechanical and viscoelastic properties of BC [29]. Additionally, a co-culture strategy has also been used for the *in-situ* production of HA/BC nanocomposites, like in the previously mentioned example. However, instead of using a recombinant *N. hansenii* strain, the wild strain was co-cultured with a *Lactococcus lactis* strain that was engineered for HA production. The authors also demonstrated that the HA yield was dependent on the pH of the culture, enabling the use of pH as a modulating parameter for the final physical properties of the material [95].

1.4.3.2 Engineered Living Materials

ELMs are another interesting and potentially disruptive strategy for the creation of BC-based smart products. Such ELMs can consist of organisms from one or multiple species, with the first major proof of concept dating to 2014 [96]. In 2019, Walker *et al.* developed a self-patterning ELM by adapting a Lux quorum sensing system from the Registry of Standard Biological parts for use in *K. rhaeticus* iGEM. The ELM was composed by two *K. rhaeticus* iGEM-derived strains – "sender" and "receiver" – were the "sender" strain produced AHL through the constitutive expression of an AHL synthase, and the "receiver" strain produced red fluorescence in response [81]. A follow up paper reported the production of "sender" and "receiver" BC spheroids, which serve as modular building blocks for constructing three-dimensional structures and patterned ELMs. These spheroids can be genetically functionalized to serve as dynamic

biosensors, producing visible or hidden signals in response to environmental stimuli. Potential applications include smart wound dressings that monitor tissue repair or sweat-analyzing patches, capable of detecting biomarkers related to various physiological conditions. Furthermore, BC spheroids exhibited potential for material regeneration by fusing damaged BC components or assembling separate cellulose and synthetic sections into cohesive structures [97].

As previously mentioned, non-model organisms, such as BC producers, often lack the essential tools needed to expand the potential applications of their capabilities. In such cases, it might be useful to use BC producers, exclusively or not, as responsible for matrix production, while an engineered strain of a model organism brings functionality to the living material [29, 65, 98]. As a proof of concept, an isopropyl β-D-1-thiogalactopyranoside (IPTG)-responsive BC membrane was developed by co-culturing *K. xylinus* ATCC 10245 with engineered *E. coli* strains. In this case, two *E. coli* strains were individually expressing the green and red fluorescent proteins (GFP and RFP, respectively) upon induction [96]. Furthermore, a modular positive-feedback genetic amplifier was designed to enhance reporter gene signals, improving the detection sensitivity of transcriptional responses. This system, based on the LuxR system from *Vibrio fischeri*, enables amplified green fluorescent protein (GFP) expression upon IPTG induction in *E. coli* BL21 star (DE3). When *E. coli* is incorporated in BC membranes, the genetic amplifier significantly increased fluorescence output, even at low bacterial loads, demonstrating its potential for enhancing biosensing applications [96].

Although the previous example was successful, BC's permeability allows microorganisms to escape. Moreover, the simplest biosensor implementations do not allow the distinction between the absence of the target analyte and cell death [99, 100]. To tackle this, *K. xylinus* and *E. coli* cells were "trapped" in the BC scaffold by addition of reconstituted silk fibroin (SF) to the membrane. Additionally, a biosensor module including the FimS promoter, flanked by inverted repeats, two fluorescent proteins (GFPa1 and mKate2), and a riboswitch-controlled FimE recombinase was developed [101]. *E. coli* constitutively expresses GFPa1 unless theophylline is present. When theophylline binds, the riboswitch activates FimE expression, resulting in the inversion of the FimS promoter, switching off GFPa1 expression, and activating mKate2. These results demonstrate the potential of BC-SF composite scaffolds for stabilizing recombinant *E. coli* in biotechnological applications. The improved metabolic activity and stress resistance enhance biosensor performance. Further optimization could tailor scaffold properties for specific uses in biosensing and biomedicine [99].

Still using *E. coli* to provide functionality to the BC-based ELMs, there is another example of an innovation but, this time, at the materials' geometry. Instead of conventional pellicles, hollow spherical BC capsules were designed to create topologically distinct regions, where *N. hansenii* ATCC 53582 forms a dense cellulose outer shell, while engineered *E. coli* occupies the inner core, enabling programmable genetic functionalities [65]. These capsules were produced by incubating droplets of fresh media containing *N. hansenii* on top of superhydrophobic polytetrafluoroethylene (PTFE) powder, allowing for spatial separation of bacterial populations. Capsules expressing curli-tethered nanobodies efficiently captured green fluorescent protein (GFP) from solution, demonstrating high specificity [65]. Additionally, capsules

engineered to display α-amylase exhibited significant enzymatic activity, breaking down starch-based substrates [65]. Another ELM was engineered for biomineralization, where *E. coli* HB101, transformed with pBR322-Ure, catalyzed urea hydrolysis, leading to carbonate ion formation and $CaCO_3$ precipitation within the cellulose matrix. When incubated in urea and $CaCl_2$-supplemented media, these capsules showed rapid mineralization, as indicated by a decrease in soluble calcium levels, increased mechanical stiffness, and a visible transformation into yellowish, pebble-like structures. X-ray powder diffraction (XRPD) analysis confirmed the presence of calcite and vaterite, suggesting that the BC network influences the mineralization process, making the material structurally adaptive and self-modifying [65].

The synthetic symbiotic culture of bacteria and yeast (Syn-SCOBY) approach, demonstrates the possibility of a modular co-culture system that integrates engineered *S. cerevisiae* into BC-based ELMs, enabling them to sense and respond to environmental stimuli [29]. Yeast biosensors were developed to detect β-oestradiol (BED) and express GFP as a reporter, maintaining functionality even after drying and long-term storage. Additionally, a yeast strain secreting laccase under a BED-inducible promoter enabled the biodegradation of BED, showcasing the potential for dynamic, responsive biomaterials [29]. Beyond chemical sensing, optogenetics was used to create light-responsive BC materials by co-culturing *K. rhaeticus* iGEM with *S. cerevisiae* engineered to express NanoLuc luciferase under a blue-light-inducible promoter. Light patterning techniques, such as masking and projection, allowed for precise spatial control over bioluminescence, with sharper patterns in yeast displaying surface-anchored NanoLuc compared to those secreting a cellulose-binding version [29]. This spatial programming of protein functionalization in BC materials highlights the potential for multicolor optogenetic systems, enabling spatially controlled enzymatic cascades for advanced biosensing and biocatalysis applications [29].

The future of BC functionalization lies in advancing synthetic biology and co-culture techniques to expand the repertoire of functional molecules integrated into the matrix. As researchers develop more efficient protein secretion mechanisms in BC-producing bacteria and refine metabolic engineering strategies, the potential for creating tailored BC composites with multifunctional properties will continue to grow. This progress will open new avenues for applications in medicine, environmental remediation, and next-generation smart materials.

1.5 Conclusions

While BC has been gaining attractiveness due to its outstanding characteristics, BC production methods are facing significant challenges with by-product formation, metabolic competition and the high precursor demands for cellulose biosynthesis, to name a few [1, 5, 22, 23]. Synthetic biology holds the potential to be a disruptive approach to overcoming these limitations, not only enabling the creation of more productive strains, but also the modulation of the material's properties and functionalization, expanding its application in several industries [14, 15, 19–21, 39, 40].

The development of synthetic biology tools has enabled a plethora of strategies that aim at fine tuning metabolic pathways, optimizing substrate utilization and regulating gene expression with high precision [13,

38, 61, 77]. In example, CRISPRi has been used to modulate the activity of key metabolic steps allowing the fine tuning of BC's porosity and crystallinity [28, 67]. Moreover, improving UDP-glucose biosynthesis through the overexpression of genes such as *pfkA*, *gnd*, and *pgi* resulted increased cellulose yields [75]. Additionally, the implementation of quorum-sensing mechanisms and synthetic gene circuits has further enabled autonomous control over BC biosynthesis, allowing for the spatial and temporal patterning of cellulose production [81, 97].

Genetic engineering has enabled the fine tuning of mechanical properties of BC, and also the direct incorporation of functional molecules into the BC matrix [65, 73, 92, 99]. A notable example is the introduction of motility genes which resulted in modified cellulose fiber morphology and increased porosity [74, 91]. Similarly, engineered BC composites obtained by *in situ* co-production of hyaluronan or curdlan into the cellulose matrix excel in its biodegradability, biofunctionality, and mechanical performance [72, 92]. The potential of BC is expanding to an increasing number of industries (e.g. electronics, regenerative medicine, sustainable biofabrication) due to the continuous innovations in BC functionalization research [2–4, 9, 22].

Co-culture systems are among the most significant advances in BC research since it opens the possibility to use more tractable organisms for in situ functionalization [14, 15, 21, 29, 99]. Due to the availability of well-established synthetic biology toolkits, *Escherichia coli* and *Saccharomyces cerevisiae* have been used in co-culture strategies for BC functionalization [14, 29, 99]. The co-culture strategies enabled the creation of BC-based living materials with enzyme activity, biosensing capabilities and self-patterning properties, thus demonstrating the feasibility of using BC as a platform for smart and interactive materials [14, 15, 21, 29, 99].

The future of BC research lies at the intersection of synthetic biology, systems biology, and bioprocess engineering [10, 12, 15, 21, 38]. By integrating multi-omics approaches (e.g. genomics, transcriptomics, metabolomics) the community might obtain deeper insights into the regulatory mechanisms over BC biosynthesis, which can potentially translate into more precise metabolic engineering strategies [38]. Computational modelling and genome-scale metabolic network reconstruction methodologies are being continuously developed aiming at facilitating the rational design of microbial BC factories through the predictive optimization of metabolic pathways. Moreover, advances in automation (e.g. high-throughput screening) can accelerate the development of superior strains [13, 38].

Looking ahead, we speculate that synthetic biology is set to play an even greater role in the advancement of BC-based materials. The potential applications of engineered BC should continue to expand in diverse fields (e.g. tissue engineering, sustainable packaging, biophotonic devices) as research continuously innovates genetic and bioprocessing strategies. The ability to program self-assembled multifunctional microbial communities is closer to become a reality in the industry, thus strengthening the role of BC-based materials as a paradigm shift in biofabrication due to their potential to outperform their synthetic counterparts [10, 12, 14, 15, 19, 21, 39, 40].

In conclusion, BC is gradually becoming a bioengineering platform for the materials of the future. The success depends on an interdisciplinary effort to integrate methodologies from synthetic biology,

metabolic engineering, and materials science, with potential to set a new era in biofabrication where living systems can be leveraged to create sustainable, responsive, high-performance materials tailored to meet the evolving demands of modern industries [10, 15, 21].

1.6 Objectives

The overarching aim of this thesis was to develop and evaluate synthetic biology and metabolic engineering strategies to increase bacterial cellulose (BC) production in the non-model acetic acid bacterium *Komagataeibacter sucrofermentans* ATCC 700178. Rather than targeting immediate economic viability, the work sought to identify the metabolic and genetic determinants of BC yield and to assess the applicability of the available genetic toolkit in this host, providing a foundation for future strain optimisation.

The specific objectives were:

- to identify and relieve the metabolic bottlenecks limiting BC production, by knocking out the four PQQ-dependent membrane dehydrogenases and evaluating ethanol supplementation as a complementary strategy (Chapter II);
- to engineer cytoplasmic glucose uptake through heterologous transporter–glucokinase modules, complementing membrane glucose dehydrogenase deletion to further redirect carbon flux towards BC synthesis (Chapter III);
- to critically assess the design considerations and constraints for implementing CRISPR–Cas9 genome editing in *K. sucrofermentans*, informing future genome-engineering efforts in this non-model strain (Chapter IV).

1.7 References

[1] Zhongjuan Wang et al. “Applications of bacterial cellulose in the food industry and its health-promoting potential”. In: *Food Chemistry* 464 (2025), p. 141763.

[2] Zi-Jian Zheng, Huan Ye, and Zai-Ping Guo. “Bacterial Cellulose Applications in Electrochemical Energy Storage Devices”. In: *Advanced Materials* n/a.n/a (2024), p. 2412908.

[3] Chunyan Zhong. “Industrial-Scale Production and Applications of Bacterial Cellulose”. In: *Frontiers in Bioengineering and Biotechnology* 8 (2020).

[4] Dian Andriani, Arina Yuthi Apriyana, and Myrtha Karina. “The optimization of bacterial cellulose production and its applications: a review”. In: *Cellulose* 27.12 (2020), pp. 6747–6766.

[5] Snehasish Mishra et al. “Biochemistry, Synthesis, and Applications of Bacterial Cellulose: A Review”. In: *Frontiers in Bioengineering and Biotechnology* 10 (2022).

[6] SP Gautam et al. “A review on systematic study of cellulose”. In: *INDIA Journal of Applied and Natural Science* 2.2 (2010), pp. 330–343.

[7] Sherif M.A.S. Keshk. “Vitamin C enhances bacterial cellulose production in Gluconacetobacter xylinus”. In: *Carbohydrate Polymers* 99 (2014), pp. 98–100.

[8] Matej Skočaj. “Bacterial nanocellulose in papermaking”. In: *Cellulose* 26.11 (2019), pp. 6477–6488.

[9] Soon Mo Choi and Eun Joo Shin. “The nanofication and functionalization of bacterial cellulose and its applications”. In: *Nanomaterials* 10.3 (2020).

[10] Vid Potočnik, Selestina Gorgieva, and Janja Trček. “From Nature to Lab: Sustainable Bacterial Cellulose Production and Modification with Synthetic Biology”. In: *Polymers* 15.16 (2023), p. 3466.

[11] Nasrullah Shah et al. “Overview of bacterial cellulose composites: A multipurpose advanced material”. In: *Carbohydrate Polymers* 98.2 (2013), pp. 1585–1598.

[12] Sundaravadanam Vishnu Vadanan, Anindya Basu, and Sierin Lim. “Bacterial cellulose production, functionalization, and development of hybrid materials using synthetic biology”. In: *Polymer Journal* 54.4 (2022), pp. 481–492.

[13] Gizem Buldum and Athanasios Mantalaris. “Systematic understanding of recent developments in bacterial cellulose biosynthesis at genetic, bioprocess and product levels”. In: *International Journal of Molecular Sciences* 22.13 (2021).

[14] Kai Jin, Chenyang Jin, and Yihan Wu. “Synthetic biology-powered microbial co-culture strategy and application of bacterial cellulose-based composite materials”. In: *Carbohydrate Polymers* 283 (2022).

[15] Koray Malcı et al. “Modulating Microbial Materials - Engineering Bacterial Cellulose with Synthetic Biology”. In: *ACS Synthetic Biology* (2024).

[16] Taisa Regina Stumpf et al. “In situ and ex situ modifications of bacterial cellulose for applications in tissue engineering”. In: *Materials Science and Engineering: C* 82 (2018), pp. 372–383.

[17] Marzena Jedrzejczak-Krzepkowska et al. “Chapter 2 - Bacterial NanoCellulose Synthesis, Recent Findings”. In: *Bacterial Nanocellulose*. Elsevier, 2016, pp. 19–46.

[18] Ana Cristina Rodrigues et al. “Response surface statistical optimization of bacterial nanocellulose fermentation in static culture using a low-cost medium”. In: *New Biotechnology* 49 (2019), pp. 19–27.

[19] Ahmad S. Khalil and James J. Collins. “Synthetic biology: Applications come of age”. In: *Nature Reviews Genetics* 11.5 (2010), pp. 367–379.

[20] Ernesto Andrianantoandro et al. “Synthetic biology: New engineering rules for an emerging discipline”. In: *Molecular Systems Biology* 2 (2006).

[21] Amritpal Singh et al. “Engineering Bacterial Cellulose by Synthetic Biology”. In: *International Journal of Molecular Sciences* 21.23 (2020), p. 9185.

[22] Maximiliano L. Cacicedo et al. “Progress in bacterial cellulose matrices for biotechnological applications”. In: *Bioresource Technology* 213 (2016), pp. 172–180.

[23] Hamada El-Gendi et al. “Recent advances in bacterial cellulose: a low-cost effective production media, optimization strategies and applications”. In: *Cellulose* 29.14 (2022), pp. 7495–7533.

[24] Angela Faustino Jozala et al. “Bacterial nanocellulose production and application: a 10-year overview”. In: *Applied Microbiology and Biotechnology* 100.5 (2016), pp. 2063–2072.

[25] Poulami Mukherjee et al. “Bacterial cellulose production, scale-up, and applications: a techno-economic study of industry-ready bacterial cellulose production from industrial and agro wastes”. In: *Cellulose* 33 (2025), pp. 541–570.

[26] Emergen Research. *Bacterial Cellulose Market Size, Share, Industry Trends and Forecast*. Emergen Research. 2024. (Visited on 06/29/2026).

[27] Małgorzata Ryngajłło et al. “Effect of ethanol supplementation on the transcriptional landscape of bionanocellulose producer Komagataeibacter xylinus E25”. In: *Applied Microbiology and Biotechnology* 103.16 (2019), pp. 6673–6688.

[28] Min Yan Teh et al. “An Expanded Synthetic Biology Toolkit for Gene Expression Control in Acetobacteraceae”. In: *ACS Synthetic Biology* 8.4 (2019), pp. 708–723.

[29] Charlie Gilbert et al. “Living materials with programmable functionalities grown from engineered microbial co-cultures”. In: *Nature Materials* 20.5 (2021), pp. 691–700.

[30] Iain D. Hay et al. “Microbial alginate production, modification and its applications”. In: *Microbial Biotechnology* 6.6 (2013), pp. 637–650.

[31] Julio Báez, David Olsen, and James W. Polarek. “Recombinant microbial systems for the production of human collagen and gelatin”. In: *Applied Microbiology and Biotechnology* 69.3 (2005), pp. 245–252.

[32] Rita C. Campebell et al. “Evaluation of Bacterial Cellulose/Alginate-Based Hydrogel and Frog Skin Dressings in Equine Skin Wound Healing”. In: *Gels* 11.2 (2025), p. 107.

[33] Yong Kwan Noh et al. “Fabrication of bacterial cellulose-collagen composite scaffolds and their osteogenic effect on human mesenchymal stem cells”. In: *Carbohydrate Polymers* 219 (2019), pp. 210–218.

[34] Suman Bose et al. “A retrievable implant for the long-term encapsulation and survival of therapeutic xenogeneic cells”. In: *Nature Biomedical Engineering* 4.8 (2020), pp. 814–826.

[35] Chelsea M. Heveran et al. “Engineered Ureolytic Microorganisms Can Tailor the Morphology and Nanomechanical Properties of Microbial-Precipitated Calcium Carbonate”. In: *Scientific Reports* 9.1 (2019).

[36] Yangxiaolu Cao et al. “Programmable assembly of pressure sensors using pattern-forming bacteria”. In: *Nature Biotechnology* 35.11 (2017), pp. 1087–1093.

[37] Ana M. Hernández-Arriaga et al. “When microbial biotechnology meets material engineering”. In: *Microbial Biotechnology* 15.1 (2022), pp. 149–163.

[38] Małgorzata Ryngajłło et al. “Towards control of cellulose biosynthesis by Komagataeibacter using systems-level and strain engineering strategies: current progress and perspectives”. In: *Applied Microbiology and Biotechnology* 104.15 (2020), pp. 6565–6585.

[39] Gregory Stephanopoulos. “Synthetic biology and metabolic engineering”. In: *ACS Synthetic Biology* 1.11 (2012), pp. 514–525.

[40] Jens Nielsen and Jay D Keasling. “Synergies between synthetic biology and metabolic engineering”. In: *Nature Biotechnology* 29.8 (2011), pp. 693–695.

[41] Jay D. Keasling. “Synthetic biology and the development of tools for metabolic engineering”. In: *Metabolic Engineering* 14.3 (2012), pp. 189–195.

[42] Ling-Pu Liu et al. “A Lambda Red and FLP/FRT-Mediated Site-Specific Recombination System in Komagataeibacter xylinus and Its Application to Enhance the Productivity of Bacterial Cellulose”. In: *ACS Synthetic Biology* 9.11 (2020), pp. 3171–3180.

[43] Vivianne J Goosens et al. “Komagataeibacter Tool Kit (KTK): A Modular Cloning System for Multigene Constructs and Programmed Protein Secretion from Cellulose Producing Bacteria”. In: *ACS Synthetic Biology* 10.12 (2021), pp. 3422–3434.

[44] Maria Gullo et al. “Biotechnological production of cellulose by acetic acid bacteria: current state and perspectives”. In: *Applied Microbiology and Biotechnology* 102.16 (2018), pp. 6885–6898.

[45] Hiroshi Toyosaki et al. “The characterization of an acetic acid bacterium useful for producing bacterial cellulose in agitation cultures: the proposal of Acetobacter xylinum subsp. sucrofermentans subsp. nov.” In: *The Journal of General and Applied Microbiology* 41.4 (1995), pp. 307–314.

[46] National Center for Biotechnology Information. *Komagataeibacter sucrofermentans DSM 15973 (ATCC 700178) genome assembly ASM4058140v1, GenBank accession GCF_040581405.1*. NCBI. 2024. (Visited on 06/29/2026).

[47] Guohui Li et al. “Research progress of the biosynthetic strains and pathways of bacterial cellulose”. In: *Journal of Industrial Microbiology and Biotechnology* 49.1 (2022).

[48] Svein Valla et al. “Cloning of a gene involved in cellulose biosynthesis in Acetobacter xylinum: Complementation of cellulose-negative mutants by the UDPG pyrophosphorylase structural gene”. In: *Molecular and General Genetics MGG* 217.1 (1989), pp. 26–30.

[49] Ute Römling and Michael Y. Galperin. “Bacterial cellulose biosynthesis: Diversity of operons, subunits, products, and functions”. In: *Trends in Microbiology* 23.9 (2015), pp. 545–557.

[50] Paulina Jacek et al. “Molecular aspects of bacterial nanocellulose biosynthesis”. In: *Microbial Biotechnology* 12.4 (2019), pp. 633–649.

[51] Takaaki Fujiwara et al. “The c-di-GMP recognition mechanism of the PilZ domain of bacterial cellulose synthase subunit A”. In: *Biochemical and Biophysical Research Communications* 431.4 (2013), pp. 802–807.

[52] Ute Römling, Michael Y. Galperin, and Mark Gomelsky. “Cyclic di-GMP: the First 25 Years of a Universal Bacterial Second Messenger”. In: *Microbiology and Molecular Biology Reviews* 77.1 (2013), pp. 1–52.

[53] Ute Römling. “Cyclic di-GMP, an established secondary messenger still speeding up”. In: *Environmental Microbiology* 14.8 (2012), pp. 1817–1829.

[54] Song-Qing Hu et al. “Structure of bacterial cellulose synthase subunit D octamer with four inner passageways”. In: *Proceedings of the National Academy of Sciences of the United States of America* 107.42 (2010), pp. 17957–17961.

[55] Alan L Chang et al. “Phosphodiesterase A1, a Regulator of Cellulose Synthesis in Acetobacter xylinum, Is a Heme-Based Sensor”. In: *Biochemistry* 40.12 (2001), pp. 3420–3426.

[56] Ute Römling. *Molecular biology of cellulose production in bacteria*. Tech. rep. 2002.

[57] Raquel Portela et al. “Bacterial cellulose: a versatile biopolymer for wound dressing applications”. In: *Microbial Biotechnology* 12.4 (2019), pp. 586–610.

[58] M. Iguchi, S. Yamanaka, and A. Budhiono. “Bacterial cellulose—a masterpiece of nature’s arts”. In: *Journal of Materials Science* 35.2 (2000), pp. 261–270.

[59] Chia Hung Kuo, Hsin Yin Teng, and Cheng Kang Lee. “Knock-out of glucose dehydrogenase gene in Gluconacetobacter xylinus for bacterial cellulose production enhancement”. In: *Biotechnology and Bioprocess Engineering* 20.1 (2015), pp. 18–25.

[60] Toru Shigematsu et al. “Cellulose production from glucose using a glucose dehydrogenase gene (gdh)-deficient mutant of gluconacetobacter xylinus and its use for bioconversion of sweet potato pulp”. In: *Journal of Bioscience and Bioengineering* 99.4 (2005), pp. 415–422.

[61] Zhaojun Peng et al. “Engineering PTS-based glucose metabolism for efficient biosynthesis of bacterial cellulose by Komagataeibacter xylinus”. In: *Carbohydrate Polymers* 343 (2024).

[62] Pedro Montenegro-Silva et al. “Enhanced bacterial cellulose production in Komagataeibacter sucrofermentans: impact of different PQQ-dependent dehydrogenase knockouts and ethanol supplementation”. In: *Biotechnology for Biofuels and Bioproducts* 17.1 (2024).

[63] Annette M Griffin, Victor J Morris, and Michael J Gasson. “Genetic analysis of the acetan biosynthetic pathway in Acetobacter xylinum: nucleotide sequence analysis of the aceB aceC aceD and aceE genes”. In: *DNA Sequence* 6.5 (1996), pp. 275–284.

[64] Takehiko Ishida et al. *EŠects of Acetan on Production of Bacterial Cellulose by Acetobacter xylinum*. Tech. rep. 8. 2002.

[65] Daniel P. Birnbaum et al. “Hybrid Living Capsules Autonomously Produced by Engineered Bacteria”. In: *Advanced Science* 8.11 (2021).

[66] Charlie Gilbert and Tom Ellis. “Biological Engineered Living Materials: Growing Functional Materials with Genetically Programmable Properties”. In: *ACS Synthetic Biology* 8.1 (2019), pp. 1–15.

[67] Long-Hui Huang et al. “Tailoring bacterial cellulose structure through CRISPR interference-mediated downregulation of galU in Komagataeibacter xylinus CGMCC 2955”. In: *Biotechnology and Bioengineering* 117.7 (2020), pp. 2165–2176.

[68] Michael Florea et al. “Engineering control of bacterial cellulose production using a genetic toolkit and a new celluloseproducing strain”. In: *Proceedings of the National Academy of Sciences of the United States of America* 113.24 (2016), E3431–E3440.

[69] Naoto Tonouchi et al. “A Host–Vector System for a Cellulose-Producing Acetobacter Strain”. In: *Bioscience, Biotechnology, and Biochemistry* 58.10 (1994), pp. 1899–1901.

[70] Tomonori Nakai et al. *Enhancement of cellulose production by expression of sucrose synthase in Acetobacter xylinum (cellulose synthesissucrose metabolism)*. Tech. rep. 1999.

[71] Magdiel Inggrid Setyawati, Liang Jung Chien, and Cheng Kang Lee. “Expressing Vitreoscilla hemoglobin in statically cultured Acetobacter xylinum with reduced O2 tension maximizes bacterial cellulose pellicle production”. In: *Journal of Biotechnology* 132.1 (2007), pp. 38–43.

[72] Vikas Yadav et al. “Novel in vivo-degradable cellulose-chitin copolymer from metabolically engineered gluconacetobacter xylinus”. In: *Applied and Environmental Microbiology* 76.18 (2010), pp. 6257–6265.

[73] Ju Fang et al. “In Vivo Curdlan/Cellulose Bionanocomposite Synthesis by Genetically Modified Gluconacetobacter xylinus”. In: *Biomacromolecules* 16.10 (2015), pp. 3154–3160.

[74] Paulina Jacek et al. “Modification of bacterial nanocellulose properties through mutation of motility related genes in Komagataeibacter hansenii ATCC 53582”. In: *New Biotechnology* 52 (2019), pp. 60–68.

[75] Hyeokjo Gwon et al. “A safe and sustainable bacterial cellulose nanofiber separator for lithium rechargeable batteries”. In: *Proceedings of the National Academy of Sciences of the United States of America* 116.39 (2019), pp. 19288–19293.

[76] S. O. Bae et al. “Features of bacterial cellulose synthesis in a mutant generated by disruption of the diguanylate cyclase 1 gene of Acetobacter xylinum BPR 2001”. In: *Applied Microbiology and Biotechnology* 65.3 (2004), pp. 315–322.

[77] Dong Hoon Hur et al. “Enhanced production of bacterial cellulose in komagataeibacter xylinus via tuning of biosynthesis genes with synthetic RBS”. In: *Journal of Microbiology and Biotechnology* 30.9 (2020), pp. 1430–1435.

[78] Gibyuck Byun, Jina Yang, and Sang Woo Seo. “CRISPRi-mediated tunable control of gene expression level with engineered single-guide RNA in Escherichia coli”. In: *Nucleic Acids Research* 51.9 (2023), pp. 4650–4659.

[79] Jason M Peters et al. “A Comprehensive, CRISPR-based Functional Analysis of Essential Genes in Bacteria”. In: *Cell* 165.6 (2016), pp. 1493–1506.

[80] Luke A. Gilbert et al. “CRISPR-Mediated Modular RNA-Guided Regulation of Transcription in Eukaryotes”. In: *Cell* 154.2 (2013), pp. 442–451.

[81] Kenneth T. Walker et al. “Engineered cell-to-cell signalling within growing bacterial cellulose pellicles”. In: *Microbial Biotechnology* 12.4 (2019), pp. 611–619.

[82] Fan Yang et al. “A recombinant strain of Komagataeibacter xylinus ATCC 23770 for production of bacterial cellulose from mannose-rich resources”. In: *New Biotechnology* 76 (2023), pp. 72–81.

[83] Evelyn Battad-Bernardo et al. “Insertion of an E. coli lacZ gene in Acetobacter xylinus for the production of cellulose in whey”. In: *FEMS Microbiology Letters* 231.2 (2004), pp. 253–260.

[84] H. Kornmann et al. “Influence of residual ethanol concentration on the growth of Gluconacetobacter xylinus I 2281”. In: *Applied Microbiology and Biotechnology* 62.2-3 (2003), pp. 168–173.

[85] Dong Hoon Hur et al. “Enhanced production of cellulose in Komagataeibacter xylinus by preventing insertion of IS element into cellulose synthesis gene”. In: *Biochemical Engineering Journal* 156 (2020).

[86] Minenosuke Matsutani et al. “Adaptive mutation related to cellulose producibility in Komagataeibacter medellinensis (Gluconacetobacter xylinus) NBRC 3288”. In: *Applied Microbiology and Biotechnology* 99.17 (2015), pp. 7229–7240.

[87] Jae Yong Jung et al. “Production of bacterial cellulose by Gluconacetobacter hansenii using a novel bioreactor equipped with a spin filter”. In: *Korean Journal of Chemical Engineering* 24.2 (2007), pp. 265–271.

[88] Woo Dae Jang et al. “Genomic and metabolic analysis of Komagataeibacter xylinus DSM 2325 producing bacterial cellulose nanofiber”. In: *Biotechnology and Bioengineering* 116.12 (2019), pp. 3372–3381.

[89] Daniela F S Fonseca et al. “Bacterial nanocellulose-hyaluronic acid microneedle patches for skin applications: In vitro and in vivo evaluation”. In: *Materials Science and Engineering: C* 118 (2021), p. 111350.

[90] Ji-Yan Qiao et al. “Autonomously Assembled Living Capsules by Microbial Coculture for Enhanced Bacteriotherapy of Inflammatory Bowel Disease”. In: *Nano Letters* 23.10 (2023), pp. 4375–4383.

[91] Paulina Jacek, Małgorzata Ryngajłło, and Stanisław Bielecki. “Structural changes of bacterial nanocellulose pellicles induced by genetic modification of Komagataeibacter hansenii ATCC 23769”. In: *Applied Microbiology and Biotechnology* 103.13 (2019), pp. 5339–5353.

[92] Ryo Takahama et al. “Biofabrication of a Hyaluronan/Bacterial Cellulose Composite Nanofibril by Secretion from Engineered Gluconacetobacter”. In: *Biomacromolecules* 22.11 (2021), pp. 4709–4719.

[93] Kenneth T. Walker et al. “Self-pigmenting textiles grown from cellulose-producing bacteria with engineered tyrosinase expression”. In: *Nature Biotechnology* (2024).

[94] Armin Baumschlager, Stephanie K Aoki, and Mustafa Khammash. “Dynamic Blue Light-Inducible T7 RNA Polymerases (Opto-T7RNAPs) for Precise Spatiotemporal Gene Expression Control”. In: *ACS Synthetic Biology* 6.11 (2017), pp. 2157–2167.

[95] Ke Liu and Jeffrey M. Catchmark. “Bacterial cellulose/hyaluronic acid nanocomposites production through co-culturing Gluconacetobacter hansenii and Lactococcus lactis under different initial pH values of fermentation media”. In: *Cellulose* 27.5 (2020), pp. 2529–2540.

[96] Guokui Qin, Bruce J. Panilaitis, and Zhongyuan Sun David L. Kaplan. “A cellulosic responsive ”living” membrane”. In: *Carbohydrate Polymers* 100 (2014), pp. 40–45.

[97] Joaquin Caro-Astorga et al. “Bacterial cellulose spheroids as building blocks for 3D and patterned living materials and for regeneration”. In: *Nature Communications* 12.1 (2021).

[98] Aleixandre Rodrigo-Navarro et al. “Engineered living biomaterials”. In: *Nature Reviews Materials* 6.12 (2021), pp. 1175–1190.

[99] Irina Drachuk et al. “Immobilization of Recombinant E. coli Cells in a Bacterial Cellulose-Silk Composite Matrix to Preserve Biological Function”. In: *ACS Biomaterials Science and Engineering* 3.10 (2017), pp. 2278–2292.

[100] Irina Drachuk et al. “Cell Surface Engineering with Edible Protein Nanoshells”. In: *Small* 9.18 (2013), pp. 3128–3137.

[101] Svetlana Harbaugh et al. “Riboswitch-Based Reversible Dual Color Sensor”. In: *ACS Synthetic Biology* 6.5 (2017), pp. 766–781.

2 Impact of Different PQQ-Dependent Dehydrogenase Knockouts and Ethanol Supplementation in BC production

2.1 Abstract

Bacterial cellulose (BC) is a biocompatible material with unique mechanical properties, thus holding a significant industrial potential. Despite many acetic acid bacteria (AAB) being BC overproducers, cost-effective production remains a challenge. The role of pyrroloquinoline quinone (PQQ)-dependent membrane dehydrogenases (mDH) is crucial in the metabolism of AAB since it links substrate incomplete oxidation in the periplasm to energy generation. Specifically, glucose oxidation to gluconic acid substantially lowers environmental pH and hinders BC production. Conversely, ethanol supplementation is known to enhance BC yields in *Komagataeibacter spp.* by promoting efficient glucose utilization. *K. sucrofermentans* ATCC 700178 was engineered, knocking out the four PQQ-mDHs, to assess their impact on BC production.

The strain KS003, lacking PQQ-dependent glucose dehydrogenase (PQQ-GDH), did not produce gluconic acid and exhibited a 5.77-fold increase in BC production with glucose as the sole carbon source, and a 2.26-fold increase under optimal ethanol supplementation conditions. In contrast, the strain KS004, deficient in the PQQ-dependent alcohol dehydrogenase (PQQ-ADH), showed no significant change in BC yield in the single carbon source experiment but showed a restrained benefit from ethanol supplementation.

The results underscore the critical influence of PQQ-GDH and PQQ-ADH and clarify the effect of ethanol supplementation on BC production in *K. sucrofermentans* ATCC 700178. This study provides a foundation for further metabolic pathway optimization, emphasizing the importance of diauxic ethanol metabolism for high BC production.

2.2 Introduction

Bacterial cellulose (BC) is a biomaterial with properties that allow its application in a diversity of industrial sectors such as medical biotechnology, food, textiles and electronics [1]. Acetic acid bacteria (AAB) are among the best BC producers, with *Komagataeibacter spp.* being the most remarkable within the group [2]. BC is a glucose-based polymer that grows by the sequential addition of uridine diphosphate glucose (UDP-glucose) monomers to the forming cellulosic fibril through the BC synthase complex. This is composed of 4 main sub-units - A, B, C and D: BcsA is a glycosyl transferase whose activity is controlled by

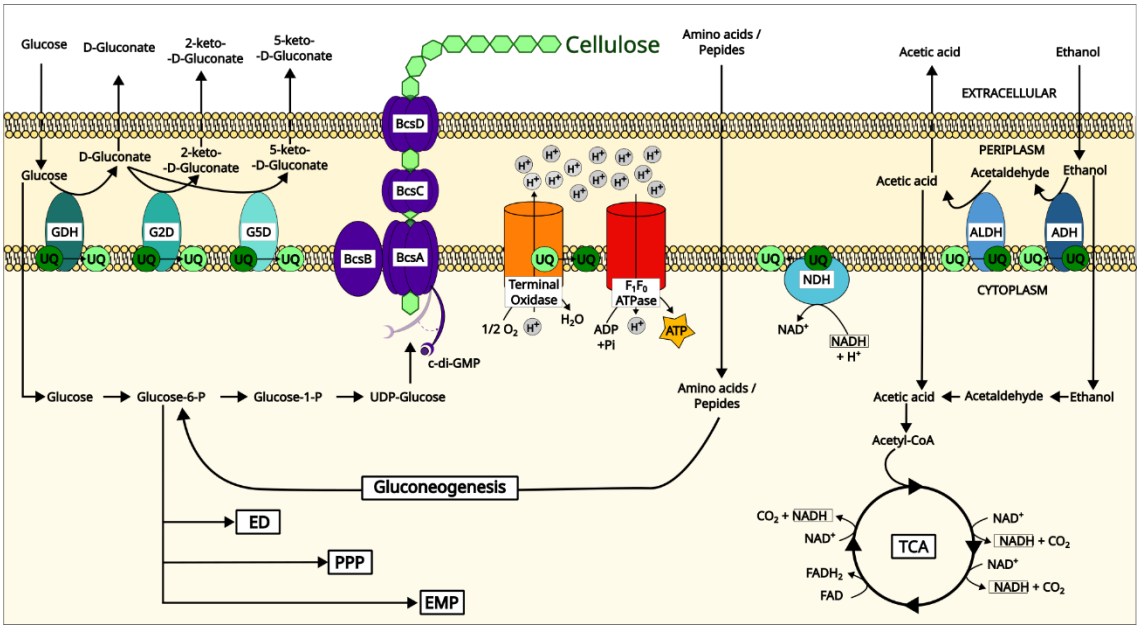


Figure II.1: Overview of the key metabolic steps and pathways involved in BC production and energy generation in the presence of glucose and ethanol. The periplasmic oxidation of the sugars, alcohols, and sugar alcohols is linked to the electron transport chain (ETC) – the dehydrogenases transfer the reducing equivalents to ubiquinone (UQ – dark green) converting it to its reduced form, ubiquinol (UQ – light green). UQ can be further re-oxidized by terminal oxidases in a process coupled with oxygen (O_2) reduction to water (H_20) and the generation of a proton (H^+) gradient. Then, F_1F_0 ATPase facilitates H^+ translocation, owing to the H^+ gradient, in a process coupled with adenosine triphosphate (ATP) generation.

the allosteric regulator cyclic diguanylate monophosphate (c-di-GMP); BcsB is responsible for membrane-anchoring, being also essential for the catalysis; while BcsC and BcsD are optional for BC biosynthesis, their presence is required for maximum productivity (**Figure II.1**) [3].

In the periplasm, glucose can be partially oxidised to D-gluconate, 2-keto-D-gluconate, and 5-D-ketogluconate by PQQ-dependent glucose dehydrogenase (GDH), flavin-dependent gluconate-2-dehydrogenase (G2D) and PQQ-dependent gluconate-5-dehydrogenase (G5D). Glucose can also be imported and used for cellulose biosynthesis or metabolized through the Entner-Doudoroff (ED), Embden-Meyerhof (EMP) or Pentose Phosphate Pathway (PPP). Ethanol can be oxidized to acetaldehyde and further to acetic acid in the periplasm by PQQ-dependent alcohol dehydrogenase (ADH) and further to acetaldehyde by flavin-dependent aldehyde dehydrogenase (ALDH). When ethanol, acetaldehyde, or acetate are assimilated by the cell, the metabolites are converted to acetyl-CoA for biomass generation, or complete oxidation through the tricarboxylic acid cycle (TCA). This is also coupled with ATP generation at different points. Additionally, NADH can also be oxidized to NAD^+ in the cytosolic membrane by NADH dehydrogenase (NADH), which is also linked to the ETC.

Efforts have been made over the years to identify conditions that allow for maximum BC productivity by *Komagataeibacter* strains, attempting to unlock the economic viability of many BC products. Such optimizations have been focused on media composition [4–8], cultural environmental conditions (pH

[9, 10], temperature [11, 12], and oxygen supply [9, 13–15]), operation mode (static/agitated cultures [4, 7, 16]) and bioreactor design [9, 13–15]. Additionally, some *Komagataeibacter* strains have been engineered with some degree of success at increasing productivity [17–23]. Despite several strategies that have demonstrated significant increases, the production process is not yet cost-effective for most applications, thus imposing an entry barrier to the markets [24].

While AAB can catabolize sugars and/or alcohols in the cytosol, the group typically prefers to perform incomplete oxidation of those substrates in the periplasm, releasing the products to the culture medium [25]. This process allows AAB to control the environmental pH while rapidly generating large amounts of energy, and converting ubiquitous carbon sources into ones that most organisms cannot consume [26]. The periplasmic oxidation is usually catalysed by co-factor-dependent membrane dehydrogenases (mDHs) that transfer the electrons from substrate oxidation to the ubiquinone (UQ) pool and further to the ETC [25]. *Komagataeibacter spp.* oxidize a significant fraction of the available glucose into gluconic acid through this pathway by the action of PQQ-dependent glucose dehydrogenase (PQQ-GDH), diverting a great amount of carbon away from cellulose production (**Figure II.1**) [22, 27, 28]. Additionally, the consequent pH decrease negatively affects BC production [9, 10]. Two different studies report noticeable increases in BC yields in *K. xylinus* BCRC12334 [18] and *K. xylinus* BPR2001 [22], through the knockout of the *gcd* gene, which codes for PQQ-GDH. Eliminating PQQ-GDH activity in *K. xylinus* BCRC12334 directly resulted in 40% and 230% increases in BC production in static and shaken cultures, respectively [18]. On the other hand, a similar strategy was employed to engineer *K. xylinus* BPR2001, but the mutant showed impaired glucose consumption and required a lower initial pH to produce comparable amounts of BC to the control strain. A mutant that overexpresses the *glf* gene from *Z. mobilis* partially restored the ability to consume glucose with a large improvement in the conversion yield. The highest yield was reported for a strain that simultaneously overexpresses *glf* and endogenous glucokinase [22].

Ethanol supplementation is known to stimulate BC biosynthesis in *Komagataeibacter* [28–32]. Since the ethanol partial oxidation in the periplasm by the membrane-anchored PQQ-dependent alcohol dehydrogenase (PQQ-ADH) is linked to the ETC, it directly contributes to ATP generation [25] (**Figure II.1**). BC biosynthesis is speculated to be favoured when high intracellular concentrations of ATP are available in the cytosol. One explanation is that high ATP levels inhibit glucose-6-phosphate dehydrogenase, blocking the metabolic flow toward the PPP [32]. Additionally, ethanol supplementation has been correlated with the induction of the expression of glucokinase and genes related to the synthesis of UDP-glucose, and repression of genes involved in glycolysis and acetan formation [28]. Overall, it seems that glucose metabolism is directed toward BC biosynthesis, while the cell uses ethanol and acetate for carbon assimilation and energy generation [33].

The genome of *K. sucrofermentans* ATCC700178 codes four PQQ-dependent mDHs (PQQ-mDHs), one belonging to the methanol/ethanol family (PYD81037), and three to the glucose/quinate/shikimate family (PYD80650, PYD79881, PYD78835). In this study, we evaluate the effects of knocking out each of the four PQQ-mDHs in the genome and assess the effect on glucose conversion to gluconic acid and BC biosynthesis. Since PQQ-mDHs link directly to the ETC, we evaluate the effect of ethanol supplementation

on the best BC-yielding strain, deficient in the PQQ-GDH (PYD79881), and on the mutant lacking the PQQ-ADH (PYD81037).

2.3 Materials and Methods

2.3.1 Bacterial strains and growth conditions

Komagataeibacter sucrofermentans ATCC700178 (KS001) and derived mutants (KS002, KS003, KS004, and KS005) were propagated in Hestrin and Schramm (HS) medium [34]. Excluding carbon sources, the medium comprises 5.0 g/L yeast extract, 2.7 g/L sodium biphosphate basic, 1.15 g/L citric acid, and 0.5 g/L magnesium sulphate. The pH was set to 5.5 with 5 M hydrochloric acid if necessary. Bacterial stocks consisted of liquid culture suspensions in 15% (v/v) glycerol and were stored at -80 °C. Before all experiments, propagation and culture synchronisation were performed as follows: 5.0 mL of HS medium with 20.0 g/L glucose, 1.5% (v/v) ethanol, and 1.0% cellulase was inoculated with the strains' glycerol stocks; the cultures were incubated for 3 days at 30 °C and 200 rpm orbital shaking, transferred to 50.0 mL of medium with the same composition, and incubated for 1 additional day in the same conditions. The bacterial biomass was then washed twice by centrifuging at 3200 *g* for 12 minutes and resuspended in the same volume of HS medium without a carbon source. Fermentations were then performed under different experimental conditions, being inoculated with a 1:10 volumetric ratio.

For growth curve monitoring, all bacterial strains were grown at 30 °C and 200 rpm orbital shaking in 50.0 mL HS medium with 1% (v/v) cellulase, and 20.0 g/L glucose or 1.5% (v/v) ethanol. BC production from a single carbon source was accessed by growing the strains statically at 30 °C in 20.0 mL of the same media without the addition of cellulase.

The ethanol supplementation experiment was performed by growing the bacterial strains statically at 30 °C, in 5.0 mL of HS medium with 20.0 g/L glucose and varying ethanol concentrations (0.5-5.0% (v/v)), in 25.0 mL culture tubes.

2.3.2 Gene disruption of PQQ-mDHs

Genomic DNA (gDNA) extraction from KS001 was performed as described elsewhere [35]. The strains KS002, KS003, KS004, and KS005, were constructed by genomic interruption of the CRF77_01730, CRF77_05025, CRF77_00430, and CRF77_09325 *loci*, respectively, by homologous recombination with the suicide vectors KS002-KO, KS003-KO, KS004-KO, and KS005-KO.

The vectors were assembled, using the InFusion Cloning® HD kit, from gel-extracted PCR fragments. The PCR reactions were set up according to the kit's instructions and the PCR products were purified with the QIAquick® Gel Extraction Kit. The assembly modules, for all constructs, consisted of a pUC19 backbone amplified from KTK_354 [36], a chloramphenicol resistance cassette amplified from KTK_137 [36], and upstream and downstream homologous regions, which were amplified from KS001 gDNA with sizes varying between 600 bp and 678 bp. The assembly reactions were transformed in *Escherichia*

coli NZY5α competent cells by heat shock according to the suppliers' protocol and transformants were selected in Luria-Bertani agar plates with 100 μg/mL ampicillin and 34 μg/mL chloramphenicol. Positive transformants were screened with colony PCR using the NZYTaq II 2x Green Master Mix, and Sanger Sequencing. Plasmid DNA was extracted using the GenElute™ Plasmid Miniprep Kit. All the primers used are listed in **Table II.1**.

For genomic interruption of the target genes, the strain KS001 was transformed with 1 μg of suicide plasmid DNA by electroporation as described elsewhere [37]. Transformants were selected in HS-agar plates with 20.0 g/L glucose and 340 μg/mL chloramphenicol and screened by colony PCR, and the correct genomic integration was confirmed by Sanger sequencing.

Table II.1: List of primers used for construction of suicide plasmids for knockout of the genes coding for PQQ-mDHs. Overhangs for assembly with InFusion® Cloning HD are represented in lower case letters, while template specific bases are in upper case letters.

Primer name	**Template**	**Target locus**	**Primer sequence (5'-3')**	**Reference**
CmR_FW	KTK_137	chloramphenicol resistance cassette	ttgatcgggcacgtaTGATCGGCACGTAAGAGGTTCCAAC	This work
CmR_RV	KTK_137	chloramphenicol resistance cassette	accaataaaaaacgcAGCGGAAAAGGACAAAAGTCA	This work
pUC_FW	KTK_354	plasmid backbone (pUC19-based)	catgtgagcaaaaggccagcaa	This work
pUC_RV	KTK_354	plasmid backbone (pUC19-based)	tatggtgcactctcagtacaatctgct	This work
KS003-UF	KS001 gDNA	CFR77_05025	tgagagtgcaccataATGAATAGCCTCATACGCTCG	This work
KS003-UR	KS001 gDNA	CFR77_05025	tacgtgcccgatcaaTGTCCAGGCCACCTTCAG	This work
KS003-DF	KS001 gDNA	CFR77_05025	gcgtttttttattggtGCAATCTCGGCATGTTCGAA	This work
KS003-DR	KS001 gDNA	CFR77_05025	ccttttgctcacatgTCAGTTCCCGTCAGGCAGG	This work
KS002-UF	KS001 gDNA	CFR77_01730	tgagagtgcaccataATGCGAGAAACCACCAAGAGG	This work

Primer name	Template	Target locus	Primer sequence (5'-3')	Reference
KS002-UR	KS001 gDNA	CFR77_01730	tacgtgcccgatcaaGACTTCAAGGTTGAACTCATG ACCC	This work
KS002-DF	KS001 gDNA	CFR77_01730	gcgtttttttattggtTCATGCTGGCCAATGCGAG	This work
KS002-DR	KS001 gDNA	CFR77_01730	ccttttgctcacatgTTATTGGGCTGCATTGCCTGCC	This work
KS004-UF	KS001 gDNA	CFR77_00430	tgagagtgcaccataATGATTTCTGCCGTTTTCGGAA AAAGACG	This work
KS004-UR	KS001 gDNA	CFR77_00430	tacgtgcccgatcaaGCCATCAACCGTGTAGGAAC GC	This work
KS004-DF	KS001 gDNA	CFR77_00430	gcgtttttttattggtGTCTGGCCAACGGCGAAT	This work
KS004-DR	KS001 gDNA	CFR77_00430	ccttttgctcacatgTTATGGCTGCTGCTCGGGAAT ACCG	This work
KS005-UF	KS001 gDNA	CFR77_09325	tgagagtgcaccataATGCTGCGCACTCTGCTG	This work
KS005-UR	KS001 gDNA	CFR77_09325	tacgtgcccgatcaaGGAAGTGTAATACACCACCGC CTTACAC	This work
KS005-DF	KS001 gDNA	CFR77_09325	gcgtttttttattggtCGTATGACGAAAAGACCGGTATCC TGA	This work
KS005-DR	KS001 gDNA	CFR77_09325	ccttttgctcacatgTCAGTTCACGTCGTCCAGCGC	This work

2.3.3 Analytical procedures

Growth curve monitoring was performed by measuring the OD_{600nm}, with undiluted samples, using the Cytation™ 3 (Biotek) microplate reader. pH was qualitatively measured using pH strips. Metabolite concentrations were determined by High-Pressure Liquid Chromatography (HPLC) using a BioRad Aminex HPC-87H column at 55 °C, with a mobile phase of 5 mM H_2SO_4 and a flow rate of 0.5 mL/min.

2.3.4 BC preparation

The BC pellicles were treated with 1% (w/v) NaOH until white or transparent and then washed with distilled water until pH neutralization. The treated membranes were then dried at 100 °C and weighed.

2.3.5 Statistics and data analysis

Data treatment and pairwise t-tests for statistical significance were performed using the pandas and matplotlib Python libraries [38, 39]. BC production per mol of consumed glucose (BPCG), ethanol (BPCE), and carbon (BPCC) were calculated using **Equations 1**, **2**, and **3**, respectively.

Equation 1 - $BPCG = \frac{BC\ (g)}{\Delta glucose\ (mol)}$

Equation 2 - $BPCE = \frac{BC\ (g)}{\Delta ethanol\ (mol)}$

Equation 3 - $BPCC = \frac{BC\ (g)}{(\Delta glucose\ (mol)*6)+(\Delta ethanol\ (mol)*2)}$

2.4 Results

In this work, we investigate the effect of knocking out the PQQ-mDHs present in the genome of the wild-type *K. sucrofermentans* ATCC 700178 (KS001) on BC production. The strains KS002, KS003, KS004, and KS005 were obtained by disrupting the *loci* CFR77_01730, CFR77_05025, CFR77_00430, and CFR77_09325, respectively. According to the protein annotation, the strains KS002, KS003 and KS005 lack PQQ-mDHs belonging to the glucose/quinate/shikimate family, while KS004 lacks a PQQ-mDH from the methanol/ethanol family.

The five strains were grown in agitated culture in the presence of cellulase, and in static culture for BC pellicle formation, in HS-glucose or HS-ethanol, in a range of ethanol concentrations from 0.5% to 5.0%. In all cases, the substrate consumption, extracellular metabolite accumulation, pH and BC production were monitored.

2.4.1 CFR77_05025 and CFR77_00430 are responsible for the periplasmic oxidation of glucose and ethanol, respectively.

In shake flask culture, distinct metabolic behaviours were observed among the strains. All except for KS003 were able to consume all glucose in the HS-glucose medium within the first 24 hours. Over the same period, pH dropped abruptly to 3.0 due to the incomplete oxidation of glucose to gluconic acid (**Figures II.2A**, **II.2B**, **II.2D**, **II.2E**, and **II.3A**). KS003, on the other hand, slowly consumed glucose without accumulating gluconate in the culture medium. In this case, pH increased slightly until a final value of 5.5 (**Figures II.2C** and **II.3A**)**.** These findings corroborate previous research [17, 18, 22], demonstrating consistent metabolic behaviours across similar studies.

In shake flask cultures using HS-ethanol medium, a distinct pattern in ethanol consumption and acetic acid production was observed for the strain KS004. For the remaining strains' cultures, ethanol was depleted after 72 hours of culturing in HS-ethanol, coincidently with the peak of extracellular accumulation of acetic acid (**Figure II.4**). However, OD_{600nm} barely varied during the second day of culturing, indicating that ethanol was probably depleted from the culture medium. After a diauxic shift that lasted for approximately 24 hours, strains KS001, KS002, KS003 and KS005 started assimilating the acetate until

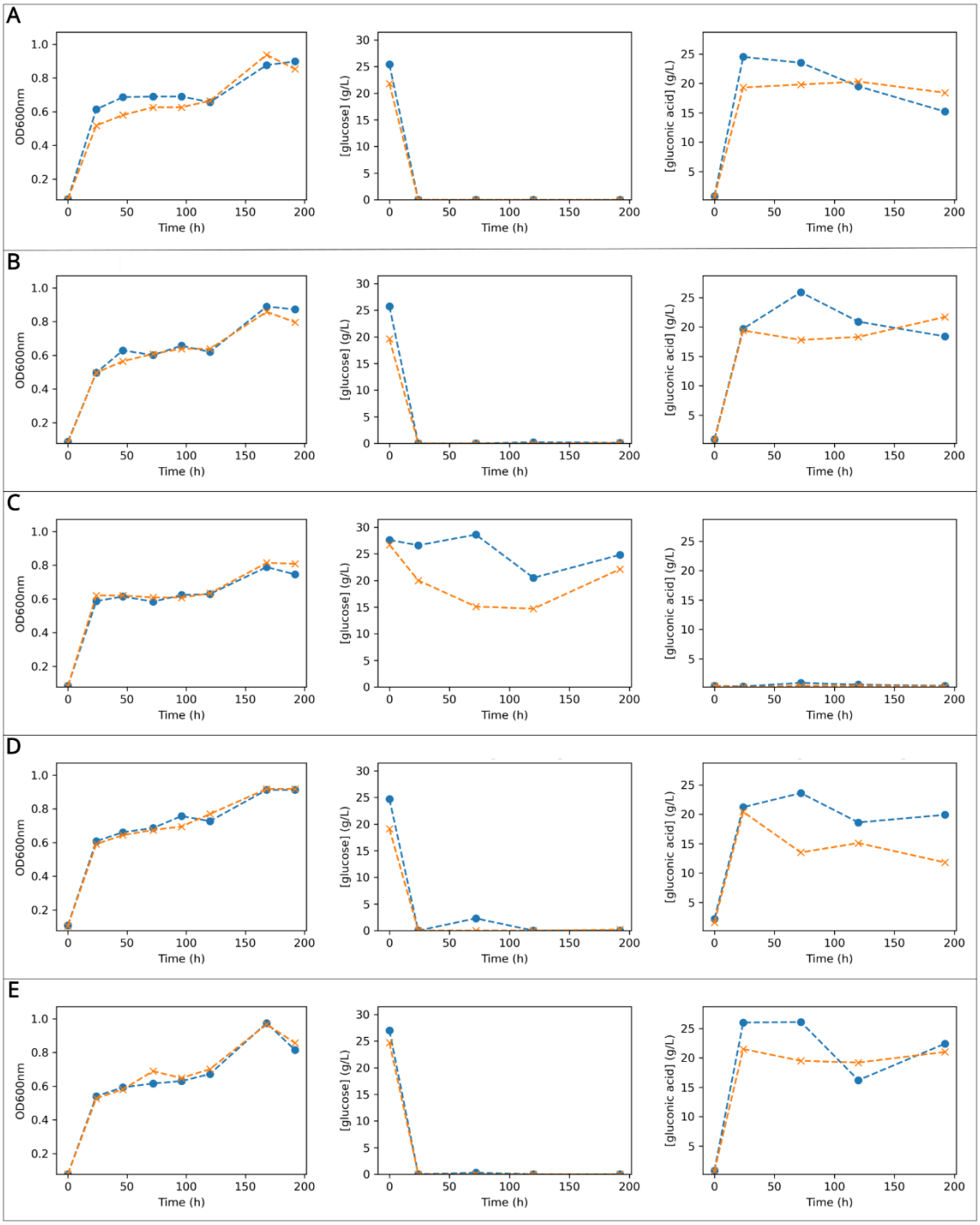


Figure II.2: Time-course growth and metabolic profiles of agitated cultures in HS-glucose medium for five K. sucrofermentans strains - A: KS001; B: KS002; C: KS003; D: KS004; E: KS005. For each strain: The left panel shows OD_{600nm} monitoring; the middle panel depicts glucose concentration (g/L); the right panel represents gluconic acid concentration (g/L). In all panels, Replicate 1 (orange lines with dot markers) and Replicate 2 (blue lines with cross markers) are shown.

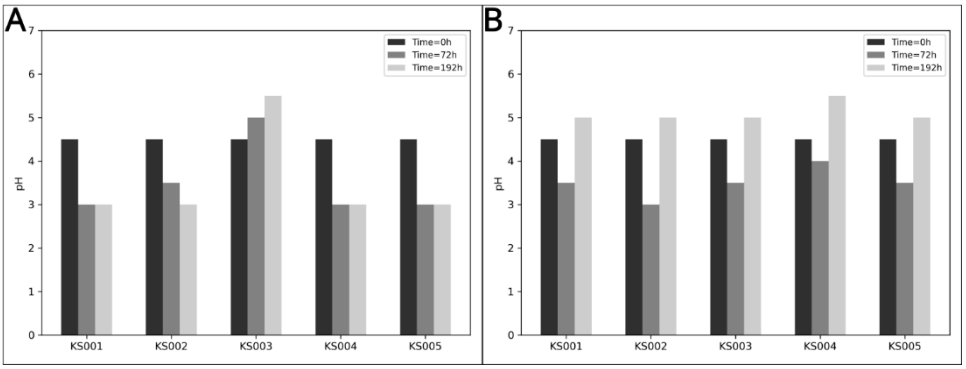


Figure II.3: pH variation during fermentations of K. sucrofermentans strains in different media – A: pH measurements for strains KS001 to KS005 over time in HS-glucose medium; B: pH values for the same strains in HS-ethanol medium.

it became undetectable by the end of the culture (**Figures II.4A**, **II.4B**, **II.4C**, and **II.4E**), as expected according to what is observed in other studies [28, 33, 40, 41]. KS004, on the other hand, slowly consumed the ethanol. The results suggest that ethanol was in this case being metabolized in the cytoplasm, in contrast to the remaining strains, since acetate was only detected in small amounts at the 72-hour time point, coinciding with the period of steepest ethanol consumption (**Figure II.4D**). This result is in alignment with research in other AAB. For example, even though *Acetobacter* typically display diauxic growth in ethanol media [42], an *A. pasteurianus* SKU118 mutant deficient in the PQQ-ADH lost the ability to accumulate acetate but retained the ethanol consumption ability [43]. Regarding pH changes, all strains except KS004 displayed pH drops ranging between 1.0 and 1.5, depending on the extent of ethanol oxidation to acetate. The four cultures ended up with a final pH of 5.0 after all acetate was consumed. On the other hand, the pH in the KS004 cultures decreased slightly after 72 hours due to the accumulation of small amounts of acetate in the medium and had the highest pH values at the end of the culture with a value of 5.5 (**Figure II.3B**).

In summary, the strains KS003 and KS004 display an absence of extracellular accumulation of large amounts of gluconic and acetic acids, respectively. This strongly suggests that the PQQ-mDHs coded by the *loci* CFR77_05025 and CFR77_00430, are responsible for the periplasmic partial oxidation of glucose and ethanol, respectively.

2.4.2 The strain KS003 shows improved BC production in static culture

The four knock-out mutants were further compared with the wild-type strain KS001 for their ability to produce BC in static culture in the presence of glucose or ethanol as the sole carbon source.

In the experiment using HS-glucose medium, all mutants achieved higher average VPE than KS001, but the improvement was not statistically significant for KS004 (p=0.05). In ascending rank of BC production: KS001 (0.25 ± 0.01 g/L) < KS004 (0.27 ± 0.01 g/L) < KS002 (0.34 ± 0.02 g/L) < KS005

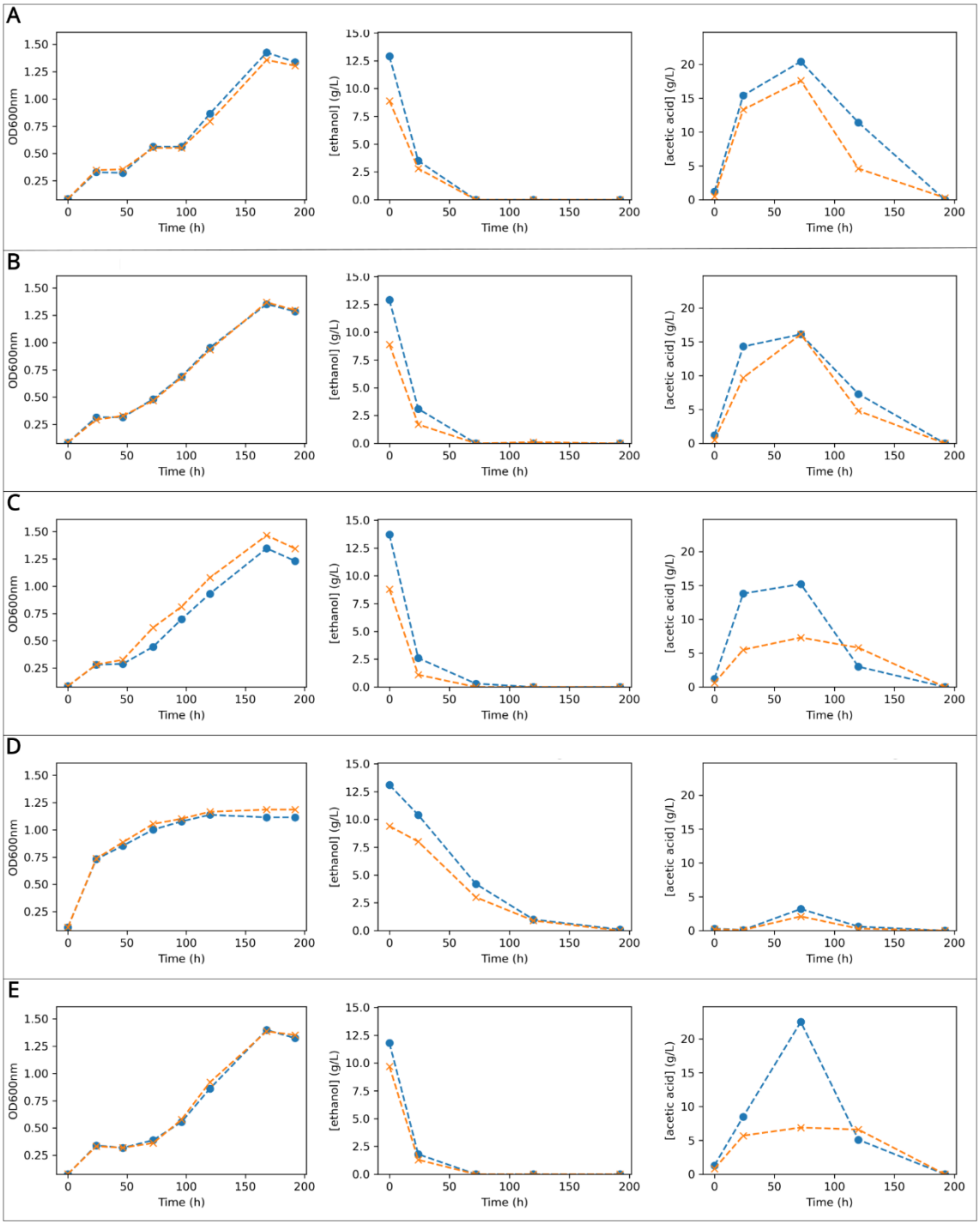


Figure II.4: Time-course growth and metabolic profiles of agitated cultures in HS-ethanol medium for five K. sucrofermentans strains - A: KS001; B: KS002; C: KS003; D: KS004; E: KS005. For each strain: The left panel shows OD_{600nm} monitoring; the middle panel depicts ethanol concentration (g/L); the Right panel represents acetic acid concentration (g/L). In all panels, Replicate 1 (orange lines with dot markers) and Replicate 2 (blue lines with cross markers) are shown.

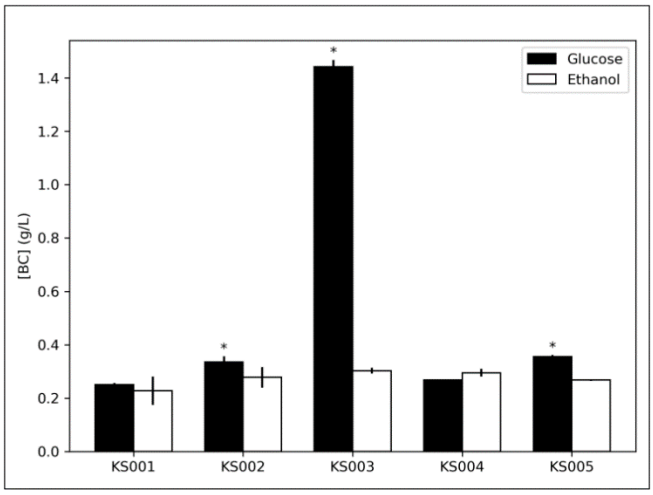


Figure II.5: BC production (g/L) of K. sucrofermentans strains KS001 to KS005 grown in HS-glucose (black bars) and HS-ethanol (white bars) media, in static culture. Error bars denote standard deviations.* Statistically significant difference in BC concentration compared to the KS001 strain for the corresponding carbon source (N=2; $p<0.05$).

(0.36 ± 0.01 g/L) < KS003 (1.44 ± 0.01 g/L). Although most strains showed marginal improvement in BC production, KS003 remarkably showed a 5.77-fold increase when compared to KS001 (**Figure II.5**). This finding aligns with previous observations in other *Komagataeibacter* species, where a knockout of PQQ-GDH enzyme led to increased BC production in glucose media [17, 18, 22]. In HS-ethanol, all mutant strains achieved non-significantly higher VPE than KS001, ranking as follows: KS001 (0.23 ± 0.04 g/L) < KS005 (0.27 ± 0.03 g/L) < KS002 (0.28 ± 0.03 g/L) < KS004 (0.30 ± 0.01 g/L) < KS003 (0.30 ± 0.01 g/L) (**Figure II.5**).

2.4.3 Ethanol concentration modulates BC production and metabolic responses in *Komagataeibacter* strains

It is widely reported in the literature that ethanol supplementation drives glucose toward BC production in *Komagataeibacter spp.*, boosting the yield of the polymer [17, 28, 30, 32, 44]. As AAB partially oxidize glucose and ethanol in the periplasm while supplying the reducing equivalents to the ETC, both reactions are directly coupled with energy generation [25]. Since KS003 and KS004 lack PQQ-GDH and PQQ-ADH, respectively, we decided to evaluate the impact of knocking out those genes on the typical BC production boost observed in cultures where both glucose and ethanol are present.

By testing a range of increasing concentrations, we were able to observe that the optimal ethanol levels required for peak BC production in the strains KS003 and KS004 shifted when compared to KS001. Specifically, while KS001 has its peak of BC production at an ethanol concentration of 1.0 % (v/v), KS004 and KS003 had their maximum VPE at 1.5 % (v/v) and 2.0 % (v/v) respectively. The shift in the optimal ethanol concentration might reflect a lower competition for ubiquinone in the ETC, which is a typical limiting step in catalysis by PQQ-mDHs [25]. The VPE at each strain's optimal ethanol concentration ranked as



Figure II.6: Comparative Analysis of Bacterial Cellulose Production Efficiency in K. sucrofermentans strains in HS-glucose-ethanol media in a range of ethanol concentrations, in static culture - A: KS001; B: KS003; C: KS004. The top panel (VPE) represents Volumetric Production Efficiency (g/L), the second panel (BPCG) shows Bacterial Cellulose Production Per Consumed Glucose (g/mol), the third panel (BPCE) denotes Bacterial Cellulose Production Per Consumed Ethanol (g/mol), and the bottom panel (BPCC) illustrates Bacterial Cellulose Production Per Consumed Carbon (g/mol). Red bars represent data at 7 days, while green bars denote data at 14 days. Error bars indicate the standard deviation. * Significance against strain KS001 for the same condition and timepoint (N= 2; $p<0.1$). ** Significance when comparing 14 days to 7 days for a given condition (N=2; $p<0.1$).

follows: KS004 (0.52 ± 0.02 g/L) < KS001 (0.88 ± 0.1 g/L) < KS003 (1.99 ± 0.01 g/L) (**Figure II.6A**, **II.6B** and **II.6C** – top panels).

Knocking out the PQQ-ADH (strain KS004), was not favourable for BC production when glucose and ethanol were simultaneously present in the culture medium (**Figure II.6C**). On the other hand, the absence of periplasmic glucose dehydrogenase activity was beneficial since KS003 had an increase of 2.26-fold in BC production when compared to KS001 at their respective optimal ethanol concentrations (**Figure II.6B**). While a mutant lacking the PQQ-GDH was previously found to benefit from ethanol supplementation, this is the first report of a systematic comparison of the response to different ethanol concentrations against the wild-type strain [17].

The initial 7-day cultivation period revealed a negative correlation between escalating ethanol concentrations and BC production for KS001 (**Figure II.6A** – top panel). This lagging effect was manifested through heightened levels of residual glucose present in the medium, coupled with a diminished formation of gluconate (**Figure II.7A**). Slower glucose consumption and gluconate production rates in dual carbon source media, in comparison with media with glucose as the sole carbon source, were expected [17]. Moreover, a relationship was observed between acetate accumulation and the initial concentration of ethanol. After 7 days, ethanol was scarcely detected in the cultures of KS001 except in those initiated with a 5.0% (v/v) ethanol concentration. Transitioning into the subsequent week of cultivation, a shift in the metabolic dynamics was noted. Glucose was predominantly detected in cultures supplemented with 2.0% and 5.0% ethanol, while a standardization occurred in gluconate concentrations, stabilizing at approximately 4 g/L across all experimental conditions (**Figure II.7A**). At first sight, this result contrasts with what was observed by Ryngajłło et al., where the supplemented cultures left a substantial amount of residual glucose and produced less gluconate. However, in contrast to our results, there was still a large amount of acetate in the medium, and it is unclear whether glucose consumption and gluconate production would have further progressed [28]. In terms of BC production, a substantial increase was measured, particularly in the conditions with ethanol concentrations calibrated to 1.0% (v/v) and 1.5% (v/v). In this period an acceleration in BC production is apparent, coincidently with the assimilation of acetate, but this increase in respect to the first week was only significant (p<0.1) for the cultures initiated with 1.0% and 2.0% (v/v) due to the variability between the replicates (**Figures II.6A** and **II.7A**). A substantial increase in BC production during the acetate assimilation phase was also observed by Yunoki et al. in *K. xylinus* ATCC 10245 in a similar culture medium composition [33].

Regarding strain KS003, a distinct metabolic behaviour was observed when contrasted with KS001, characterized by the absence of gluconate formation. This phenomenon is closely tied to the pronounced retention of glucose in the medium, with 30-50% remaining post-experiment. Despite this, the KS003 strain maintained residual ethanol and acetate levels comparable to those found in KS001 at both examined time points (**Figure II.7B**). When focusing on BC production, the initial week exhibited a minor difference between the conditions with initial ethanol concentrations of 0.5% (v/v) and 1.0% (v/v), while higher values resulted in lagged exopolysaccharide secretion. This trend sharply contrasted in the second week where acetate assimilation spurred significant boosts in BC production (p<0.1), when compared to the first week, in the cultures initiated with ethanol concentrations of 1.5% (v/v) and 2.0% (v/v) (**Figure II.6B**). The increase in these two conditions, in comparison with KS001, was also significant (p<0.1).

A distinct pattern of BC production was observed for the strain KS004. Despite a significant 1.9-fold augmentation from the first to the second week of cultivation (p<0.1) at the ethanol concentration of 2.0% (**Figure II.6C**), it is critical to note the strain's overall diminished BC production. This observation starkly contrasts with its ability to maintain the lowest levels of residual glucose, and higher conversion to gluconate, across all examined conditions and temporal checkpoints (all significant; p<0.1). Furthermore, the KS004 strain demonstrated a restrained extracellular acetate accumulation, maintaining low levels in most conditions with a noTable II.increase observed in cultures supplemented with a 5.0% ethanol



Figure II.7: Metabolic profiles of K. sucrofermentans strains in HS-glucose-ethanol media. Each panel shows the residual concentration of (from top to bottom) glucose, gluconic acid, ethanol, and acetic acid (all in g/L) for strains KS001 (A), KS003 (B), and KS004 (C). Red and green bars indicate measurements at 7 and 14 days, respectively; error bars represent standard deviation; the horizontal blue dashed line represents the initial glucose concentration (g/L). * Significant differences from strain KS001 under identical conditions (N=2; p<0.1). ** Significant differences between the time points for each strain (N=2; p<0.1).

concentration (**Figure II.7C**).

The BPCG in the KS001 strain tended to decrease with increased initial ethanol concentrations during the first week of cultivation. However, with extended culturing to 14 days, a substantial increase in BPCG was observed in cultures with 1.0% (v/v) and 1.5% (v/v) ethanol concentrations. The 1.0% (v/v) ethanol condition reached the highest BPCG of 8.03 ± 1.01 g/mol for this strain (**Figure II.6A** – second panel). The BPCE showed a consistent decline with increasing ethanol concentrations across both the 7 and 14-day culturing periods (**Figure II.6A** – third panel). In the first 7 days, there was a downward trend in BPCC as ethanol concentration increased. In the second week, significant increases in BPCC were noted for the 1.0% and 2.0% ethanol conditions (p<0.1). The BPCC was notably higher at lower ethanol concentrations (0.5% and 1.0% v/v) (**Figure II.6A** – bottom panel).

During the initial cultivation week, strain KS003 demonstrated a declining BPCG with increased ethanol concentration. However, a significant increase in BPCG was observed in the 1.5% (v/v) and

2.0% (v/v) ethanol conditions over 14 days (p<0.1), with increases of approximately 1.71- and 2.1-fold, respectively. The optimal condition of 2.0% (v/v) ethanol yielded an average BPCG of 29.04 ± 1.87 g/mol, which was the highest value in the experiment (**Figure II.6B** – second panel). In contrast to KS001, KS003 showed a more sTable II.BPCE in the second week of culturing, maintaining levels around 4.97 ± 0.28 g/mol across mediums with 1.0%, 1.5%, and 2.0% (v/v) ethanol. In media with 1.5% (v/v) and 2.0% (v/v), at the end of the experiment, the increase in BPCE was significantly higher when compared with the strain KS001 and with the intermediate time-point (p<0.1) (**Figure II.6B** – third panel). The BPCC pattern in KS003 over the two-week period showed the highest yields at the lowest tested ethanol concentration. The BPCC levelled off at an average of 1.58 ± 0.03 g/mol in trials with 1.5% and 2.0% initial ethanol concentrations, with a marked downturn at 5.0% (v/v) ethanol concentration (**Figure II.6B** - bottom panel).

Strain KS004 exhibited the lowest BPCGs of the experiment. The highest BPCG was 4.68 ± 0.18 g/mol under the 1.5% (v/v) ethanol condition, which was considerably lower when compared to the other two strains (**Figure II.6C** – second panel). Throughout the initial 7-day period, the BPCC in KS004 was slightly affected within the ethanol range of 0.5-2.0% (v/v), with an average value of 0.23 ± 0.02 g/mol. However, a more fluctuating BPCC pattern was observed over 14 days, with values oscillating between 0.30 ± 0.05 and 0.41 ± 0.01 g/mol (**Figure II.6C** – bottom panel). KS004 demonstrated restrained benefits from ethanol supplementation due to the removal of PQQ-ADH, contrasting with other strains that showed improved BC production in ethanol-containing media.

2.5 Discussion

Ethanol supplementation in glucose-containing media is an established method to enhance BC production [28, 30, 33, 41]. *Komagataeibacter spp.* express mDHs specific for the oxidation of both substrates in a reaction coupled with energy generation by electron channelling through the ETC [25, 28]. Interestingly, multiple studies reported that the attenuation, or elimination, of extracellular accumulation of gluconic acid is typical in high BC-producing strains [17, 18, 22]. As PQQ-mDHs are key players in the metabolic landscape of AAB [22], combining both strategies can generate useful insights for a better understanding of their role in BC production and allow the achievement of better yields.

Among the mutants generated in this work, the strains KS003 and KS004 stood out due to their inability to accumulate gluconate and acetate in the medium, respectively. This indicates that the loci CFR77_05025 and CFR77_00430 code the PQQ-mDHs responsible for the periplasmic oxidation of glucose and ethanol in *K. sucrofermentans*, respectively. While neither strain was able to show significantly increased BC production when grown in HS-ethanol, by comparison with KS001, KS003 showed a substantial increase in HS-glucose.

Three previous studies have reported the loss of gluconate production by interruption of the *gcd* gene, with the respective KO strains preventing the typical pH drop [17, 18, 22]. Shigematsu et. al and Kuo et. al reported slower glucose consumption rates, in *K. xylinus* BPR 2001 and *K. xylinus* BCRC 12334,

respectively, with the KO strains reaching higher $OD600_{nm}$ than the unmodified ones, in agitated cultures with cellulase [17, 18]. Without further optimization, the KO strains consumed all available glucose and achieved 1.4 and 1.7-fold increased BC production in the static mode of cultivation, respectively. Knocking out the *gcd* gene in *K. xylinus* CGMCC 2955, on the other hand, resulted in a strain with severe growth, BC production, and glucose consumption deficiencies, thus requiring further modifications to improve the yield [22]. While the overexpression of the glucose facilitator protein (*glf* from *Zymomonas mobilis*) and the native glucokinase (*glk*) did not fully restore the glucose consumption ability, it has improved its conversion to BC thus unlocking a similar volumetric yield to the control strain from a lower glucose concentration. In our study, KS003 was able to reach the same OD_{600nm} as KS001 in an agitated culture in the presence of cellulase. However, the simultaneous production and degradation of BC caused oscillating glucose levels in the medium. This was only observed in this strain's cultures, thus evidencing its impaired glucose consumption. As the glucose oxidation to gluconic acid occurs in the periplasm, and the latter is mostly released to the extracellular medium, the fact that the strain KS003 can reach a similar OD_{600nm} as KS001 can be an indicator that both strains are equally efficient at importing glucose to the cytoplasm. Nonetheless, the strain was able to produce 5.77-fold more BC than the unmodified strain in static cultures with glucose as the sole carbon source.

All strains showed low BC production levels with ethanol as the sole carbon source but were able to metabolize the alcohol with no exception. However, acetate was barely detected in the extracellular medium, in agitated cultures with the strain KS004. This is corroborated by the pH measurements. The residual extracellular levels of acetate are probably due to the efflux by ABC transporters, associated with the high acetic acid resistance phenotype typically observed in bacteria from the *Komagataeibacter* genus [28, 45].

In *Komagataibacter*, ethanol metabolism has two distinct phases: 1) ethanol oxidation in the periplasm, which causes acetate to accumulate in the medium; and 2) acetic acid assimilation [28, 32, 33]. The prioritization of extracellular accumulation of acetate is corroborated by gene expression in *K. xylinus* E25, where the authors found acetate kinase, succinyl-CoA:acetate-CoA-transferase and most genes from the TCA cycle to be down-regulated while ethanol is not depleted from the culture medium [28]. Our results suggest that KS004 was able to metabolize the ethanol, but through the cytosolic route, instead of the signature periplasmic incomplete oxidation. While the growth curves in the remaining strains show the occurrence of a diauxic shift, the same was not observed in KS004 (Figure II.4D – left panel). Given that KS004 does not accumulate acetate, and that the strain displays a distinct growth curve, our results point to a different mode for ethanol metabolization than the typical two-staged metabolism. This was previously observed in a PQQ-ADH-deficient *A. pasteurianus* mutant, that ceased to accumulate acetate extracellularly while retaining the ethanol metabolization ability [43].

Bacteria from the *Komagataeibacter* genus seem to increase the glucose flow toward BC production and its necessary precursors in ethanol supplementation setups [28, 33]. The presence of ethanol induced the expression of galP3, a putative glucose transporter, glucokinase, UDP-glucose pyrophosphorylase, and phosphoglucomutase, in *K. xylinus* E25. Repression of the *gcd* gene, and others involved in

glycolysis and the PPP was also observed. Overall, their results suggested enhanced direct polymerization of glucose instead of its use for biomass and energy [28]. Our results are in alignment with their observations since KS001, KS003, and KS004 showed a higher volumetric production when grown in an ethanol supplementation setup than in the single carbon source experiment.

Ethanol supplementation is usually associated with slower glucose consumption and lower gluconate production. In strain KS001, the glucose consumption and gluconate production rates decrease with the increase of the initial concentration of ethanol during the first week of cultivation, which is when the ethanol oxidation phase occurs. However, strain KS004 was significantly faster at consuming the glucose and produced more gluconate than strain KS001. As our results suggest that the strain directly oxidizes ethanol to CO_2 and H_20 in the cytoplasm, thus not requiring a diauxic shift to allow acetate assimilation [43], it's then possible that KS004 does not operate under the same regulatory rules.

During the ethanol oxidation phase, the ETC is fed electrons mainly from the PQQ-mDHs, since the NADH dehydrogenase is down-regulated [25, 28]. However, in *K. xylinus* E25 the ubiquinol re-oxidation to UQ appeared to be on demand since up-regulation of the cytochrome ba_3 was observed, thus suggesting a high respiration rate during ethanol oxidation [28]. Since the substrate oxidation reactions of PQQ-GDH and PQQ-ADH both require the reoxidation of PQQ, an increase in the activity of the former might be partially caused by a decreased competition for UQ in the strain KS004, due to the absence of the latter [25]. This might also explain why both KS003 and KS004 show a preference for higher concentrations of ethanol than KS001. Nonetheless, our results suggest that the absence of PQQ-ADH is, at least partially, being compensated by higher PQQ-GDH activity.

After 7 days, glucose concentrations between 8.19 ± 0.64 g/L and 10.19 ± 0.43 g/L were measured in cultures of the strain KS003 with up to 2.0% (v/v) ethanol. Those values were all significantly superior to ones obtained with the strain KS001 under similar conditions, which further corroborates that strains lacking a functional PQQ-GDH show slower glucose consumption [17, 18, 22]. Additionally, a putatively increased expression of a galP3 homolog in the presence of ethanol, as observed by Ryngajłło et al. [28], did not fully restore the ability of KS003 to import glucose. Despite that, the strain KS003 showed significantly higher VPEs than KS001 for the conditions with 1.0-2.0% ethanol. In fact, during the first half of the culturing period, the strain KS003 was able to produce more BC than KS001 during the full duration of the experiment.

On one hand, while ethanol supplementation narrowed the fold increase between KS003 and KS001 in terms of BC production, by comparison with cultures in HS-glucose, the strain lacking the PQQ-GDH was still the best-performing strain in the experiment. On the other hand, KS004 was the worst BC producer in the presence of both carbon sources. As previously mentioned, substrate oxidation by PQQ-mDHs is tightly linked to the ETC and thus ATP biosynthesis [25]. As BC production is an energy-demanding process, the extra ATP generated by ethanol oxidation is thought as one of the factors that cause increased yields [28, 30, 32, 33, 41]. Additionally, ATP can have aregulatory effect by inhibiting the activities of glucose-6-phosphate dehydrogenases [32].

Two different studies that compare the intracellular ATP levels in glucose-based media, with and

without ethanol supplementation, obtain contrasting results. While Naritomi et al. verified that ethanol supplementation resulted in increased ATP levels in *Komagataeibacter sucrofermentans* BPR 3001A [32], Ryngajłło verified the opposite in *K. xylinus* E25 [28]. The striking differences between both studies were the sugars used and the fermentation mode. Naritomi et al. grew the bacteria in continuous culture, with fructose and ethanol feed. Ryngajłło et al. performed a static batch culture where glucose was used instead of fructose. The PQQ-ADH activity is concentration-dependent [46] and, due to the diauxic metabolism that *Komagataeibacter* display in the presence of ethanol, the bacteria was continuously generating ATP at a virtually fixed rate, in Naritomi et al [32]. In batch culture, the ethanol concentration decreases over time, partially explaining why Ryngajłło et al. measured lower ATP levels at the latter stage of the ethanol oxidation, while the TCA was still down-regulated. Interestingly, the ATP levels were still much lower during the acetate assimilation phase when compared with the non-supplemented medium, which the authors justify with an increased energy demand due to efflux of acetate, nutrient import from the culture medium, and BC biosynthesis [28].

The results of the ethanol supplementation experiment show that, the higher the initial concentration of ethanol is in the medium, the longer it takes for the BC production boost to occur. Although the BC production after 7 days was higher than in HS-glucose both for KS001 and KS003, a significant boost occurred during the second week of cultivation in mid-range ethanol concentrations. Although our study lacks temporal resolution, one assumes that the higher the ethanol concentration, the more prolonged the ethanol oxidation phase will be. The increased lag for the production boost to occur as the initial ethanol concentration increases suggests that the major production of BC occurs during the acetate assimilation phase, as observed in other studies [28, 33]. This was especially visible for the strain KS003 which suffered a penalizing effect with the increase from 0.5-2.0% ethanol during the first week but prospered in BC production over the second week in more acetic environments. Interestingly, the glucose concentration in the media barely varied within the same timeframe.

Upon ethanol depletion from the culture medium, a diauxic shift occurs and *Komagateibacter* species start catabolizing the previously accumulated acetate. Kornmann et al. [41] and Sakurai et al. [42] reported that the TCA cycle is more active on acetate than it is on ethanol in *K. xylinus* I2281 and *A. aceti* NBRC 14818, respectively. It appears that during the second phase, of acetate utilization, the acetyl-CoA synthase plays a major role in converting the acetate into acetyl-CoA, which can further be used to generate biomass or be channelled to the TCA cycle for energy generation [41, 42]. When comparing the BPCEs and BPCCs of the strains KS001 and KS003, both metrics showed an inverse relationship with the ethanol concentration during the first week, when the ethanol was converted to acetate, which was not immediately assimilated (**Figures II.6A**, **II.6B**, **II.7A**, and **II.7B**). Since acetate is assimilated upon cessation of ethanol oxidation [28, 30, 33, 41, 42], further BC production could only impact the BPCE positively. The fact that, at the end of the fermentation with the strain KS003, the BPCE barely changed within cultures initiated with 1.0-2.0% (v/v) ethanol, suggests that BC production was nearly proportional to the amount of acetate that's being assimilated in such conditions.

Interestingly, the evidence in the literature suggests that carbon from acetate is unlikely to be incorporated into BC. Yunoki et al. [33] conducted tests in *K. xylinus* with D-(1-^{13}C)-, D-(2-^{13}C)- and D-(6-^{13}C)-glucose, and (1-^{13}C)-ethanol labelling, demonstrating that in ethanol supplementation setups with ^{13}C-labeled ethanol, there's no evidence of labelled cellulose following ethanol oxidation or acetic acid assimilation [33]. That study also observed impaired BC production during the ethanol oxidation phase and a subsequent boost during acetate assimilation. The absence of labelled BC in cultures with (1-^{13}C)-ethanol indicates that acetate was rather fuelling the metabolism through the TCA cycle. The rearrangement of the glucose ring in BC synthesized in cultures with differently labelled glucose suggests that not only ethanol favours direct polymerization of glucose but also gluconeogenesis from peptides and amino acids imported from the culture medium [33]. The transcriptome of *K. xylinus* E25 also suggests that the active transport of nutrients from the culture medium is increased by ethanol supplementation [28]. Moreover, we were unable to find a coding sequence for homologs of *E. coli*'s phosphoenolpyruvate carboxykinase in the genome of the large majority of *Komagataeibacter spp.* through a BLAST search (not shown). This might be indicative that a metabolic route that could divert oxaloacetate to gluconeogenesis might be absent. Additionally, independent studies have found that supplementation with glucogenic and amphibolic amino acids boosts BC production in *Komagataeibacter spp* [47, 48]. One study reports that L-methionine (glucogenic) boosts BC production in 50%, in basal medium, in *Komagataeibacter sucrofermentans* BPR2001 [47]. Another study reports that aspartic acid and serine (glucogenic), and phenylalanine (amphibolic) boost BC production in *Komagataeibacter intermedius* V-05 [48].

Altogether, the evidence in the literature suggests that ethanol promotes a more efficient use of glucose and nutrients contained in the peptone and yeast extract, while not being a source of carbon for BC production [28, 33, 47, 48]. This would imply that, if that's the case, most of the glucose monomers in the BC being produced by the strain KS003 during the acetate assimilation phase were originated by neogenesis from imported amino acids, since the levels of glucose barely change during that period. This work suggests that the PQQ-ADH is an important component at increasing the BC productivity in the presence of ethanol. PQQ-ADH overexpression in KS003 might further improve the strain's productivity by increasing the rate of ethanol oxidation while simultaneously conferring acetic acid tolerance [25]. This might have a positive influence on the strains' bioenergetics and, consequently, on BC productivity.

2.6 Conclusions

Our study underlines the importance of membrane-anchored PQQ- mDHs, specifically PQQ-GDH and PQQ-ADH, in BC production by *K. sucrofermentans*. The metabolic differences in the strains KS003 and KS004, characterized by altered patterns of gluconate and acetate extracellular accumulation, respectively, allowed a better understanding of their role in substrate oxidation, and the impact on BC yield. Notably, the impaired glucose consumption coupled with enhanced BC production in KS003, despite its metabolic limitations, highlights the complex interplay between pH, metabolic fluxes, and product synthesis.

Furthermore, our findings suggest that ethanol supplementation, while might not directly contribute

carbon for BC biosynthesis, plays a crucial role in modulating cellular metabolism towards optimal BC production, possibly through the regulation of energy generation and nutrient assimilation pathways. Additionally, our results suggest that the extracellular accumulation of acetate is advantageous over direct metabolization of ethanol through the cytosolic route. The importance of PQQ-ADH for increased BC yield through ethanol supplementation was already hypothesized in the literature. However, to our knowledge, this is the first report of a *Komagataeibacter* strain unable to express a functional PQQ-ADH displaying a restrained benefit from ethanol supplementation.

Therefore, this study establishes the groundwork for further strain improvement, by offering potential strategies for targeted manipulation of metabolic pathways to enhance BC production.

2.7 References

[1] Soon Mo Choi et al. “Bacterial Cellulose and Its Applications”. In: *Polymers* 14.6 (2022), p. 1080.

[2] Maria Gullo et al. “Biotechnological production of cellulose by acetic acid bacteria: current state and perspectives”. In: *Applied Microbiology and Biotechnology* 102.16 (2018), pp. 6885–6898.

[3] Ute Römling and Michael Y. Galperin. “Bacterial cellulose biosynthesis: Diversity of operons, subunits, products, and functions”. In: *Trends in Microbiology* 23.9 (2015), pp. 545–557.

[4] Andrea F. S. Costa et al. “Production of Bacterial Cellulose by Gluconacetobacter hansenii Using Corn Steep Liquor As Nutrient Sources”. In: *Frontiers in Microbiology* 8 (2017).

[5] Dehui Lin et al. “Production of bacterial cellulose by Gluconacetobacter hansenii CGMCC 3917 using only waste beer yeast as nutrient source”. In: *Bioresource Technology* 151 (2014), pp. 113–119.

[6] Erminta Tsouko et al. “Integrated biorefinery development for the extraction of value-added components and bacterial cellulose production from orange peel waste streams”. In: *Renewable Energy* 160 (2020), pp. 944–954.

[7] Seung-Hyeon Moon et al. “Comparisons of physical properties of bacterial celluloses produced in different culture conditions using saccharified food wastes”. In: *Biotechnology and Bioprocess Engineering* 11.1 (2006), pp. 26–31.

[8] Feng Hong et al. “Bacterial cellulose production from cotton-based waste textiles: Enzymatic saccharification enhanced by ionic liquid pretreatment”. In: *Bioresource Technology* 104 (2012), pp. 503–508.

[9] Jung Wook Hwang et al. “Effects of pH and dissolved oxygen on cellulose production by Acetobacter xylinum BRC5 in agitated culture”. In: *Journal of Bioscience and Bioengineering* 88.2 (1999), pp. 183–188.

[10] Zhaofeng Li et al. “Effect of pH Buffer and Carbon Metabolism on the Yield and Mechanical Properties of Bacterial Cellulose Produced by *Komagataeibacter hansenii* ATCC 53582”. In: *Journal of Microbiology and Biotechnology* 31.3 (2021), pp. 429–438.

[11] Ahmed K. Saleh et al. “Statistical optimization and characterization of a biocellulose produced by local Egyptian isolate Komagataeibacter hansenii AS.5”. In: *International Journal of Biological Macromolecules* 144 (2020), pp. 198–207.

[12] Kallayanee Naloka et al. “Komagataeibacter diospyri sp. nov., a novel species of thermotolerant bacterial nanocellulose-producing bacterium”. In: *International Journal of Systematic and Evolutionary Microbiology* 70.1 (2020), pp. 251–258.

[13] Sangok Bae, Yasushi Sugano, and Makoto Shoda. “Improvement of bacterial cellulose production by addition of agar in a jar fermentor”. In: *Journal of Bioscience and Bioengineering* 97.1 (2004), pp. 33–38.

[14] Y. Chao et al. “Effect of Addition of Water-Soluble Polysaccharides on Bacterial Cellulose Production in a 50-L Airlift Reactor”. In: *Biotechnology Progress* 17.4 (2001), pp. 781–785.

[15] Y Chao et al. “Bacterial cellulose production by Acetobacter xylinum in a 50-L internal-loop airlift reactor.” In: *Biotechnology and bioengineering* 68.3 (2000), pp. 345–52.

[16] Joaquin Caro-Astorga et al. “Bacterial cellulose spheroids as building blocks for 3D and patterned living materials and for regeneration”. In: *Nature Communications* 12.1 (2021).

[17] Toru Shigematsu et al. “Cellulose production from glucose using a glucose dehydrogenase gene (gdh)-deficient mutant of gluconacetobacter xylinus and its use for bioconversion of sweet potato pulp”. In: *Journal of Bioscience and Bioengineering* 99.4 (2005), pp. 415–422.

[18] Chia Hung Kuo, Hsin Yin Teng, and Cheng Kang Lee. “Knock-out of glucose dehydrogenase gene in Gluconacetobacter xylinus for bacterial cellulose production enhancement”. In: *Biotechnology and Bioprocess Engineering* 20.1 (2015), pp. 18–25.

[19] Hyeokjo Gwon et al. “A safe and sustainable bacterial cellulose nanofiber separator for lithium rechargeable batteries”. In: *Proceedings of the National Academy of Sciences of the United States of America* 116.39 (2019), pp. 19288–19293.

[20] Magdiel Inggrid Setyawati, Liang Jung Chien, and Cheng Kang Lee. “Expressing Vitreoscilla hemoglobin in statically cultured Acetobacter xylinum with reduced O2 tension maximizes bacterial cellulose pellicle production”. In: *Journal of Biotechnology* 132.1 (2007), pp. 38–43.

[21] Miao Liu et al. “Enhanced bacterial cellulose production by Gluconacetobacter xylinus via expression of Vitreoscilla hemoglobin and oxygen tension regulation.” In: *Applied microbiology and biotechnology* 102.3 (2018), pp. 1155–1165.

[22] Ling-Pu Liu et al. “A Lambda Red and FLP/FRT-Mediated Site-Specific Recombination System in Komagataeibacter xylinus and Its Application to Enhance the Productivity of Bacterial Cellulose”. In: *ACS Synthetic Biology* 9.11 (2020), pp. 3171–3180.

[23] Woo Dae Jang et al. “Genomic and metabolic analysis of Komagataeibacter xylinus DSM 2325 producing bacterial cellulose nanofiber”. In: *Biotechnology and Bioengineering* 116.12 (2019), pp. 3372–3381.

[24] Zohaib Hussain et al. “Production of bacterial cellulose from industrial wastes: a review”. In: *Cellulose* 26.5 (2019), pp. 2895–2911.

[25] Zhijie Qin et al. “Dehydrogenases of acetic acid bacteria”. In: *Biotechnology Advances* 54 (2022), p. 107863.

[26] Kieran M. Lynch et al. “Physiology of Acetic Acid Bacteria and Their Role in Vinegar and Fermented Beverages”. In: *Comprehensive Reviews in Food Science and Food Safety* 18.3 (2019), pp. 587–625.

[27] Pietro Cannazza et al. “Characterization, genome analysis and genetic tractability studies of a new nanocellulose producing Komagataeibacter intermedius isolate”. In: *Scientific Reports* 12.1 (2022), p. 20520.

[28] Małgorzata Ryngajłło et al. “Effect of ethanol supplementation on the transcriptional landscape of bionanocellulose producer Komagataeibacter xylinus E25”. In: *Applied Microbiology and Biotechnology* 103.16 (2019), pp. 6673–6688.

[29] Carlos Molina-Ramírez et al. “Effects of alternative energy sources on bacterial cellulose characteristics produced by Komagataeibacter medellinensis”. In: *International Journal of Biological Macromolecules* 117 (2018), pp. 735–741.

[30] Joong Kon Park, Jae Yong Jung, and Youn Hee Park. “Cellulose production by Gluconacetobacter hansenii in a medium containing ethanol”. In: *Biotechnology Letters* 25.24 (2003), pp. 2055–2059.

[31] A Krystynowicz et al. “Factors affecting the yield and properties of bacterial cellulose”. In: *Journal of Industrial Microbiology and Biotechnology* 29.4 (2002), pp. 189–195.

[32] Takaaki Naritomi et al. *Effect of Ethanol on Bacterial Cellulose Production in Continuous Culture from Fructose*. Tech. rep. 6. 1998.

[33] Shunji Yunoki et al. “Role of Ethanol in Improvement of Bacterial Cellulose Production: Analysis Using 13C-Labeled Carbon Sources”. In: *Food Science and Technology Research* 10.3 (2004), pp. 307–313.

[34] S. Hestrin and M. Schramm. “Synthesis of cellulose by *Acetobacter xylinum* . 2. Preparation of freeze-dried cells capable of polymerizing glucose to cellulose”. In: *Biochemical Journal* 58.2 (1954), pp. 345–352.

[35] Fanglian He. “E. coli Genomic DNA Extraction”. In: *BIO-PROTOCOL* 1.14 (2011).

[36] Vivianne J Goosens et al. “Komagataeibacter Tool Kit (KTK): A Modular Cloning System for Multigene Constructs and Programmed Protein Secretion from Cellulose Producing Bacteria”. In: *ACS Synthetic Biology* 10.12 (2021), pp. 3422–3434.

[37] Michael Florea et al. “Engineering control of bacterial cellulose production using a genetic toolkit and a new cellulose-producing strain”. In: *Proceedings of the National Academy of Sciences of the United States of America* 113.24 (2016), E3431–E3440.

[38] John D. Hunter. “Matplotlib: A 2D Graphics Environment”. In: *Computing in Science & Engineering* 9.3 (2007), pp. 90–95.

[39] Wes McKinney. “Data Structures for Statistical Computing in Python”. In: 2010, pp. 56–61.

[40] François Barja et al. “Physiology of Komagataeibacter spp. During Acetic Acid Fermentation”. In: *Acetic Acid Bacteria*. Springer Japan, 2016, pp. 201–221.

[41] H. Kornmann et al. “Influence of residual ethanol concentration on the growth of Gluconacetobacter xylinus I 2281”. In: *Applied Microbiology and Biotechnology* 62.2-3 (2003), pp. 168–173.

[42] Kenta Sakurai et al. “Changes in the gene expression profile of Acetobacter aceti during growth on ethanol”. In: *Journal of Bioscience and Bioengineering* 113.3 (2012), pp. 343–348.

[43] Piyawan Chinnawirotpisan et al. “Quinoprotein alcohol dehydrogenase is involved in catabolic acetate production, while NAD-dependent alcohol dehydrogenase in ethanol assimilation in Acetobacter pasteurianus SKU1108”. In: *Journal of Bioscience and Bioengineering* 96.6 (2003), pp. 564–571.

[44] Joong Kon Park, Youn Hee Park, and Jae Yong Jung. “Production of bacterial cellulose byGluconacetobacter hansenii PJK isolated from rotten apple”. In: *Biotechnology and Bioprocess Engineering* 8.2 (2003), p. 83.

[45] Bin Wang, Yanchun Shao, and Fusheng Chen. “Overview on mechanisms of acetic acid resistance in acetic acid bacteria”. In: *World Journal of Microbiology and Biotechnology* 31.2 (2015), pp. 255–263.

[46] Xuefeng Wu et al. “Improving Acetic Acid Production by Over-Expressing PQQ-ADH in Acetobacter pasteurianus”. In: *Frontiers in Microbiology* 8 (2017).

[47] Masanobu Matsuoka et al. “A Synthetic Medium for Bacterial Cellulose Production by *Acetobacter xylinum* subsp. *sucrofermentans*”. In: *Bioscience, Biotechnology, and Biochemistry* 60.4 (1996), pp. 575–579.

[48] Rodrigo José Gomes, Elza Iouko Ida, and Wilma Aparecida Spinosa. “Nutritional Supplementation with Amino Acids on Bacterial Cellulose Production by Komagataeibacter intermedius: Effect Analysis and Application of Response Surface Methodology”. In: *Applied Biochemistry and Biotechnology* 194.11 (2022), pp. 5017–5036.

3 Engineering cytoplasmic glucose uptake in *Komagataeibacter sucrofermentans* ATCC 700178 lacking membrane glucose dehydrogenase

3.1 Abstract

Bacterial cellulose (BC) synthesis in *Komagataeibacter* is strongly influenced by the oxidative metabolism characteristic of acetic acid bacteria, in which the pyrroloquinoline quinone (PQQ)-dependent membrane glucose dehydrogenase (mGDH) oxidizes glucose to gluconic acid in the periplasm. This reaction diverts a large fraction of glucose away from intracellular metabolism, limiting carbon availability for cellulose biosynthesis. Previous work demonstrated that disruption of the mGDH gene in *K. sucrofermentans* ATCC 700178 generated the mutant strain KS003, which eliminates gluconic acid accumulation and increases BC production by 5.77-fold relative to the wild type. However, removal of the oxidative pathway also reduced the rate of glucose consumption, suggesting that intracellular glucose uptake becomes a metabolic bottleneck.

To address this limitation, the present study evaluated whether strengthening cytoplasmic glucose assimilation could further improve BC production. Two transporter–kinase modules were introduced: a heterologous glucose facilitator–glucokinase system (*Zm*GLF–*Ks*GLK) derived from *Zymomonas mobilis*, and a *Ks*GALP3–*Ks*GLK module inspired by transcriptomic evidence indicating that the galactose permease homolog GalP3 may function as a native glucose transporter in *Komagataeibacter*. These constructs were expressed in both the wild-type and KS003 backgrounds using the Komagataeibacter Toolkit modular cloning system.

Disruption of mGDH remained the dominant determinant of carbon partitioning. The plasmid-free KS003 strain produced 1.45 ± 0.07 g L^{-1} BC compared with 0.57 ± 0.32 g L^{-1} in the wild type, while gluconic acid accumulation decreased from approximately 11–16 g L^{-1} in wild-type strains to less than 1.35 g L^{-1} in KS003 derivatives. Normalization to glucose consumption revealed substantially higher conversion efficiency in the mutant background, reaching 0.150 ± 0.014 mg BC per mg glucose consumed, compared with 0.0267 ± 0.0153 mg mg^{-1} in the wild type. Introduction of the transporter–kinase modules produced modest phenotypic changes: KS003-*Zm*GLF–*Ks*GLK yielded 1.10 ± 0.14 g L^{-1} BC, whereas KS003-*Ks*GALP3–*Ks*GLK produced 0.90 ± 0.10 g L^{-1}. In the wild-type background, BC titers remained low regardless of construct.

These results confirm that periplasmic glucose oxidation via mGDH is the primary metabolic constraint limiting cellulose production in glucose-fed *Komagataeibacter*. Once this pathway is removed, intracellular

glucose assimilation becomes more relevant but does not alone determine productivity, indicating additional physiological limitations such as plasmid burden or downstream metabolic capacity. Overall, the study reinforces a hierarchical model of carbon allocation in acetic acid bacteria and suggests that future strain improvement should focus on chromosomal integration of optimized glucose uptake systems and more comprehensive metabolic rewiring to support efficient intracellular glucose flux toward cellulose biosynthesis.

3.2 Introduction

Bacterial cellulose (BC) is a highly pure and crystalline extracellular polysaccharide produced by several acetic acid bacteria (AAB), particularly species of the genus *Komagataeibacter* [1–3]. Owing to its high mechanical strength, water-holding capacity, and biocompatibility, BC has attracted increasing interest for applications in food, biomedical materials, and advanced composites [1, 2, 4–8]. When glucose is used as the primary carbon source, however, BC production in AAB is strongly influenced by the characteristic oxidative metabolism of these organisms. A defining feature of this metabolism is the presence of membrane-bound dehydrogenases located in the periplasmic space that catalyse incomplete oxidation of sugars and sugar alcohols in a reaction coupled directly to the respiratory chain [6, 9–12].

A central enzyme in this system is the pyrroloquinoline quinone (PQQ)-dependent membrane glucose dehydrogenase (mGDH), which catalyses the oxidation of D-glucose to D-glucono-δ-lactone on the outer surface of the cytoplasmic membrane [13–17]. The lactone is subsequently hydrolyzed to gluconic acid, which accumulates in the extracellular medium and can reduce the environmental pH to values as low as 3.0–3.5 [9–12, 17]. While this oxidative route enables rapid energy generation through the respiratory chain, it also diverts a substantial fraction of the available glucose away from intracellular metabolism. As a result, a large portion of the carbon substrate is secreted as gluconate rather than assimilated into central metabolic pathways required for BC biosynthesis [9–12, 17, 18].

Elimination of this oxidative pathway has been shown to fundamentally alter carbon allocation in cellulose-producing bacteria [9–11, 17, 18]. In work reported in **Chapter 2**, the strain *K. sucrofermentans* ATCC 700178 was engineered to generate the mutant KS003 by disrupting the gene encoding the PQQ-dependent mGDH. Removal of this enzyme prevented gluconic acid accumulation during glucose fermentation and maintained a more stable culture pH. Under these conditions, the KS003 strain exhibited a 5.77-fold increase in BC production relative to the wild-type strain when grown on glucose as the sole carbon source. However, this improvement in cellulose yield was accompanied by a significantly slower rate of glucose consumption, reflecting the loss of the rapid periplasmic oxidation pathway and the resulting dependence on cytoplasmic transport systems for glucose assimilation [11].

There are reports of metabolic engineering strategies have therefore focused on improving intracellular glucose uptake and phosphorylation in *Komagataeibacter* glucose dehydrogenase-deficient strains [10, 19]. Liu et al. [10] addressed this limitation in *K. xylinus* CGMCC 2955 using a markerless λ-Red and FLP/FRT-mediated recombination system to generate a *gcd* knockout strain. To compensate for the

reduced glucose assimilation caused by elimination of periplasmic oxidation, the authors introduced the glucose facilitator protein Glf from *Zymomonas mobilis*, which enables passive glucose transport across the cytoplasmic membrane [10, 20, 21]. This facilitator was combined with overexpression of the endogenous glucokinase gene (*glk*), reinforcing phosphorylation of glucose to glucose-6-phosphate and thereby strengthening flux into central metabolism [10]. The resulting *Zm*GLF–*Ks*GLK module significantly improved carbon conversion efficiency. Under standard conditions (25 g L^{-1} glucose, pH 6.0), the engineered strain produced 4.37 g L^{-1} BC while consuming 53.22% less glucose than the control strain, resulting in a 111.11% increase in glucose-to-cellulose conversion efficiency. Further optimization showed that the system performed best at an initial pH of 4.5, where the strain achieved a BC titer of 5.91 g L^{-1} and a yield of 0.52 g g^{-1} glucose, representing a 173.68% improvement in yield relative to the control. These results demonstrated that reinforcing cytoplasmic glucose uptake and phosphorylation can effectively redirect carbon flux toward cellulose synthesis once the competing oxidative pathway has been removed [10].

Parallel efforts explored alternative glucose uptake mechanisms based on the phosphoenolpyruvate-dependent glucose phosphotransferase system (PTSGlc). In their early work, Liu *et al.* tested heterologous PTS components from *Escherichia coli*, constructing strains expressing the glucose transporter *ptsG* alone or together with the *ptsHIcrr* operon. Although coexpression of these genes increased BC production relative to the *gcd* knockout control, the engineered strains did not surpass wild-type performance. The authors attributed this limitation to insufficient intracellular phosphoenolpyruvate (PEP), since each glucose molecule transported by the PTS consumes one mole of PEP as a phosphate donor [22, 23]. This energetic constraint suggested that the native glycolytic machinery of *K. xylinus* was unable to support efficient PTS-based glucose uptake [10].

Peng et al. [19] subsequently addressed this bottleneck through a more comprehensive metabolic engineering strategy. Recognizing that limited PEP availability constrained the functionality of heterologous PTS systems, the authors introduced the *E. coli* genes *ptsHIcrr* and *ptsG* together with a heterologous phosphofructokinase gene (*pfkA*) to reinforce glycolytic flux and increase the intracellular PEP pool. To avoid excessive metabolic burden caused by strong promoters, they also constructed an endogenous promoter library and identified the moderate-strength promoter P10220 as optimal for balanced expression of the transport and glycolytic modules. The resulting strain, GX08PTS03, demonstrated efficient glucose utilization without gluconic acid accumulation and achieved a BC titer of 7.74 g L^{-1} with a yield of 0.39 g g^{-1} glucose under optimized fermentation conditions. This represented an 87.41% increase in BC titer compared with the wild-type strain and confirmed that appropriate metabolic reinforcement can transform PTS-based transport into an effective strategy for improving BC production [19].

In addition to heterologous engineering approaches, transcriptomic studies have provided insight into potential native glucose transport systems in *Komagataeibacter*. Genome-wide expression profiling of *K. xylinus* E25 by Ryngajłło *et al.* revealed coordinated regulation of genes involved in glucose transport and phosphorylation during cellulose production. Among several homologs of the *E. coli* galactose permease

(GalP), the gene *galP3* was identified as the most highly expressed member of the family and was significantly upregulated under ethanol-supplemented conditions known to stimulate cellulose synthesis. The simultaneous induction of GalP3 and glucokinase expression suggests that this transporter may represent a key route for cytoplasmic glucose uptake in *Komagataeibacter* species [24].

Based on these observations, improving cytoplasmic glucose assimilation may represent an effective strategy to further enhance BC production in strains where the oxidative glucose pathway has already been removed [10, 19]. The present work therefore investigates whether strengthening glucose transport and phosphorylation can improve BC production in the KS003 background. Two transporter–kinase modules were evaluated: the heterologous *Zm*GLF–*Ks*GLK system previously demonstrated to enhance glucose assimilation in *Komagataeibacter*, and a *Ks*GALP3–*Ks*GLK module inspired by transcriptomic evidence of native glucose transport. By testing these constructs in both KS003 and wild-type backgrounds, this study aims to determine whether enhancing intracellular glucose uptake can alleviate metabolic limitations associated with mGDH deletion and further increase the efficiency of carbon conversion into BC.

3.3 Materials and Methods

3.3.1 Strains and culture conditions

K. sucrofermentans ATCC 700178 was used as the wild-type parental strain (KS001). A previously described mutant strain deficient in the PQQ-dependent glucose dehydrogenase (KS003) was used as an alternative genetic background. Each background was transformed either with the empty control vector KTK_015 or with constructs expressing the heterologous glucose uptake systems *Zm*GLF–*Ks*GLK or GAL–GLK. All strains, plasmids, and primers used in this study are listed in **Tables III.1** and **III.2**.

Komagataeibacter strains were propagated in Hestrin–Schramm (HS) medium composed of 5.0 g L^{-1} yeast extract, 2.7 g L^{-1} sodium phosphate dibasic, 1.15 g L^{-1} citric acid, and 0.5 g L^{-1} magnesium sulfate [25]. The pH was adjusted to 5.5 when required. Glycerol stocks were prepared from liquid cultures supplemented with 15% (v/v) glycerol and stored at -80 °C. Prior to experiments, cultures were synchronized by inoculating 5 mL HS medium containing 20 g L^{-1} glucose, 1.5% (v/v) ethanol and 1% (w/v) cellulase from glycerol stocks and incubating for three days at 30 °C with orbital shaking at 200 rpm. Cultures were subsequently transferred to 50 mL of fresh medium of the same composition and incubated for an additional 24 h under the same conditions. Cells were harvested by centrifugation at 3200 × g for 12 min, washed twice with HS medium lacking carbon source, and resuspended to the original volume. Fermentations were inoculated at a 1:10 volumetric ratio.

All plasmid assembly steps were performed in *E.* NZY5α competent cells using the manufacturer's protocol.

Table III.1: Strains used in this study.

Strain	**Relevant genotype / description**	**Reference**
Komagataeibacter sucrofermentans ATCC 700178	Wild-type parental strain	ATCC / this study
KS003	*K. sucrofermentans* ATCC 700178 Δ*mGDH* mutant lacking the PQQ-dependent membrane glucose dehydrogenase	Montenegro-Silva et al., 2024
KS001-KTK_015	Wild-type strain carrying empty KTK_015 destination vector	This study
KS001-*Zm*GLF–*Ks*GLK	Wild-type strain carrying KTK-D2.2a-*Ks*GALP3–*Ks*GLK	This study
KS001-*Ks*GALP3–*Ks*GLK	Wild-type strain carrying KTK-D2.2a-KsGALP3-KsGLK	This study
KS003-KTK_015	KS003 carrying empty KTK_015 destination vector	This study
KS003-*Zm*GLF–*Ks*GLK	KS003 carrying KTK-D2.2a-*Ks*GALP3–*Ks*GLK	This study
KS003-*Ks*GALP3–*Ks*GLK	KS003 carrying KTK-D2.2a-KsGALP3-KsGLK	This study
Escherichia coli NZY5α	Cloning host used for plasmid propagation and assembly	This study

Table III.2: Plasmids used in this study.

Plasmid / module	**KTK type**	**Antibiotic resistance**	**Description**	**Reference**
KTK_001	E1.0 dropout	Amp	Entry-level backbone used for cloning basic parts into the KTK system	Adapted from YTK / this study
KTK_002	E1.1	Amp	Constitutive promoter module, J23104 promoter	Adapted from Florea et al., 2016
KTK_029	E1.2	Amp	Ribosome binding site module, BBa_B0035	Adapted from Florea et al., 2016
KTK-E-GalP3	E1.3	Amp	Entry-level CDS module carrying *galP3*	This study
KTK-E-GLF	E1.3	Amp	Entry-level CDS module carrying *glf* from *Zymomonas mobilis*	This study
KTK-E-GLK	E1.3	Amp	Entry-level CDS module carrying *glk* from *Zymomonas mobilis*	This study

Plasmid / module	**KTK type**	**Antibiotic resistance**	**Description**	**Reference**
KTK_005	E1.4(I)	Amp	Terminator module, BBa_B0015	This study / KTK library
KTK_009	D1.1 dropout	Cm	Destination vector for assembly of the first transcription unit (TU1)	This study, adapted from pSEVA
KTK_010	D1.2 dropout	Cm	Destination vector for assembly of the second transcription unit (TU2)	This study, adapted from pSEVA
KTK-D1.1-GalP3	D1.1	Cm	TU1 expressing J23104–B0035–GalP3–B0015	This study
KTK-D1.1-GLF	D1.1	Cm	TU1 expressing J23104–B0035–GLF–B0015	This study
KTK-D1.2-GLK	D1.2	Cm	TU2 expressing J23104–B0035–GLK–B0015	This study
KTK_015	D2.2a	Spec	Destination vector for multigene assembly of two transcription units	This study, adapted from pSEVA
KTK-D2.2a-KsGALP3-KsGLK	D2.2a	Spec	Multigene construct carrying D1.1-GalP3 and D1.2-GLK	This study
KTK-D2.2a-*Ks*GALP3–*Ks*GLK	D2.2a	Spec	Multigene construct carrying D1.1-GLF and D1.2-GLK	This study

3.3.2 DNA assembly

Genetic constructs were assembled using the *Komagataeibacter* Toolkit (KTK) modular cloning system based on hierarchical Golden Gate assembly. All primers used in this study are listed in **Table III.3**. In this system, KTK_001 functions as the entry vector backbone for cloning individual genetic parts. After cloning into KTK_001, the resulting plasmids become entry modules whose identity is defined by their flanking Type IIS restriction overhangs. These overhangs determine the position of the part in downstream assemblies, corresponding to promoter (E1.1), ribosome binding site (E1.2), coding sequence (E1.3), and transcription terminator (E1.4) modules. Entry modules are assembled into D1 vectors to generate complete transcription units, and multiple transcription units can subsequently be assembled into D2 vectors to generate multigene constructs.

Table III.3: Primers used in this study.

Primer	**Sequence (5' – 3')**	**Purpose**
GalP3_FW	gataaccgtagTCGGTCTCCTATGGAAAATCAGCCCGCG	Amplification of *galP3* fragment 1 for cloning into KTK_001
GalP3_M_RV	TGCGCAGATCTTCCAGCAC	Internal reverse primer for *galP3* fragment split to remove internal BsaI site
GalP3_M_FW	TGGAAGATCTGCGCAGCG	Internal forward primer for *galP3* fragment split to remove internal BsaI site
GalP3_RV	ttgataatcttggtcTCAAGAACTACTTCTCCTGCGGCAG	Amplification of *galP3* fragment 2 for cloning into KTK_001
KS001_GalFW	gaccaagattatcaaaaaggatc	Amplification of KTK_001 backbone for In-Fusion cloning of *galP3*
KS001_GalRV	CCGActacggttatccac	Amplification of KTK_001 backbone for In-Fusion cloning of *galP3*
F1-GLF-FW	TCGGTCTCCTATGAGTTCTGAAAGTAGTCAGGGTCTAGTCAC	Amplification of *glf* fragment 1
F1-GLF-RV	AAGCCGGCGACCAGCACC	Amplification of *glf* fragment 1
F2-GLF-FW	GCTGGTCGCCGGCTTCAGAAG	Amplification of *glf* fragment 2
F2-GLF-RV	GGTCTCAAGAACTACTTCTGGGAGCGCCACATCTCC	Amplification of *glf* fragment 2

Primer	**Sequence (5' – 3')**	**Purpose**
KTK001glf_FW	GTAGTTCTTGAGACCAAGATTATCAAAAAGGATCTTCAC	Amplification of KTK_001 backbone for In-Fusion cloning of *glf* / *glk*
KTK001glf_RV	CTCATAGGAGACCGACTACGGTTATCCACAGAATCAGG	Amplification of KTK_001 backbone for In-Fusion cloning of *glf* / *glk*
F1-GLK-FW	TCGGTCTCCT ATGAAAGAGATCGTAGCAGTTGACATTG	Amplification of *glk* fragment 1
F1-GLK-RV	CCTCGGTTTCGCACACGAAG	Amplification of *glk* fragment 1
F2-GLK-FW	TGTGCGAAACCGAGGGTG	Amplification of *glk* fragment 2
F2-GLK-RV	TCAAGAATCAGTCTTGGCGGTAAGCC	Amplification of *glk* fragment 2
GLK-iPCR-FW	CCAGCTGGAAGACCGGAT	Inverse PCR primer for removal of internal BpiI site from *glk* construct
GLK-iPCR-RV	ATCCGGTCTTCCAGCTGG	Inverse PCR primer for removal of internal BpiI site from *glk* construct

The *galP3* coding sequence, which encodes the endogenous galactose permease homologue of *K. sucrofermentans* ATCC 700178, was amplified from the genomic DNA of this strain and cloned into the KTK_001 entry vector by In-Fusion cloning using two PCR fragments designed to remove an internal BsaI restriction site. GalP3 was amplified using the primer pairs GalP3_FW/GalP3_M_RV and GalP3_M_FW/GalP3_RV, while the vector backbone was amplified from KTK_001 using primers KS001_GalFW and KS001_GalRV. The resulting plasmid constituted the E1.3 entry module KTK-E-GalP3. Correct assemblies were verified by colony PCR and Sanger sequencing.

The GLF gene from *Z. mobilis* was cloned into KTK_001 using a similar strategy. Two PCR fragments were amplified from a boiled colony of *Z. mobilis* subsp. *mobilis* ZM4 (ATCC 31821) using primers F1-GLF-FW/F1-GLF-RV and F2-GLF-FW/F2-GLF-RV to remove an internal BsaI restriction site. The vector backbone was amplified using primers KTK001glf_FW and KTK001glf_RV. The fragments were assembled by In-Fusion cloning to generate the entry module KTK-E-GLF (E1.3). Correct assemblies were confirmed by

colony PCR and sequencing.

The GLK gene from *Z. mobilis* was cloned into KTK_001 following the same approach. Two PCR fragments were amplified with primers F1-GLK-FW/F1-GLK-RV and F2-GLK-FW/F2-GLK-RV and assembled with a backbone amplified using primers KTK001glf_FW and KTK001glf_RV. An internal BpiI site was subsequently removed by inverse PCR using primers GLK-iPCR-FW and GLK-iPCR-RV, followed by In-Fusion circularization, forming KTK-E-GLK. Final constructs were verified by colony PCR and Sanger sequencing.

The next step consisted in the assembly of the entry level coding sequences into D1 expression plasmids, named KTK-D1.1-GalP3, KTK-D1.1-GLF and KTK-D1.2-GLK. Transcription units were assembled using BsaI-HFv2 (New England Biolabs) Golden Gate reactions. Assemblies contained 25 fmol of the promoter module KTK_002 (J23104), the ribosome binding site module KTK_029 (BBa_B0035), the respective coding sequence module (KTK-E-GalP3, KTK-E-GLF or KTK-E-GLK), and the terminator module KTK_005 (BBa_B0015), together with 12.5 fmol of the D1 backbone vector (KTK_009 for D1.1 constructs or KTK_010 for D1.2 constructs). Reactions were performed with an initial digestion at 37 °C for 30 min followed by 25 cycles of 5 min at 37 °C and 5 min at 16 °C, and a final digestion at 37 °C for 30 min. Assemblies were transformed into *E. coli* NZY5α and verified by colony PCR and BpiI-HF restriction digestion.

The multigene constructs, KTK-D2.2a-*Ks*GALP3–*Ks*GLK and KTK-D2.2a-*Zm*GLF-*Ks*GLK, were assembled by combining D1 transcription units into the D2.2a vector KTK_015, which carries spectinomycin resistance. Reactions contained 25 fmol of the respective D1 constructs (KTK-D1.1-*Ks*GalP3 or KTK-D1.1-*Zm*GLF together with KTK-D1.2-GLK) and 12.5 fmol of the D2 backbone KTK_015. Golden Gate assembly was performed using BpiI-HF with the same cycling conditions described above. Correct assemblies were verified by colony PCR and BsaI-HFv2 digestion.

3.3.3 Transformation of *K. sucrofermentans*

Electrocompetent cells of *K. sucrofermentans* ATCC 700178 were prepared following the optimized conditions described in **Chapter 4**. Briefly, cells grown in HS medium supplemented with cellulase were harvested in mid-exponential phase, washed with ice-cold 1 mM HEPES, and resuspended in 15% glycerol to obtain electrocompetent cells. For transformation, electrocompetent cells were mixed with plasmid DNA and transferred to 0.1 cm (1 mm) electroporation cuvettes. Electroporation was performed using 1.80 kV, 25 μF, and 200 Ω. Immediately after the pulse, cells were recovered in HS medium and incubated at 30 °C for 8 hours prior to plating on selective HS agar plates. *K. sucrofermentans* transformants were screened and confirmed by colony PCR.

3.3.4 Metabolite analysis and BC quantification

Metabolite concentrations were determined by high-performance liquid chromatography (HPLC) using a Bio-Rad Aminex HPX-87H column operated at 55 °C with 5 mM H_2SO_4 as the mobile phase at a flow rate

of 0.5 mL min^{-1}. BC pellicles were treated with 1% (w/v) NaOH until white or transparent, washed with distilled water until neutral pH, dried at 100 °C, and weighed to determine BC production.

3.3.5 Data analysis

Data processing and statistical analysis were performed in Python using the pandas, numpy, and matplotlib libraries. Pairwise comparisons between strains were performed using two-sided Welch's t-tests.

3.4 Results and Discussion

As described in Chapter 2, disruption of the PQQ-dependent membrane glucose dehydrogenase (mGDH) in *K. sucrofermentans* ATCC 700178 generated the mutant strain KS003, which exhibits strongly reduced gluconic acid formation and improved BC (BC) production [11]. In acetic acid bacteria, mGDH catalyzes the periplasmic oxidation of glucose to glucono-δ-lactone, which subsequently hydrolyzes to gluconic acid [3, 13, 16, 17]. Because this enzyme transfers electrons directly to the respiratory chain, it enables rapid energy generation without requiring cytoplasmic glucose transport [3, 13–17]. As a consequence, a large fraction of extracellular glucose can be oxidized and secreted as gluconate rather than assimilated into intracellular metabolism, effectively diverting carbon away from biosynthetic pathways such as cellulose formation [9–11, 17, 18]. The metabolic phenotype of KS003 observed in the present work is therefore consistent with the strain characterization described previously, where deletion of the PQQ-dependent glucose dehydrogenase prevented gluconate accumulation and increased BC production approximately 5.77-fold compared with the parental strain [11].

Once this oxidative pathway is removed, however, the metabolic bottleneck shifts. In the absence of mGDH, glucose utilization becomes dependent on transport across the cytoplasmic membrane and subsequent phosphorylation to glucose-6-phosphate, the entry point into central metabolism and the precursor route toward UDP-glucose, the direct substrate for cellulose synthase [5, 9–11, 13, 15–18, 26]. Several metabolic engineering studies have therefore proposed that intracellular glucose assimilation may become limiting in gcd-deficient strains [9–11, 17, 18]. Liu *et al.* demonstrated this concept in *K. xylinus*, where expression of the glucose facilitator Glf from *Z. mobilis* combined with glucokinase increased the efficiency with which glucose was converted into cellulose by improving cytoplasmic glucose uptake and phosphorylation [10]. The fact that the Glf expressing *K. xylinus* strain still wasn't able to consume a considerable fraction of the available glucose motivated a more extensive engineering strategy that pursued the same objective through alternative uptake mechanisms [19]. Peng *et al.* reconstructed a heterologous phosphotransferase system (PTSGlc) in a gcd-deficient *K. xylinus* strain, redirecting glucose metabolism away from gluconate formation and substantially increasing BC titers and yield by strengthening intracellular glucose flux [19].

Transcriptomic analyses of *Komagataeibacter* metabolism provide additional insight into why these strategies may succeed. In *K. xylinus* E25, genes involved in glucose transport and phosphorylation are coordinately upregulated under conditions that stimulate cellulose synthesis, while pathways competing

for carbon are repressed. In particular, homologs of the *E. coli* galactose permease (*galP*) have been proposed to function as glucose transporters in the cytoplasmic membrane, and among these isoforms the gene *galP3* was reported as the most highly expressed member of the family and significantly induced together with glucokinase expression under ethanol-supplemented conditions that enhance cellulose production [24]. These observations support the interpretation that enhanced cytoplasmic glucose uptake and phosphorylation favor the formation of glucose-6-phosphate and its downstream conversion to UDP-glucose, thereby reinforcing the metabolic flux toward cellulose biosynthesis rather than oxidative glucose metabolism.

Building upon this framework, the present study examined whether strengthening intracellular glucose uptake could further improve BC production in the KS003 background, where the dominant oxidative carbon sink had already been removed. Two transporter–kinase modules were therefore evaluated: *Zm*GLF–*Ks*GLK, previously explored in *Komagataeibacter* as a strategy to compensate for reduced glucose assimilation in gcd-deficient strains, and *Ks*GALP3–*Ks*GLK, based on the highly expressed GalP-family permease suggested by transcriptomic analyses. By testing these modules in both KS003 and wild-type backgrounds, the study aimed to determine whether alternative glucose transport routes could further increase the fraction of carbon directed toward cellulose synthesis.

BC production, glucose consumption, and organic acid formation were quantified for the parental strains and their plasmid-bearing derivatives. Consistent with the phenotype previously reported for the mGDH knockout, the KS003 background produced substantially higher BC titers than the wild-type strain. The plasmid-free KS003 strain produced 1.45 ± 0.07 g L^{-1} BC, whereas the parental wild-type strain produced only 0.57 ± 0.32 g L^{-1} (**Figure III.1-A**). This difference reflects the removal of gluconate formation as a dominant carbon sink and illustrates the fundamental metabolic asymmetry between the two genetic backgrounds. Introduction of the empty D2.2a vector (KTK_015) reduced BC production in both backgrounds, yielding 0.70 ± 0.00 g L^{-1} in KS003-KTK_015 and 0.50 ± 0.28 g L^{-1} in KS001-KTK_015. Expression of the transporter–kinase modules produced intermediate phenotypes. The KS003-*Ks*GALP3–*Ks*GLK strain produced 1.10 ± 0.14 g L^{-1} BC, while KS003-*Ks*GALP3-*Ks*GLK produced 0.90 ± 0.10 g L^{-1}. The fact that the difference between KS003-KTK_015 and KS003-*Ks*GALP3–*Ks*GLK did not hit any of the statistical significance thresholds despite the considerable difference in volumetric productivity can be attributed to the N=2 in both datapoints. In the wild-type background, BC titers remained low, with KS001-*Ks*GALP3–*Ks*GLK producing 0.40 ± 0.00 g L^{-1} and KS001-*Ks*GALP3-*Ks* GLK producing 0.47 ± 0.06 g L^{-1} (**Figure III.1-A**).

Normalization of BC production to glucose consumption revealed even larger differences between the two genetic backgrounds (**Figure III.1-B**). The plasmid-free KS003 strain achieved a BC yield of 0.150 ± 0.014 mg BC per mg glucose consumed, whereas the wild-type strain exhibited a yield of only 0.0267 ± 0.0153 mg mg^{-1}. In KS003-KTK_015 this value decreased to 0.080 ± 0.014 mg mg^{-1}, while KS003-*Ks*GALP3–*Ks*GLK and KS003-*Ks*GALP3-*Ks*GLK reached 0.150 ± 0.014 mg mg^{-1} and 0.090 ± 0.010 mg mg^{-1}, respectively (**Figure III.1-B**). Overall, the KS003 background therefore converted glucose to BC approximately three- to seven-fold more efficiently than the wild-type strain.

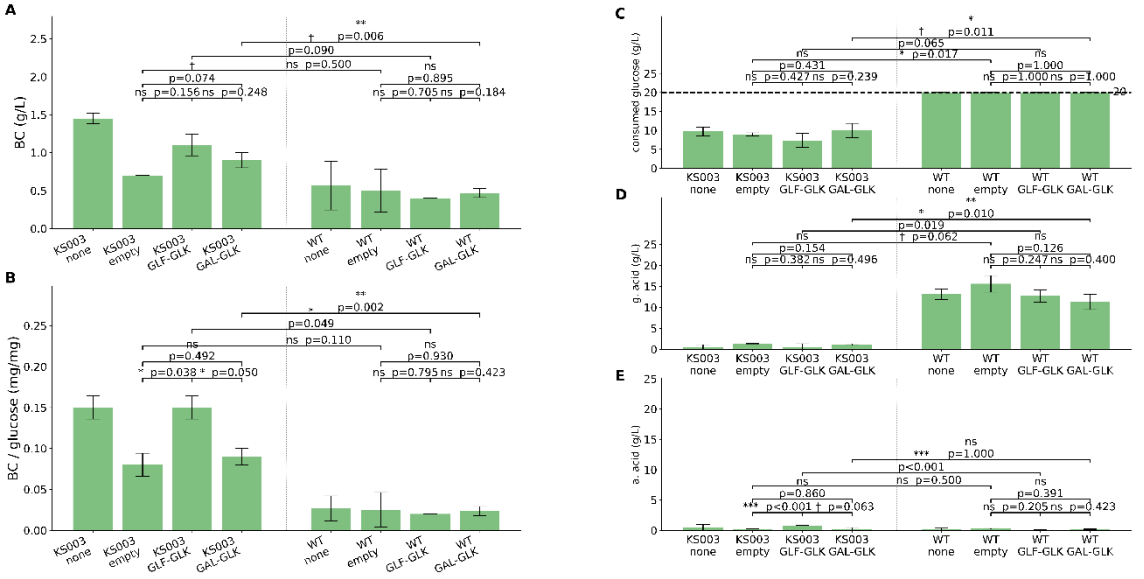


Figure III.1: Effects of heterologous glucose uptake modules on bacterial cellulose production and metabolite formation in K. sucrofermentans. Strains derived from the wild-type (KS001) K. sucrofermentans ATCC 700178 and from the ΔmGDH mutant KS003 were transformed with either no plasmid ("none"), an empty vector control, or plasmids encoding the glucose facilitator–glucokinase module (*Zm*GLF–*Ks*GLK) or the galactose permease–glucokinase module (GAL–GLK). (A) Final BC (BC) concentration (g L^{-1}). (B) BC yield relative to consumed glucose (mg mg^{-1}). (C) Total glucose consumed during cultivation (g L^{-1}). The dashed line indicates the initial glucose concentration (20 g L^{-1}). (D) Gluconic acid produced (g L^{-1}). (E) Residual acetic acid concentration (g L^{-1}). Bars represent mean values of biological replicates (n = 2–3) and error bars indicate standard deviation. Statistical significance between selected conditions was evaluated using Welch's t-test; p values are indicated above brackets. Significance levels are denoted as $p \leq 0.001$, $p \leq 0.01$, $p \leq 0.05$*, † $p \leq 0.10$, and ns (not significant). The vertical dotted line separates KS003-derived strains from KS001-derived strains. The glucose consumption profiles further illustrate the metabolic divergence between the two strains. All wild-type derivatives consumed essentially all available glucose (20 g L^{-1}) during cultivation, whereas KS003 strains consumed only approximately half of the available glucose.

The contrast between the two genetic backgrounds is even more evident when examining gluconic acid production (**Figure III.1-D**). Wild-type strains accumulated large amounts of gluconate, reaching approximately 11–16 g L^{-1} depending on the construct present. In the KS003 background, by contrast, gluconate accumulation remained minimal, ranging only from approximately 0.45 to 1.35 g L^{-1} across constructs (**Figure III.1-D**). Interestingly, when comparing the gluconate production between KS001-KTK_015 and KS001-*Ks*GALP3–*Ks*GLK, the p-value of 0.126 suggests that increasing the N in this experiment could give significance to the observation that that, at least this construct, might be diverging the glucose flux away from gluconate production. However, it is not possible to rule out the hypothesis that the difference may lie in the profile of different gluconic acids, since in this work, only D-gluconate was quantified [13].

Residual acetic acid concentrations remained low across all strains and conditions, with no consistent trend related to either genetic background or heterologous gene expression. According to our knowledge

about the strains' diauxic acetate metabolism, acquired in the characterization made in **Chapter 2**, the most prolific BC production phase during growth corresponds to the acetate assimilation phase (specially in KS003) [11]. As neither ethanol or acetate was detected at significant amounts, we can extrapolate that all datapoints capture the most significant production timeframe (**Figure III.1-E**).

Taken together, the results reveal a clear hierarchy of metabolic constraints governing cellulose production in these strains. In the presence of mGDH, the oxidative pathway dominates glucose metabolism and limits the effectiveness of intracellular transport engineering [9, 13, 17]. Once this pathway is removed, however, intracellular glucose assimilation becomes a more relevant control point [9–11, 18]. The modest improvements observed for *Zm*GLF–*Ks*GLK and *Ks*GALP3–*Ks*GLK relative to the empty-vector control in KS003 are therefore consistent with a model in which transporter engineering can enhance intracellular flux but cannot fully compensate for physiological constraints such as plasmid burden, energetic costs, or downstream metabolic limitations (Figure III.**1A**, **B**, and **C**) [10, 19, 27–29].

Comparison with previous engineering studies supports this interpretation. Liu *et al.* showed that combining a facilitator-type transporter with glucokinase could improve glucose-to-cellulose conversion in gcd-deficient *K. xylinus*, whereas the transporter alone had only limited effect [10]. Peng *et al.* extended this principle by introducing a heterologous phosphotransferase system together with additional metabolic modifications, achieving substantially higher BC titers in engineered gcd-deficient strains [19]. Within this broader context, the present work demonstrates that the same metabolic principles apply in *K. sucrofermentans*. The KS003 strain confirms the dominant role of mGDH in determining carbon allocation between gluconate production and cellulose biosynthesis, while the transporter-kinase modules illustrate how intracellular glucose uptake can provide incremental improvements once that dominant pathway is eliminated.

3.5 Conclusion

Collectively, these results reinforce a simple hierarchy of constraints for glucose-fed *Komagataeibacter*: as long as mGDH is present, periplasmic oxidation dominates carbon partitioning and drives substantial gluconate accumulation, limiting the impact of intracellular uptake engineering on BC formation [9–11, 18, 19]. After mGDH disruption (KS003), carbon is forced through cytoplasmic entry points, yielding markedly higher glucose-to-BC conversion efficiency, but at the cost of slower overall glucose utilization. In this context, the *Zm*GLF–*Ks*GLK and *Ks*GALP3–*Ks*GLK modules provided only incremental gains relative to the empty-vector control, consistent with a scenario where (i) intracellular uptake and phosphorylation can be partially strengthened, yet (ii) plasmid burden, expression imbalance, and downstream pathway capacity become the dominant limitations.

From a forward-looking strain-design standpoint, literature indicates that the phosphotransferase system approach is mechanistically superior for forcing glucose into intracellular metabolism because transport and phosphorylation are coupled, which can reduce futile cycling and tighten control over intracellular glucose-6-phosphate supply [10, 19]. However, in *Komagataeibacter* this advantage is not "plug-and-play":

PTS functionality requires sufficient phosphoenolpyruvate (PEP) availability and balanced expression of multiple heterologous components, and overly strong expression can impose severe burden and impair transformant fitness [10, 19]. Peng *et al.* explicitly demonstrate that a performant PTS platform in a *gcd*-deficient background required (a) installation of *ptsHIcrr* + *ptsG* and (b) reinforcement of glycolytic flux via *pfkA*, together with promoter optimization to avoid growth inhibition, ultimately enabling high BC titer without gluconate accumulation [19]. In practical terms, PTS-based solutions appear "better" in principle, but they demand substantially higher engineering effort and tuning than two-gene transporter–kinase modules.

A clear next step is to repeat this experiment with more replicates and in larger vessels (in example, 250 mL volumetric flasks) to increase certainty in the phenotypes, and then to eliminate plasmid-associated burden and stabilize phenotypes by integrating uptake modules into the chromosome. Given that KS003 was generated by interrupting the mGDH locus, the same landing-pad architecture can be repurposed for functional replacement: the disrupted mGDH region can serve as a defined genomic insertion site to install *Ks*GALP3–*Ks*GLK or *Zm*GLF–*Ks*GLK as single-copy, insulated cassettes, converting the original oxidative "carbon sink" locus into a hardwired intracellular assimilation module. This strategy would (i) preserve the low-gluconate phenotype, (ii) improve genetic stability, and (iii) reduce variability associated with copy number and maintenance costs. In parallel, a longer-term route would be to implement a chromosomal PTS cassette (e.g., *ptsHIcrr/ptsG* with glycolytic reinforcement such as *pfkA*), but this should be approached as a multi-parameter optimization problem (PEP supply, promoter strength, expression ratios, and growth/BC trade-offs) rather than a single construct swap, consistent with the engineering burden highlighted in PTS-based studies.

3.6 References

[1] Shan Liu, Muxuan Yang, and Weinan Xu. "Three-Dimensional Hierarchical Cellulose Structures Based on Microbial Synthesis and Advanced Biofabrication". In: *Chem & Bio Engineering* 1.10 (2024), pp. 876–886.

[2] Gerald Enos Shija. "Bacterial cellulose for emerging contaminants: A review of applications for PFAS, nanoplastics, and endocrine disruptors in water treatment". In: *Science of The Total Environment* 1008 (2025), p. 180976.

[3] Maria Gullo et al. "Biotechnological production of cellulose by acetic acid bacteria: current state and perspectives". In: *Applied Microbiology and Biotechnology* 102.16 (2018), pp. 6885–6898.

[4] Michael Florea et al. "Engineering control of bacterial cellulose production using a genetic toolkit and a new cellulose-producing strain". In: *Proceedings of the National Academy of Sciences of the United States of America* 113.24 (2016), E3431–E3440.

[5] P Ross, R Mayer, and M Benziman. "Cellulose biosynthesis and function in bacteria". In: *Microbiological Reviews* 55.1 (1991), pp. 35–58.

[6] Kieran M. Lynch et al. “Physiology of Acetic Acid Bacteria and Their Role in Vinegar and Fermented Beverages”. In: *Comprehensive Reviews in Food Science and Food Safety* 18.3 (2019), pp. 587–625.

[7] Ronagul Turganova et al. “Bacterial Cellulose for Sustainable Food Packaging: Production Pathways, Structural Design, and Functional Modification Strategies”. In: *Polymers* 17.23 (2025), p. 3165.

[8] Thomas Meslier et al. “A Comprehensive Review of Clinical Studies on Bacterial Cellulose: From the Earliest Uses to Contemporary Innovations”. In: *Advanced Healthcare Materials* 14.27 (2025).

[9] Chia Hung Kuo, Hsin Yin Teng, and Cheng Kang Lee. “Knock-out of glucose dehydrogenase gene in Gluconacetobacter xylinus for bacterial cellulose production enhancement”. In: *Biotechnology and Bioprocess Engineering* 20.1 (2015), pp. 18–25.

[10] Ling-Pu Liu et al. “A Lambda Red and FLP/FRT-Mediated Site-Specific Recombination System in Komagataeibacter xylinus and Its Application to Enhance the Productivity of Bacterial Cellulose”. In: *ACS Synthetic Biology* 9.11 (2020), pp. 3171–3180.

[11] Pedro Montenegro-Silva et al. “Enhanced bacterial cellulose production in Komagataeibacter sucrofermentans: impact of different PQQ-dependent dehydrogenase knockouts and ethanol supplementation”. In: *Biotechnology for Biofuels and Bioproducts* 17.1 (2024).

[12] D Mikkelsen et al. “Influence of different carbon sources on bacterial cellulose production by Gluconacetobacter xylinus strain ATCC 53524”. In: *Journal of Applied Microbiology* 107.2 (2009), pp. 576–583.

[13] Zhijie Qin et al. “Dehydrogenases of acetic acid bacteria”. In: *Biotechnology Advances* 54 (2022), p. 107863.

[14] Bin Wang, Yanchun Shao, and Fusheng Chen. “Overview on mechanisms of acetic acid resistance in acetic acid bacteria”. In: *World Journal of Microbiology and Biotechnology* 31.2 (2015), pp. 255–263.

[15] François Barja et al. “Physiology of Komagataeibacter spp. During Acetic Acid Fermentation”. In: *Acetic Acid Bacteria*. Springer Japan, 2016, pp. 201–221.

[16] Kazunobu Matsushita, Hirohide Toyama, and Osao Adachi. “Respiratory Chains and Bioenergetics of Acetic Acid Bacteria”. In: *Advances in Microbial Physiology* 36 (1994), pp. 247–301.

[17] Peter Wulf, Koen Joris, and Erick J. Vandamme. “Improved Cellulose Formation by anAcetobacter xylinum Mutant Limited in (Keto)Gluconate Synthesis”. In: *Journal of Chemical Technology & Biotechnology* 67.4 (1996), pp. 376–380.

[18] Toru Shigematsu et al. “Cellulose production from glucose using a glucose dehydrogenase gene (gdh)-deficient mutant of gluconacetobacter xylinus and its use for bioconversion of sweet potato pulp”. In: *Journal of Bioscience and Bioengineering* 99.4 (2005), pp. 415–422.

[19] Zhaojun Peng et al. “Engineering PTS-based glucose metabolism for efficient biosynthesis of bacterial cellulose by Komagataeibacter xylinus”. In: *Carbohydrate Polymers* 343 (2024).

[20] Corrine Parker et al. “Characterization of the *Zymomonas mobilis* glucose facilitator gene product (*glf*) in recombinant *Escherichia coli* : examination of transport mechanism, kinetics and the role of glucokinase in glucose transport”. In: *Molecular Microbiology* 15.5 (1995), pp. 795–802.

[21] Anthony A. DiMarco and Antonio H. Romano. “d -Glucose Transport System of *Zymomonas mobilis*”. In: *Applied and Environmental Microbiology* 49.1 (1985), pp. 151–157.

[22] P W Postma, J W Lengeler, and G R Jacobson. “Phosphoenolpyruvate:carbohydrate phosphotransferase systems of bacteria”. In: *Microbiological Reviews* 57.3 (1993), pp. 543–594.

[23] Josef Deutscher, Christof Francke, and Pieter W. Postma. “How Phosphotransferase System-Related Protein Phosphorylation Regulates Carbohydrate Metabolism in Bacteria”. In: *Microbiology and Molecular Biology Reviews* 70.4 (2006), pp. 939–1031.

[24] Małgorzata Ryngajłło et al. “Effect of ethanol supplementation on the transcriptional landscape of bionanocellulose producer Komagataeibacter xylinus E25”. In: *Applied Microbiology and Biotechnology* 103.16 (2019), pp. 6673–6688.

[25] S. Hestrin and M. Schramm. “Synthesis of cellulose by *Acetobacter xylinum* . 2. Preparation of freeze-dried cells capable of polymerizing glucose to cellulose”. In: *Biochemical Journal* 58.2 (1954), pp. 345–352.

[26] Reeta Rani Singhania et al. “Genetic modification for enhancing bacterial cellulose production and its applications”. In: *Bioengineered* 12.1 (2021), pp. 6793–6807.

[27] Jiwei Mao et al. “Relieving metabolic burden to improve robustness and bioproduction by industrial microorganisms”. In: *Biotechnology Advances* 74 (2024), p. 108401.

[28] A. Rozkov et al. “Characterization of the metabolic burden on *Escherichia coli* DH1 cells imposed by the presence of a plasmid containing a gene therapy sequence”. In: *Biotechnology and Bioengineering* 88.7 (2004), pp. 909–915.

[29] William E. Bentley et al. “Plasmid□encoded protein: The principal factor in the “metabolic burden” associated with recombinant bacteria”. In: *Biotechnology and Bioengineering* 35.7 (1990), pp. 668–681.

4 Design Considerations for Implementing CRISPR–Cas9 Genome Editing in *Komagataeibacter sucrofermentans* ATCC 700178

4.1 Abstract

Bacterial cellulose (BC) produced by *Komagataeibacter* species is a high-purity, structurally crystalline biopolymer with broad applications in food, biomedical, and advanced material sectors. Industrial deployment of genetically engineered BC-producing strains requires markerless and scarless genome editing strategies to ensure genetic stability and regulatory compliance. Although CRISPR–Cas9 remains the most powerful counterselection-based genome editing platform in Gram-negative bacteria, its implementation in non-model hosts is frequently constrained by Cas9-associated toxicity and host-specific repair limitations.

This study attempted to construct a single-plasmid CRISPR–Cas9 system compatible with the *Komagataeibacter* Tool Kit (KTK) framework for genome editing of *K. sucrofermentans* ATCC 700178. Three architectures were tested, differing in promoter strength, regulatory logic, and replication origin. All nuclease-active Cas9 constructs failed to yield transformants, independently of constitutive or inducible control and irrespective of electroporation optimization. In contrast, the corresponding dCas9 plasmid was successfully transformed and maintained, and electroporation optimization increased transformation efficiency of non-toxic constructs to 1.24×10^6 CFU μg^{-1} DNA. These results demonstrate that transformation inefficiency is not the limiting factor; rather, basal Cas9 expression is sufficient to induce lethal DNA damage in this host.

To contextualize these findings, a comprehensive cross-genera analysis of CRISPR–Cas9 system design in non-model Gram-negative bacteria was performed. Replication origin choice, Cas9 dosage control, recombinase compatibility, donor architecture, plasmid curing strategies, and delivery routes were systematically compared. The analysis reveals that successful implementation depends on strict temporal separation between DNA delivery, recombination, and nuclease activation, as well as precise tuning of effective Cas9 dosage to match host repair capacity. Constitutive single-plasmid architectures commonly used in Enterobacterales are frequently incompatible with more sensitive hosts.

Collectively, the experimental data and comparative analysis indicate that CRISPR–Cas9 development in *Komagataeibacter* requires architectural redesign rather than incremental tuning. Tightly regulated dual-plasmid systems, enhanced recombination support, and delayed Cas9 activation emerge as key design principles. In parallel, CRISPRi and base-editing approaches provide immediately deployable alternatives that bypass double-strand break–associated lethality. These findings establish a rational framework for

developing robust, markerless genome editing platforms in BC-producing *Komagataeibacter* strains.

4.2 Introduction

Bacterial cellulose (BC) is a sustainable and renewable biopolymer known for its high purity, porosity, breathability structural crystallinity, and excellent water-holding capacity [1–4]. These superior physicochemical properties have led to its extensive utilization across the food, medical, paper, and electronics industries. To meet the specific requirements of these diverse applications it is crucial to develop precise genetic engineering tools to modify BC-producing strains [2, 3]. For industrial and regulatory purposes, these genome editing methods must be markerless and scarless to ensure the stability and safety of the engineered organisms [1].

Significant progress has been made in developing genetic toolkits for the *Komagataeibacter* genus, the predominant producers of BC. Traditional methods include the -Red and FLP/FRT-mediated recombineering systems, which enable site-specific recombination and marker removal [5]. Furthermore, markerless editing has been successfully achieved in 2025 using SacB-mediated systems (e.g., pK18mobsacB), which utilize a two-round homologous recombination (HR) strategy and sucrose counterselection to eliminate plasmid backbones, achieving efficiencies up to 83.33% [1]. CRISPR interference (CRISPRi) has been implemented to provide a high-throughput method for regulating BC structure by controlling the expression of essential genes like *galU* [2]. It was also demonstrated in the *Komagataeibacter* tool kit (KTK) where the catalytically inactive dCas9 is expressed under influence of a random promoter [6] . Additionally, CRISPR-guided base editors now allow for highly efficient (80%–90%) multiplex editing by introducing premature stop codons without the need for foreign DNA templates or double-strand breaks [3].

Despite these advancements, CRISPR-Cas9 remains the most powerful starting point for markerless genome editing due to its high specificity and ability to induce HR [4, 7–9]. However, implementing CRISPR-Cas9 in *Komagataeibacter* is hindered by Cas9-related toxicity, where excessive protein expression leads to high lethality rates even in the absence of target cleavage. In 2025, one successful application required significant optimization, such as tuning the ribosome-binding site (RBS) to reduce Cas9 translation levels while maintaining sufficient guide RNA expression [4].

In this work, we attempted to build a single-plasmid CRISPR–Cas9 tool for the genome editing of *K. sucrofermentans* ATCC 700178. Every assembled active-Cas9 construct failed to yield transformants. To rule out DNA delivery as the limiting factor, electroporation was systematically optimized, substantially improving transformation efficiency (validated with a catalytically dead dCas9 control); nevertheless, guideless active-Cas9 expression remained too toxic to recover colonies. The rationale, methods, and results of these attempts are presented in the Materials and Methods and Results sections that follow. To understand the basis of this recalcitrance, we then surveyed the literature on CRISPR–Cas9 implementation in non-model Gram-negative bacteria, compiled as online supplementary material (Github link), and distilled it into a set of design rules to guide genome editing in *Komagataeibacter* and other recalcitrant hosts.

4.3 Materials and Methods

4.3.1 Strains, plasmids, media and culture conditions

All strains and plasmids used in this study are listed in **Table IV.1** and **Table IV.2**, respectively.

Escherichia coli NZY5α, *E. coli* NEB Turbo, and their derived strains were cultivated in standard LB medium at 37 °C, either in liquid culture or on LB agar plates supplemented with 15 g L^{-1} agar.

Komagataeibacter sucrofermentans was cultivated in Hestrin–Schramm (HS) medium supplemented with 2% (w/v) glucose at 30 °C. Liquid cultures were supplemented with 0.1% (w/v) cellulase to prevent cellulose pellicle formation and ensure homogeneous growth. Solid media were prepared by addition of agar at standard concentration.

Unless otherwise stated, pre-cultures of *K. sucrofermentans* were initiated by inoculating static HS 2% glucose medium with a single 10 μL loop of glycerol stock stored at −80 °C. These cultures were subsequently used to inoculate fresh medium at a 1:200 dilution for preparation of electrocompetent cells.

Table IV.1: Strains used in this study.

Strain	**Genotype**	**Reference**
E. coli NZY5α	F' proA$^+$$proB^+lacI\hat{}q$ΔlacZΔM15 / fhuA2 Δ(lac-proAB) glnV galK16 galE15 R(zgb-210::Tn10) Tet^S endA1 thi-1 Δ(hsdS-mcrB)5	NZYTech©
Komagataeibacter sucrofermentans ATCC 700178	Wild-type parental strain	[10]
E. coli NEB Turbo (pKTK_001)	F' proA$^+$$proB^+lacI\hat{}q$ΔlacZΔM15 / fhuA2 Δ(lac-proAB) glnV galK16 galE15 R(zgb-210::Tn10) Tet^S endA1 thi-1 Δ(hsdS-mcrB)5; pKTK_001	[6]
E. coli NZY5α (pCasAb-apr)	fhuA2 Δ(argF-lacZ)U169 phoA glnV44 Φ80 Δ(lacZ)M15 gyrA96 recA1 relA1 endA1 thi-1 hsdR17; pCasAb-apr	[11]
E. coli NEB Turbo (pKTK_045)	F' proA$^+$$proB^+lacI\hat{}q$ΔlacZΔM15 / fhuA2 Δ(lac-proAB) glnV galK16 galE15 R(zgb-210::Tn10) Tet^S endA1 thi-1 Δ(hsdS-mcrB)5; pKTK_045	[6]
E. coli NEB Turbo (pKTK_095)	F' proA$^+$$proB^+lacI\hat{}q$ΔlacZΔM15 / fhuA2 Δ(lac-proAB) glnV galK16 galE15 R(zgb-210::Tn10) Tet^S endA1 thi-1 Δ(hsdS-mcrB)5; pKTK_095	[6]
E. coli NZY5α (pKTK001-Cas9)	fhuA2 Δ(argF-lacZ)U169 phoA glnV44 Φ80 Δ(lacZ)M15 gyrA96 recA1 relA1 endA1 thi-1 hsdR17; pKTK001-Cas9	This work
E. coli NZY5α (pKTK-D1.1-Cas9)	fhuA2 Δ(argF-lacZ)U169 phoA glnV44 Φ80 Δ(lacZ)M15 gyrA96 recA1 relA1 endA1 thi-1 hsdR17; pKTK-D1.1-Cas9	This work

Table IV.1: Strains used in this study.

Strain	**Genotype**	**Reference**
E. coli NZY5α (pKTK_095-Cas9)	fhuA2 Δ(argF-lacZ)U169 phoA glnV44 Φ80 Δ(lacZ)M15 gyrA96 recA1 relA1 endA1 thi-1 hsdR17; pKTK_095-Cas9	This work
E. coli NZY5α (pKTK_sgJ23117)	fhuA2 Δ(argF-lacZ)U169 phoA glnV44 Φ80 Δ(lacZ)M15 gyrA96 recA1 relA1 endA1 thi-1 hsdR17; pKTK_sgJ23117	This work
E. coli NZY5α (pKTK-E-lacI)	fhuA2 Δ(argF-lacZ)U169 phoA glnV44 Φ80 Δ(lacZ)M15 gyrA96 recA1 relA1 endA1 thi-1 hsdR17; pKTK-E-lacI	This work
E. coli NZY5α (pKTK-D1-lacI)	fhuA2 Δ(argF-lacZ)U169 phoA glnV44 Φ80 Δ(lacZ)M15 gyrA96 recA1 relA1 endA1 thi-1 hsdR17; pKTK-D1-lacI	This work
E. coli NEB Turbo (pKTK_002)	F' proA$^+$$proB^+lacI\hat{}q$ΔlacZΔM15 / fhuA2 Δ(lac-proAB) glnV galK16 galE15 R(zgb-210::Tn10) Tet^S endA1 thi-1 Δ(hsdS-mcrB)5; pKTK_002	[6]
E. coli NEB Turbo (pKTK_003)	F' proA$^+$$proB^+lacI\hat{}q$ΔlacZΔM15 / fhuA2 Δ(lac-proAB) glnV galK16 galE15 R(zgb-210::Tn10) Tet^S endA1 thi-1 Δ(hsdS-mcrB)5; pKTK_003	[6]
E. coli NEB Turbo (pKTK_005)	F' proA$^+$$proB^+lacI\hat{}q$ΔlacZΔM15 / fhuA2 Δ(lac-proAB) glnV galK16 galE15 R(zgb-210::Tn10) Tet^S endA1 thi-1 Δ(hsdS-mcrB)5; pKTK_005	[6]
E. coli NEB Turbo (pKTK_042)	F' proA$^+$$proB^+lacI\hat{}q$ΔlacZΔM15 / fhuA2 Δ(lac-proAB) glnV galK16 galE15 R(zgb-210::Tn10) Tet^S endA1 thi-1 Δ(hsdS-mcrB)5; pKTK_042	[6]
E. coli NEB Turbo (pKTK_009)	F' proA$^+$$proB^+lacI\hat{}q$ΔlacZΔM15 / fhuA2 Δ(lac-proAB) glnV galK16 galE15 R(zgb-210::Tn10) Tet^S endA1 thi-1 Δ(hsdS-mcrB)5; pKTK_009	[6]

Table IV.2: Plasmids used in this study.

Plasmid	**Description**	**Reference**
pKTK_001	KTK E1.0 *gfp* dropout entry-level plasmid (AmpR)	[6]
pCasAb-apr	RSF1010 oriV plasmid carrying lacIq-controlled, tac-inducible SpCas9 and RecAB recombineering functions for *Acinetobacter baumannii* (AprR)	[11]
pKTK_045	KTK E1.2 entry-level BBa_B0034 RBS part(AmpR)	[6]
pKTK_095	KTK D1.1 plasmid carrying dCas9 and *luxZ* dropout cassette with flanking D1.1 overhangs (CmR)	[6]

Table IV.2: Plasmids used in this study.

Plasmid	Description	Reference
pKTK001-Cas9	KTK E1.3 entry-level plasmid harboring SpCas9 with silent mutations introduced to remove BsmBI, BpiI and BsaI restriction sites by site-directed mutagenesis (AmpR)	This work
pKTK-D1.1-Cas9	KTK D1.1 plasmid derived from pKTK_009 carrying the J23104–BBa_B0034–*cas9*–BBa_B0015 expression unit (CmR)	This work
pKTK_002	KTK E1.1 entry-level plasmid harboring the J23104 promoter (AmpR)	[6]
pKTK_003	KTK E1.2 entry-level plasmid harboring the BBa_B0034 RBS (AmpR)	[6]
pKTK_005	KTK E1.4(I) entry-level plasmid carrying the BBa_B0015 terminator (AmpR)	[6]
pKTK_009	KTK D1.1 destination vector with lacZ dropout flanked by D1.1 overhangs (CmR)	[6]
pKTK_095-Cas9	Reversion of D10A (RuvC) and H840A (HNH) mutations in dCas9 by site-directed mutagenesis to restore nuclease activity (CmR)	This work
pKTK_sgJ23117	KTK E1.1 promoter entry-level plasmid derived from KTK_044 harboring the J23117 promoter with modified downstream fusion site enabling direct Golden Gate assembly to E1.3 CDS modules (AmpR)	This work
pKTK-E-lacI	KTK E1.3 entry-level plasmid harboring the *lacI* CDS with silent mutations introduced to remove BsmBI, BpiI and BsaI restriction sites by site-directed mutagenesis (AmpR)	This work
pKTK-D1.1-lacI	KTK D1.1 plasmid derived from pKTK_009 carrying the J23100–BBa_B0034–*lacI*–BBa_B0015 expression unit (CmR)	This work
pKTK_042	KTK E1.1 entry-level plasmid harboring the J23100 promoter (AmpR)	[6]

4.3.2 Construction of plasmids

All primers used in this study are listed in **Table IV.3**.

The *Spcas9* coding sequence was domesticated and cloned as an Entry-level CDS part in the KTK_001 backbone for subsequent Golden Gate (GG) assembly. Internal recognition sites for the type IIS restriction enzymes BsaI, BpiI, and BsmBI were removed by amplifying the gene as five overlapping fragments, introducing silent nucleotide substitutions where required. Each fragment was designed with 20 bp homologous overlaps to adjacent fragments and to the linearized KTK_001 backbone to enable seamless assembly by In-Fusion cloning.

Construction of pKTK001-Cas9

The KTK_001 backbone was amplified using primers KTK001_4cas_FW and KTK001_4cas_RV. The

five cas9 fragments (Cas9.1–Cas9.5) were amplified from plasmid pCasAb-apr (AprR) using fragment-specific primer pairs (Cas9.1_FW/RV, Cas9.2_FW/RV, Cas9.3_FW/RV, Cas9.4_FW/RV, and Cas9.5_FW/RV). PCR products were gel-purified prior to assembly.

The purified backbone and cas9 fragments were assembled using In-Fusion cloning according to the manufacturer's instructions and transformed into chemically competent *Escherichia coli* NZY5α. Correct assembly and complete removal of internal type IIS restriction sites were confirmed by Sanger sequencing of the entire cas9 coding sequence and flanking cloning junctions. Sequence-verified plasmids were subsequently used for Golden Gate assembly reactions.

Construction of pKTK-D1.1-Cas9

pKTK-D1.1-Cas9 was assembled by BsaI-HF®v2 Golden Gate assembly using the promoter PJ23104 (E1.1), RBS BBa_B0034 (E1.2), *SpCas9* CDS (E1.3), and terminator BBa_B0015 (E1.4). These parts were sourced from entry-level plasmids pKTK_002, pKTK_003, pKTK001-Cas9, and pKTK_005, respectively, and assembled into the KTK_009 (D1.1) backbone. Transformants were selected on chloramphenicol and verified by colony PCR and Sanger sequencing.

Construction of KTK-E-lacI

The lacI coding sequence was domesticated by PCR amplification in four overlapping fragments from *E. coli* NZY5α genomic DNA to remove internal type IIS restriction sites, using primer pairs lacI.1_FW/lacI.1_RV, lacI.2_FW/lacI.2_RV, lacI.3_FW/lacI.3_RV, and lacI.4_FW/lacI.4_RV. The KTK_001 backbone was amplified with primers KTK001_4lac_FW and KTK001_4lac_RV. Fragments were assembled by In-Fusion cloning and transformed by heat shock into chemically competent *E. coli* NZY5α. Transformants were selected on ampicillin and verified by colony PCR and Sanger sequencing.

Construction of KTK-D1.1-lacI

KTK-D1.1-lacI was assembled by BsaI-HF®v2 Golden Gate assembly using promoter PJ23100 (E1.1 part from pKTK_042), RBS BBa_B0034 (E1.2 part from pKTK_003), lacI CDS (E1.3 part from KTK-E-lacI), and terminator BBa_B0015 (E1.4 part from pKTK_005), into the KTK_009 backbone (D1.1). Assembled plasmids were transformed into chemically competent *E. coli* NZY5α, selected on chloramphenicol, and verified by colony PCR and Sanger sequencing.

Attempted construction of KTK-D1.1-lacI-lacUV5-Cas9

Assembly of KTK-D1.1-lacI-lacUV5-Cas9 by In-Fusion cloning was attempted but unsuccessful due to PCR amplification difficulties. The intended strategy involved amplification of the complete lacI transcriptional unit from KTK-D1.1-lacI using primers J23100_FW and B0015_RV to introduce In-Fusion overlaps, and amplification of cas9 from KTK_095-Cas9 using primers RBS8_FW and TT1_RV.

Due to repeated failure in amplifying the lacI transcriptional unit, a nested PCR approach was implemented using primers lacI_nested_FW and lacI_nested_RV to generate a larger intermediate fragment for use as template. Despite optimization attempts, amplification of cas9 with primers RBS8_FW and TT1_RV remained unsuccessful, and the construct was not obtained.

PCR amplification and Colony PCR screening

All DNA fragments were amplified using Phusion High-Fidelity DNA Polymerase (Thermo Scientific) to

minimize polymerase-induced errors. Reactions (50 μL) contained 1× HF buffer, 10 mM dNTPs, 10 μM of each primer, 60 ng template DNA, 3% (v/v) DMSO, and 1 U Phusion polymerase. Cycling conditions followed the manufacturer's recommendations, with annealing temperatures adjusted according to primer melting temperatures and extension times calculated based on fragment length.

Transformants were screened by colony PCR using NZYGreen Master Mix (NZYTech). Reactions (20 μL) contained 1× NZYGreen Master Mix and 10 μM of each primer. Diagnostic amplicons spanning assembly junctions were used to identify correct clones. Positive candidates were confirmed by Sanger sequencing.

Plasmid and gel extraction

Plasmid DNA from E. coli was extracted using the GenElute™ Plasmid Miniprep Kit (Sigma–Aldrich), following the manufacturer's instructions. DNA fragments were purified from agarose gels using the QIAquick Gel Extraction Kit (Qiagen), according to the supplier's protocol.

DNA concentration and purity were determined spectrophotometrically using a NanoDrop instrument (Thermo Scientific), and concentrations were used directly for downstream applications unless otherwise specified.

Golden Gate assembly conditions

Golden Gate reactions (10 μL total volume) contained 1× T4 DNA ligase buffer, 0.5 U T4 DNA ligase (Promega), 10 U BsaI-HF®v2, 25 fmol of each insert fragment, and 12.5 fmol of backbone vector. Reactions were incubated at 37 °C for 30 min (pre-digestion), followed by 25 cycles of 5 min at 37 °C and 5 min at 16 °C. A final digestion step was performed at 37 °C for 30 min, followed by enzyme inactivation at 80 °C for 20 min.

Table IV.3: Primers used in this study.

Primer	**Sequence (5'-3')**
KTK001_4cas_FW	CTTATCCATAGGAGACCGACTACGGTTATCCACAGAATC
KTK001_4cas_RV	GTGACTGATTCTTGAGACCAAGATTATCAAAAAGGATCTTCACC
Cas9.1_FW	TCTCCTATGGATAAGAAATACTCAATAGGCTTAGATATCG
Cas9.1_RV	GTTTGAGGCGAGTCGCTTCC
Cas9.2_FW	CGACTCGCCTCAAACGGAC
Cas9.2_RV	TCTTGTCCTCTTCCACCAAAAAAGAC
Cas9.3_FW	TGGAAGAGGACAAGAAGCATG
Cas9.3_RV	AGTCCTCTTGCCTTCTCAAAATAGC
Cas9.4_FW	GAAGGCAAGAGGACTTTTATCCATTTTTAAAAG
Cas9.4_RV	GAATGTCCTCTTTAAATGTCAAACTATCATCATG
Cas9.5_FW	TTAAAGAGGACATTCAAAAAGCACAAGTG
Cas9.5_RV	TCAAGAATCAGTCACCTCCTAGCTGACTC
A10D_RV	TGCCGATATCTAAGCCTATTGAG
A840H_FW	ATGTCGATCACATTGTTCCAC

Table IV.3: Primers used in this study.

Primer	**Sequence (5'-3')**
A10D_FW	TAGGCTTAGATATCGGCACAAATAG
A840H_RV	GAACAATGTGATCGACATCATAATCAC
J23100sg_FW	TGAGACCAAGATTATCAAAAAGGATC
J23100sg_RV	GCTAGCACTGTACCTAGGAC
lacI.1_FW	TCTCCTATGAAACCAGTAACGTTATACGATGTC
lacI.1_RV	GCGTACCATCTTCATGGGAGAAAATAATAC
lacI.2_FW	ATGAAGATGGTACGCGACTGG
lacI.2_RV	ATGAGCTATCTTCGGTATCGTCG
lacI.3_FW	CCGAAGATAGCTCATGTTATATCCCG
lacI.3_RV	CCAGTGACACGGGCAACAG
lacI.4_FW	TGCCCGTGTCACTGGTGAAAAG
lacI.4_RV	TCAAGAATCACTGCCCGCTTTCCAGTC
KTK001_4lac_RV	TGGTTTCATAGGAGACCGACTACGGTTATCCACAGAATC
KTK001_4lac_FW	GGCAGTGATTCTTGAGACCAAGATTATCAAAAAGGATCTTCACC
J23100_FW	TTGACGGCTAGCTCAGTCCTAGG
B0015_RV	TATAAACGCAGAAAGGCCCACCC
RBS8_FW	TGGGCCTTTCTGCGTTTATATTTACACTTTATGCTTCCGGCTCGTATAATGTGTGGAATT
	GTGAGCGGATAACAAAAGAATTCAAAAGCTCTACAGAGGAGAAAGG
TT1_RV	AGGACTGAGCTAGCCGTCAACTCGAGAGGCATCAAATAAAACGAAAG
lacI_nested_FW	CTCCATGCGGTAGGGGTG
lacI_nested_RV	CGTGCGAAAAAGGATGGATATACC

4.3.3 Electroporation

Initial electroporation protocol for *K. sucrofermentans* ATCC 700178

The electroporation protocol was originally developed for *K. rhaeticus* iGEM by Professor Tom Ellis and was initially applied here to *K. sucrofermentans* ATCC 700178 with no major modifications.

A 5 mL pre-culture was initiated in HS medium supplemented with 0.2% (v/v) cellulase and incubated at 30 °C, 180 rpm until turbid. The culture was used to inoculate 80 mL HS + cellulase medium and grown at 30 °C, 180 rpm to mid-exponential phase (OD_{600} 0.4–0.7). Cultures were chilled on ice for 10 minutes and all subsequent steps were performed at 4 °C.

Cells were harvested by centrifugation (12 min, 3200 ×g, 4 °C). Cells were washed twice with ice-cold 1 mM HEPES (pH 7.0). A final wash was performed (14 min, 4100 rpm, 4 °C). The final pellet was resuspended in ice-cold 15% (v/v) glycerol and adjusted to a final volume of 6 mL. Aliquots (100 μL) were prepared and either used immediately or stored at −80 °C.

Electroporation optimization through response surface methodology central composite design

To optimize transformation efficiency in *K. sucrofermentans* ATCC 700178, key electroporation-related variables were systematically evaluated using response surface methodology (RSM) based on a central composite design (CCD).

Three independent variables were selected based on biological relevance and preliminary experiments: cell concentration at harvest (OD_{600}; X_1), cell concentration of electrocompetent cells prior to electroporation (OD_{600}; X_2), and DNA concentration (ng μL^{-1}; final concentration after mixing with cells; X_3). Each variable was evaluated at five coded levels, including factorial points (−1 and +1), axial points ($\pm\alpha$), and replicated centre points (0).

The CCD comprised eight factorial (corner) points, six axial points, and three replicated centre points, totalling seventeen experimental runs (**Table IV.4**). The actual values corresponding to the coded factorial levels were 0.5, 0.7, and 0.9 for X_1; 14, 21, and 28 for X_2; and 1, 5, and 10 for X_3, corresponding to coded levels −1, 0, and +1, respectively. Axial points were included to enable estimation of curvature, while centre point replicates were used to estimate pure experimental error and assess model adequacy.

Transformation efficiency was used as the response variable. Experimental data were initially fitted to a full second-order (quadratic) polynomial model including linear, interaction, and squared terms:

$$Y = \beta_0 + \sum \beta_i X_i + \sum \beta_{ii} X_i^2 + \sum \beta_{ij} X_i X_j,$$

where Yrepresents transformation efficiency, $X_i$the coded independent variables, and $\beta$the regression coefficients. Model significance and term relevance were evaluated by analysis of variance (ANOVA). Non-significant terms ($p > 0.05$) were sequentially removed to obtain a reduced model, while preserving model hierarchy and statistically significant curvature or interaction effects.

Model adequacy was assessed using the coefficient of determination (R^2 and adjusted R^2), lack-of-fit testing, and residual analysis. Response surface and contour plots were generated to visualize variable interactions and identify optimal operating regions within the experimental space.

The final reduced quadratic model was used to predict optimal parameter combinations. These predicted conditions were experimentally validated by independent electroporation assays and observed transformation efficiencies were compared with model predictions. This statistically guided optimization enabled identification of parameter combinations that significantly improved transformation efficiency relative to the initial protocol conditions, while explicitly accounting for curvature and interaction effects inherent to the biological system.

Table IV.4: Statistical Surface Optimization conditions.

Run	OD_{600nm} at harvest	OD_{600nm} after concentration	DNA concentration (ng/μL)	Type
1	-1	-1	-1	Corner
2	-1	-1	1	Corner

Table IV.4: Statistical Surface Optimization conditions.

Run	OD_{600nm} at harvest	OD_{600nm} after concentration	DNA concentration (ng/μL)	Type
3	-1	1	-1	Corner
4	-1	1	1	Corner
5	1	-1	-1	Corner
6	1	-1	1	Corner
7	1	1	-1	Corner
8	1	1	1	Corner
9	-1	0	0	Axial
10	1	0	0	Axial
11	0	-1	0	Axial
12	0	1	0	Axial
13	0	0	-1	Axial
14	0	0	1	Axial
15	0	0	0	Center
16	0	0	0	Center
17	0	0	0	Center

4.4 Results

To establish a CRISPR–Cas9 editing platform compatible with the KTK modular cloning system, three plasmid architectures were constructed and evaluated in *Komagataeibacter sucrofermentans*, differing in promoter strength, replication origin, and regulatory logic. The experimental rationale was sequential: (i) assess the tolerance of constitutive Cas9 expression, (ii) reduce expression to minimal constitutive levels while enabling Golden Gate sgRNA cloning, and (iii) test an inducible heterologous system previously validated in other Gram-negative hosts. Electroporation parameters were systematically optimized to maximize transformation efficiency and exclude technical limitations in DNA delivery. To ensure clarity in data interpretation, the optimization results are presented separately in a dedicated subsection following the CRISPR experiments.

First, KTK-D1.1-Cas9 was assembled on the KTK_009 backbone (pBBR1 origin, Cm^R), placing *cas9* under the constitutive promoter J23104 (medium strength). The construct was designed to be later adapted for BsaI-based Golden Gate guide cloning using a GFP dropout cassette compatible with KTK parts. However, transformation attempts yielded no colonies (**Table IV.5**), indicating that constitutive Cas9 expression from J23104 is not tolerated in the absence of a guide RNA.

To mitigate toxicity, site-directed mutagenesis of KTK_095 restored nuclease-active Cas9, generating

KTK_095-Cas9, in which *cas9* is driven by the synthetic promoter RAND14 and RBS8, both designed for minimal expression [6]. The plasmid retains the pBBR1 origin and CmR marker and allows BsaI Golden Gate cloning of sgRNAs. Despite the use of a low-strength promoter/RBS combination, transformation again yielded 0 CFU μg^{-1} DNA before and after electroporation optimization (**Table IV.5**).

In parallel, the broad-host-range plasmid pCasAb-apr (RSF1010 origin) was evaluated. This vector carries inducible *cas9* and *recA* (from *Acinetobacter baumannii*) modules and has previously been shown to replicate in *Komagataeibacter* spp. Despite the inducible configuration, no transformants were obtained under non-induced conditions (**Table IV.5**), suggesting that basal transcriptional leakage is sufficient to trigger lethality.

To exclude technical limitations in DNA delivery, electroporation efficiency was optimized through a central composite design (CCD). Control transformations with the non-nuclease plasmid KTK_095 (dCas9) yielded 270 ± 46 CFU μg^{-1} DNA (N = 2) prior to optimization and 6371 ± 588 CFU μg^{-1} DNA (N = 2) after optimization (Table IV.5), representing a >20-fold improvement in transformation efficiency. Importantly, no colonies were obtained for any active Cas9 construct under either condition.

Table IV.5 and **Figure IV.1** summarize these results. While dCas9-bearing plasmids were efficiently maintained, all vectors encoding nuclease-active Cas9 failed to yield transformants, independently of promoter strength (J23104 vs RAND14), regulatory architecture (constitutive vs inducible), or replication origin (pBBR1 vs RSF1010).

Collectively, these data demonstrate that even minimal or leaky Cas9 expression in the absence of a targeting guide is prohibitive in *K. sucrofermentans*. The complete absence of colonies across independent constructs and improved transformation conditions strongly indicates Cas9-associated toxicity rather than insufficient DNA uptake. The results suggest that basal double-strand break formation—potentially mediated by non-specific or transient DNA interactions—is lethal in this host, and that tighter regulatory control or alternative editing strategies will be required for successful genome engineering.

Table IV.5: Transformation efficiency of Cas9-encoding plasmids in *K. sucrofermentans* before and after electroporation optimization.

Plasmid	**Origin of replication**	**dCas9/ Cas9 promoter**	**Cas9 inducibility**	**Transformation efficiency before optimization (CFU/μg DNA)**	**Transformation efficiency after optimization (CFU/μg DNA)**
KTK-D1.1-Cas9	pBBR1	J23104	Constitutive (medium strength)	0 ± 0 (N=5)	0 ± 0 (N=6)
KTK_095	pBBR1	RAND14	Constitutive (minimal strength)	270 ± 46 (N=2)	6371 ± 588 (N=2)

Table IV.5: Transformation efficiency of Cas9-encoding plasmids in *K. sucrofermentans* before and after electroporation optimization.

Plasmid	**Origin of replication**	**dCas9/ Cas9 promoter**	**Cas9 inducibility**	**Transformation efficiency before optimization (CFU/μg DNA)**	**Transformation efficiency after optimization (CFU/μg DNA)**
KTK_095-Cas9	pBBR1	RAND14	Constitutive (minimal strength)	0 ± 0 (N=5)	0 ± 0 (N=6)
pCasAb-apr	RSF1010	Ptac	IPTG-inducible	0 ± 0 (N=5)	0 ± 0 (N=6)

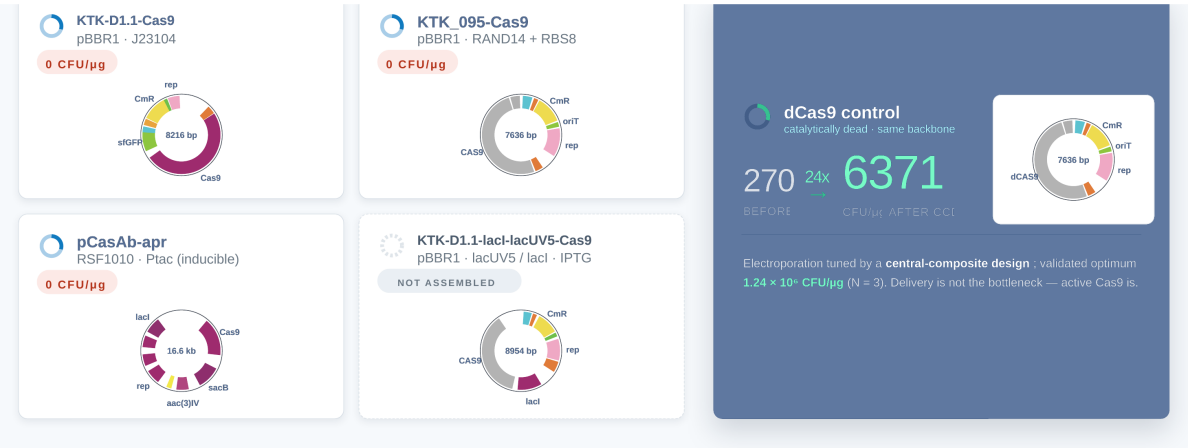


Figure IV.1: Transformation outcomes across Cas9 architectures. Promoter strength, regulatory logic, and replication origin were varied independently; every assembled active-Cas9 construct yielded no transformants (0 CFU μg^{-1}), whereas a catalytically dead dCas9 control was recovered. Electroporation was tuned by a central-composite design (validated optimum 1.24×10^6 CFU μg^{-1}; N=3), confirming that DNA delivery is not the limiting factor.

4.4.1 Electroporation optimization

Prior to this optimization study, transformation efficiency in *K. sucrofermentans* ATCC 700178 was sufficient for routine plasmid introduction and genomic integration/disruption experiments. Although not systematically quantified, electroporations typically yielded from a few dozen to a few hundred colonies using approximately 100–120 ng of plasmid DNA. However, Cas9-expression plasmids are commonly transformed at efficiencies several orders of magnitude lower than non-toxic constructs due to Cas9-associated

lethality. The intrinsically low baseline efficiency likely contributed to the difficulty in obtaining a guideless Cas9-harboring strain, motivating a systematic optimization of electroporation parameters using CCD.

Transformation efficiency (CFU μg^{-1} DNA) obtained across the 17 CCD runs (**Table IV.6**) was fitted to a full second-order quadratic model including linear, squared, and interaction terms. The model yielded R^2 = 0.854 and adjusted R^2 = 0.636, indicating that 85.4% of the variance was explained, albeit with reduced adjusted fit due to model complexity and limited degrees of freedom (n = 16; df_resid = 6). The overall model approached statistical significance (F = 3.908, p = 0.0556). Although the null hypothesis could not be rejected at α = 0.05, it was rejected at α = 0.10, indicating borderline but suggestive explanatory power given the small sample size.

Table IV.6: Electroporation efficiency values obtained for each central composite design run.

Run	OD_{600nm} at harvest	OD_{600nm} after concentration	DNA concentration (ng/μL)	Transformation efficiency (CFU/μg DNA)
1	0,403	14	1	90000
2	0,403	14	10	197000
3	0,403	28	1	330000
4	0,403	28	10	742333,3
5	0,84	14	1	40000
6	0,84	14	10	425500
7	0,84	28	1	40000
8	0,84	28	10	142000
9	0,403	21	5	516000
10	0,84	21	5	30000
11	0,59	14	5	28000
12	0,59	28	5	44000
13	0,59	21	1	10000
14	0,59	21	10	100000
15	0,59	21	5	40000
16	0,59	21	5	84000
17	0,59	21	5	56000

Inspection of **Table IV.6** suggests dependence on harvest OD_{600} (X_1). At $OD_{600} \approx 0.403$, efficiencies reached up to 742,333 CFU μg^{-1} (Run 4) and 516,000 CFU μg^{-1} (Run 9), whereas at $OD_{600} \approx 0.84$ efficiencies dropped dramatically (e.g., 30,000–142,000 CFU μg^{-1}; Runs 5–8, 10). This trend is quantitatively supported by regression analysis: X_1 exhibited a significant negative linear coefficient (β =

-9.61×10^4, p = 0.037), indicating that increasing harvest OD reduced transformation efficiency within the explored range. Simultaneously, the quadratic term $X_1{}^2$ was positive and significant ($\beta = 1.36 \times 10^5$, p = 0.029), confirming non-linear behavior and curvature along the X_1 axis. This curvature is clearly visible in **Figure IV.2A** and **IV.2B**, where efficiency varies non-monotonically along X_1.

DNA concentration (X_3) displayed a positive linear coefficient ($\beta = 8.34 \times 10^4$) with borderline significance (p = 0.058). Empirically, increasing DNA from 1 to 10 ng μL^{-1} frequently improved efficiency at low harvest OD (e.g., Run 1 vs Run 2; Run 3 vs Run 4). However, no significant quadratic effect was detected for X_3 (p = 0.858), indicating an approximately linear contribution within the tested range. This behavior is consistent with the gradual slope observed along X_3 in **Figure IV.2B** and **IV.2C**.

In contrast, OD after concentration (X_2) did not show a significant linear (p = 0.372) or quadratic (p = 0.795) effect. Nevertheless, the interaction term $X_1{:}X_2$ approached significance ($\beta = -7.52 \times 10^4$, p = 0.056), suggesting that the benefit of early harvest may partially depend on the final cell concentration. This interaction is reflected in the response surface of Figure 1A, where the curvature along X_1 shifts depending on X_2 levels. Other interaction terms ($X_1{:}X_3$ and $X_2{:}X_3$) were clearly non-significant (p > 0.95), consistent with the relatively smooth surfaces observed in **Figure IV.2B** and **IV.2C**.

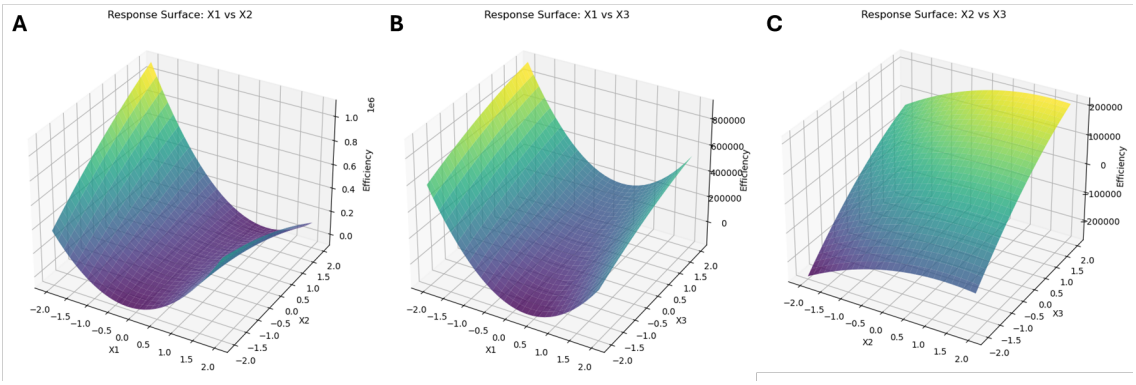


Figure IV.2: Response surface analysis of electroporation efficiency in *K. sucrofermentans* ATCC 700178. Three-dimensional response surfaces generated from the fitted quadratic model illustrating the effects of: **A)** harvest OD_{600} (X_1) and OD_{600} after concentration (X_2); **B)** harvest OD_{600} (X_1) and DNA concentration (X_3); and **C)** OD_{600} after concentration (X_2) and DNA concentration (X_3) on transformation efficiency (CFU μg^{-1} DNA). In each panel, the non-plotted factor was held at its central coded value (0).

Numerical optimization of the full model predicted a maximum transformation efficiency of 1.25×10^6 CFU μg^{-1} at coded levels [–2, 2, 2], corresponding to OD_{600} at harvest ≈ 0.291, OD_{600} after concentration ≈ 31.9, and DNA concentration ≈ 12.3 ng μL^{-1} (≈1230 ng total DNA). Importantly, this optimum lies at the boundary of the explored design space, indicating that the response surface continued to increase toward lower harvest OD and higher DNA and concentration values (**Figure IV.2**). In practical terms, the model identified a direction of improvement rather than an internal stationary point.

A reduced hierarchical model (Y ~ $X_1 + X_3 + X_1{}^2 + X_1{:}X_2$) was subsequently constructed to remove non-significant predictors while preserving model structure. The reduced model achieved statistical significance at $\alpha = 0.05$ and retained essentially the same predicted optimum (1.20×10^6 CFU μg^{-1} at coded

levels [−2, 2, 2]), confirming that X_1 and its curvature dominate the system. The predicted optimum was validated for N=3 by electroporation with the conditions identified through the reduced model, which yielded 1 243 056 ± 136579 CFU/μg.

Further experimental attempts were conducted to test lower harvest OD_{600} values; however, these repeatedly suggested that "earlier is better," with the apparent optimum continuously shifting toward the lowest practically achievable OD. At this stage, practical constraints became limiting. Very early harvest substantially reduces total biomass yield, requiring larger culture volumes to obtain sufficient competent cells. Increasing concentration factors beyond ~30 OD units becomes operationally difficult and time-consuming, while high DNA inputs introduce dilution variability and reduce reproducibility in routine workflows. Thus, although the mathematical model predicts continued improvement beyond the tested range, procedural impracticality and working-volume constraints limit the feasible operational window.

Collectively, the data demonstrate that harvest OD_{600} is the dominant determinant of electroporation efficiency, exerting both statistically significant linear and nonlinear effects. DNA concentration provides a secondary positive contribution, while OD after concentration plays a minor role primarily through interaction with harvest OD. Although the full model was statistically borderline, the biological trends are internally consistent, visually supported by the response surfaces (**Figure IV.2**), and mechanistically coherent. The boundary optimum should therefore be interpreted not as a definitive maximum, but as evidence that transformation efficiency in *K. sucrofermentans* is strongly favored by early exponential-phase harvesting and increased DNA availability, within the constraints imposed by experimental practicality and workflow scalability.

4.5 Understanding the logic behind CRISPR implementation in recalcitrant bacteria

4.5.1 Plasmids, Transformation, and Curing

The architecture of CRISPR–Cas9 plasmids in Gram-negative bacteria reveals a consistent design logic: backbone choice dictates the balance between replication stability, curing feasibility, and host adaptability, with a direct influence on Cas9 dosage and, consequently, toxicity. Three major strategies have emerged across genera—temperature-sensitive (TS) origins [12–15] and broad-host-range (BHR) replicons [16–19], which govern plasmid copy number, stability, and curing, and conjugative delivery strategies, which address plasmid entry into genetically recalcitrant hosts (**Table IV.7**, online supplementary material). Across the dataset (**Table IV.7**), the majority of uses of the TS origin SC101(Ts) are mostly employed in *Enterobacteriaceae*, whereas BHR replicons dominate non-enteric Gram-negative genera, frequently coupled to conjugative delivery.

Table IV.7: Replication origins, delivery routes, and curing strategies.

Genus	Origins of replication	Delivery routes	Curing strategies
Acidithiobacillus	IncQ (1/1)	conjugation (1/1)	passive curing (1/1)
Acinetobacter	RSF1010 (5/5) WH1266 (5/5)	electroporation (4/5) natural transformation (1/5)	sucrose counter-selection (5/5)
Aeromonas	BBR1	conjugation (1/1)	passive curing (1/1)
Agrobacterium	BBR1	conjugation (1/1)	not reported (1/1)
Cupriavidus	oriV/oriT + tfrA (1/3) pAK1900 (1/3) IncP (1/3) BBR1 (1/3)	electroporation (3/3) conjugation (1/3)	sucrose counter-selection (1/3) passive curing (2/3)
Edwardsiella	BBR1 (1/1)	conjugation (1/1)	passive curing (1/1)
Enterobacter	BBR1 (1/1) SC101-ts (1/1)	electroporation (1/1)	passive curing (1/1)
Erwinia	SC101-ts (1/1)	chemical transformation (1/1) electroporation (1/1) conjugation (1/1)	sucrose counter-selection (1/1) passive thermal curing (1/1)
Halomonas	HA020_1 (1/3) HA020_2 (1/3) RK2 (2/3) RO1600 (2/3)	conjugation (1/3) electroporation (2/3)	passive curing (2/3) not reported (1/3)
Klebsiella	SC0101-ts (5/7) ColE1 (2/7)	electroporation (7/7)	sucrose counter-selection (3/7) passive thermal curing (1/7) CRISPR curing (1/7)
Komagataeibacter	BBR1 (1/1)	electroporation (1/1)	passive curing (1/1)
Kosakonia	BBR1 (1/1) MB1 (1/1)	electroporation (1/1)	passive curing (1/1)
Leptospira	R6K (1/1)	conjugation (1/1)	not reported (1/1)
Mycoplasma	integrated (1/1)	electroporation (1/1)	not applicable (1/1)

Genus	Origins of replication	Delivery routes	Curing strategies
Photorhabdus	R6K-suicide (1/1)	conjugation (1/1)	not applicable (1/1)
Pseudomonas	oriV + trfA (6/17) msF (5/17) RK2 (8/17) RO1600 (2/17) R6K (2/17) BBR1 (7/17) RSF1010 (4/17) SC101-ts (1/17)	electroporation (15/17) conjugation (4/17)	sacharose/rhamnose counter-selection (1/17) sacharose counter-selection (6/17) passive curing (7/17) CRISPR curing (1/17) passive thermal curing (2/17)
Rhodobacter	BBR1 (1/1)	conjugation (1/1)	passive curing (1/1)
Salmonella	15A (1/7) SC101-ts (5/7) ColE1 (2/7) MB1 (2/7) SC101-ts (1/7)	chemical transformation (6/7) electroporation (1/7)	passive thermal curing (4/7) IPTG-induced CRISPR curing (1/7)
Schlegelella	BBR1 (1/1)	electroporation (1/1)	not mentioned (1/1)
Serratia	BBR1 (1/1)	electroporation (1/1)	sucrose counter-selection (1/1) rhamnose-induced CRISPR curing (1/1)
Shewanella	BBR1 (3/3) 15A (1/3)	conjugation (1/3) electroporation (2/3)	passive curing (1/3) arabinose- induced I-SceI curing (1/3)
Synechocystis	RSF1010 (1/1)	electroporation (1/1)	Ni^{2+} supplemented passive curing (1/1)
Thermus	pMK18 (1/1)	natural transformation (1/1)	passive curing (1/2)
Vibrio	ColE1 (1/2) 15A (1/2)	chemical transformation (1/1) electroporation (1/1) conjugation (1/1)	passive curing (2/2)

TS origins are particularly prominent in *Enterobacteriaceae*, with 8 out of 11 reports in the analysed corpus being about applications within the family (**Table IV.7**). They provide stable maintenance during editing and straightforward post-edit passive thermal curing through temperature upshift. The canonical *E. coli* pCas/pTarget dual-plasmid system employs a SC101(Ts) origin for the Cas9 + λ-Red helper plasmid and a pMB1 origin for the sgRNA ± donor plasmid, allowing genome editing followed by temperature-induced curing of pCas [20]. This configuration was subsequently adapted for *Salmonella* and *Enterobacter* [13, 21–25]. Comparable systems have been developed in *K. pneumoniae*, where pCasKP/pSGKP uses a temperature-sensitive plasmid expressing constitutive Cas9 and inducible λ-Red recombinase, while the sgRNA/donor module resides on a pMB1-derived plasmid, enabling scarless genome editing and efficient plasmid curing [26]. These systems exemplify how low-copy thermosensitive replicons can facilitate Cas9 dosage control during editing while simplifying plasmid removal without the need for additional counter-selection markers [13, 15, 27, 28]. Within the present corpus, related architectures employing SC101(Ts) plasmids are confirmed for *Enterobacter* [13], *Salmonella* [14], *Erwinia* [29], *Klebsiella* [26], and *Pseudomonas* [28] species. In most cases, TS replicons are used to conditionally maintain the Cas9 + λ-Red module at permissive temperature and permit efficient curing at ≥37 °C. Notably, the no-SCAR system, developed for use in *E.coli* [30] and later used in *Salmonella* [14], instead places the SC101(ts) origin on the sgRNA plasmid, thus enabling straightforward cycling of the guide plasmids, thereby supporting iterative genome editing [30].

In contrast, with 39 reports in the analysed corpus, broad-host-range replicons dominate CRISPR system design across non-enteric Gram-negative bacteria, including *Pseudomonas* [8, 31–35], *Acinetobacter* [9, 36], *Shewanella* [37, 38], and *Halomonas* [19, 39, 40], whereas temperature-sensitive origins remain numerically minor and largely confined to Enterobacteriaceae, highlighting a clear shift from lineage-specific to cross-genera backbone strategies (**Table IV.7**). These replicons, derived from pBBR1, pRSF1010, pRO1600, and pRK2, enable stable replication across diverse Proteobacteria while offering sufficient Cas9 ± recombinase payloads [33, 35, 36, 38, 39]. The corpus reveals that this design space is unevenly consolidated across genera, with some hosts relying repeatedly on few backbones (e.g. *Acinetobacter* [9, 11, 36]), whereas others exhibit pronounced architectural diversity (e.g. *Pseudomonas* [34, 35, 41–43]). Delivery route considerations further constrain viable plasmid backbones and replication origins, as DNA transfer requirements imposed by the host often pre-select for conjugation-compatible, broad-host-range vectors.

RK2-derived origins offer stable replication in many Gram-negative bacteria and are often used for plasmids that require wide host range or conjugative transfer [44], and are frequently included in CRISPR editing plasmids delivered by conjugation [7, 18, 19, 45]. RK2-derived vectors that harbor *oriT* sequences compatible with IncP-1 transfer systems, enable conjugative mobilization into transformation-recalcitrant hosts (e.g., *Pseudomonas*, *Cupriavidus, Halomonas, Shewanella*) when provided with the appropriate IncP-1 conjugative transfer machinery [7, 45, 46]. In *Pseudomonas putida*, SEVA-based multi-plasmid workflows exploit orthogonal replicons (RK2, pBBR1, RSF1010, and RO1600) to balance compatibility and gene dosage [47]. RK2 and pBBR1 derivatives frequently host Cas9 modules or guide RNA cassettes

[7, 16, 18, 34], whereas R6K suicide vectors support allelic exchange with resolution via I-SceI or Cas9 counterselection [35, 48]. Recent work reported that BBR1-based Cas9 constructs can be readily cured in *P. putida* in the absence of selection, facilitating iterative editing, demonstrating that contextual host-dependent instability can be leveraged [47, 49].

These architectural solutions—temperature-sensitive origins and broad-host-range replicons, combined in some cases with conjugative delivery—address complementary constraints in CRISPR-Cas9 system implementation, namely expression control, plasmid persistence, and access to genetically recalcitrant hosts [50]. Temperature-sensitive replicons offer a straightforward curing strategy in hosts that tolerate non-permissive temperature shifts, but their utility is limited by strain-specific thermal tolerance and physiological constraints [50–52]. Broad-host-range replicons facilitate use across diverse bacteria, but their stability can cause difficulties in curing as a trade-off [9, 41, 44, 53–55]. Conjugation-based strategies are especially useful in organisms lacking efficient electroporation or chemical transformation protocols, without intrinsically affecting Cas9 dosage, but come at the cost of increased experimental design complexity [45, 56, 57]. Across the analysed corpus, the distribution of temperature-sensitive origins, broad-host-range replicons, and conjugation-compatible backbones is highly uneven across genera (**Table IV.7**), indicating that CRISPR–Cas9 plasmid architecture is primarily shaped by host-specific constraints on replication, DNA delivery, and plasmid stability rather than by intrinsic properties of the Cas9 system itself.

In *Kosakonia oryzendophytica*, for instance, the pCas/pTarget was not functional, possibly due to poor Cas9/ λ-Red expression [20, 58]. Such assumption inspired origin swapping experiments that explicitly demonstrated the quantitative effect of copy number on expression: fluorescence output increased by approximately 55 % when the same cassette was placed on a high-copy pMB1 origin and decreased by 47 % on a low-copy p15A origin, relative to pBBR1 [58]. The fluorescent proteins in the dual reporter system were replaced by Cas9 and λ-Red, in an editing system with reportedly near 100% efficiency [58]. Although low Cas9 expression can be prohibitive, too much expression can hinder growth and even cause cell death [16, 59, 60]. The choice of an appropriate origin of replication in Cas9-harbouring plasmid backbones can be critical to properly dose Cas9 expression to ensure successful counterselection without completely hindering cell viability [58–60].

Plasmid delivery constraints further reinforce the interdependence between replication origin, transformation and curing methods in CRISPR–Cas9 system design for Gram-negative hosts [45, 49, 57, 61, 62]. In organisms where electroporation is inefficient, CRISPR components are commonly assembled in RK2-derived backbones and delivered through conjugation as demonstrated in multiple systems targeting *Pseudomonas*, *Halomonas*, and *Shewanella* [16, 19, 45]. The RSF1010, RO1600, and BBR1 origins are also commonly used in conjugation-based strategies in *Pseudomonas*, *Shewanella*, *Acidithiobacillus*, and *Rhodobacter* [8, 35, 37, 57, 63]. Whether a helper plasmid is required depends entirely on whether the construct carries its own oriT, as is the only essential cis-acting element for transfer, while all other conjugation functions can be supplied in trans by a helper plasmid [64]. Across the corpus analysed, the recurring use of RK2-, RSF1010-, and BBR1-family replicons highlights their robustness as generalizable

scaffolds for CRISPR editing in non-model Gram-negative bacteria [9, 33, 37, 53, 63]. As the plasmid should be able to replicate both in *E. coli* and in the target organism, for cloning and editing, respectively, some applications might require the use of a hybrid origin [8, 35]. Plasmids with thermosensitive replicons are convenient due to the ease of curing but can only be used when the host tolerates non-permissive temperatures [51, 65].

Collectively, these observations confirm that replication origin selection is a primary engineering variable because it dictates feasible delivery routes, achievable Cas9/sgRNA/recombinase dosage, plasmid stability, compatibility with other plasmids, fitness cost, and available curing strategies within each target genus, ultimately affecting not only the efficiency of CRISPR-Cas9 strategies but also affecting their flexibility and turnaround time [51, 62, 66–70].

4.5.1.1 Active Plasmid Curing

A central challenge in deploying CRISPR–Cas9 editing systems in non-model Gram-negative bacteria is the reliable removal of editing plasmids after the desired modification. Because these plasmids typically encode Cas9, recombinases, and sgRNAs, their continued presence increases the risk of lethal cleavage, off-target effects, and genetic instability. Plasmid curing is especially important for iterative editing, where plasmid removal is a major time bottleneck especially when passive curing is slow. Consequently, curing strategies have been built directly into system designs, with different solutions reflecting the physiology of each genus.

One of the most widely used counter-selection markers is *sacB*, which causes sucrose-dependent lethality thus facilitating plasmid curing. In *Pseudomonas aeruginosa*, Chen et al. introduced *sacB* into both pCasPA and pACRISPR, enabling rapid post-editing plasmid curing after sucrose selection [41]. In *Acinetobacter baumannii*, Wang et al. similarly placed *sacB* on both pCasAb-apr and pSGAb-km, with sucrose selection used to successfully obtain plasmid-free edited strains [9, 11]. In *Klebsiella*, *sacB* is carried on the sgRNA plasmid but not on the Cas9-Red plasmid of the KoSC system, which should facilitate iterative editing since the editing template is supplied as linear dsDNA [71]. In *Synechocystis sp.* PCC 6803, the *mazF* gene was incorporated into CRISPR plasmid, downstream of a Ni^{2+}-inducible promoter, as an active curing strategy, since its expression inhibits protein synthesis ultimately resulting in cell death [54].

In Enterobacteriaceae, temperature-sensitive Cas9 plasmids derived from the pCas/pTarget system are widely used for post-editing curing. In this architecture, pCas carries a temperature-sensitive repA101(Ts)/pSC101-type origin and a Ptrc-driven sgRNA targeting the pTarget pMB1 replicon. After editing, pTarget is first cured by IPTG induction of sgRNA-pMB1, and pCas is then eliminated by overnight growth at 37 °C [20, 25]. In *K. pneumoniae*, the pCasKP/pSGKP plasmid system adopts a similar two-plasmid design that facilitates iterative editing through the sucrose counter-selectable sgRNA plasmid, and a thermosensitive Cas9 plasmid expressing Cas9 and λ-Red [26, 72]. In applied resistance-reversal work, Tagliaferri et al. [73] showed that CRISPR-Cas9 targeting *blaKPC* can fully clear a resistance plasmid in an *E. coli* model and partially re-sensitize a clinical *K. michiganensis* isolate through reduced *blaKPC* plasmid copy

number and expression rather than complete plasmid loss [73]. With the same principle, Fan et al. [45] used a plasmid-targeting I-SceI homing nuclease, downstream of the P_{BAD} promoter, for efficient inducible plasmid curing in *Shewanella oneidensis* [45].

To accelerate the process, researchers sometimes use incompatible plasmid cycling, where the sequential use of incompatible CRISPR plasmids with different antibiotic markers (e.g., KmR and TetR) excuses a separate plasmid curing step [27]. This cycling strategy reduces experimental downtime and avoids repeated reliance on counter-selection.

Together, these findings illustrate that plasmid curing is not a secondary concern but an intrinsic design feature. *Pseudomonas* and *Acinetobacter* lean on sacB to force rapid plasmid loss, while *Salmonella* and *Klebsiella* exploit thermosensitive origins, sometimes coupled with programmed plasmid self-targeting. Meanwhile, modular systems like SEVA use incompatibility cycling to integrate curing seamlessly into iterative editing workflows. Across genera, the most successful CRISPR designs are those that treat curing as a first-class constraint, embedding strategies that allow round-after-round editing with minimal manual intervention.

4.5.2 Cas9 Expression Strategies

Regulating Cas9 expression is a decisive design variable in CRISPR–Cas9 systems for Gram-negative bacteria. Excessive Cas9 activity can be toxic via lethal chromosomal double-strand breaks or off-target promoter binding/silencing ("bad-seed" guides) and high heterologous expression also imposes general over-expression burden that can be bactericidal in *E. coli* [59, 60, 74]. Importantly, Cas9 toxicity reflects effective intracellular dosage rather than regulatory logic alone, and both constitutive and inducible expression architectures can be viable depending on promoter strength, plasmid context, host physiology, and recombination capacity [7, 41, 49]. Conversely, insufficient Cas9 dosage lowers editing/killing efficiency and increases escapers; raising cas9 copy/expression improves outcomes [75]. As a result, expression strategies often reflect host tolerance: targeted Cas9 often kills without a repair template, so systems may require Cas9/sgRNA temporal control and recombination support accordingly [9, 26, 41]. Across the analysed systems, inducible versus constitutive control should therefore not be interpreted as a binary design rule, but as alternative strategies to tune effective Cas9 dosage in conjunction with promoter strength, plasmid context, and recombination capacity. This dose-dependence is further illustrated by NT-CRISPR counterselection systems, where inducible cell killing requires a finely balanced expression ratio between Cas9 and the anti-CRISPR AcrIIA4, since insufficient AcrIIA4 fails to buffer leaky Cas9/sgRNA expression and causes premature lethality, whereas excessive AcrIIA4 can suppress CRISPR activity even upon full induction, thereby compromising counterselection efficiency [76].

This conceptual framework is directly supported by the quantitative distribution of Cas9 expression strategies in the analysed dataset (**Table IV.8**). Inducible Cas9 expression is reported in 33 cases, while constitutive expression appears in 28 cases, with the remaining studies employing mixed, alternative, or layered regulatory strategies. Importantly, inducible systems are distributed across a broader taxonomic range, whereas constitutive expression is concentrated in a limited number of well-studied genera (notably

Pseudomonas, *Salmonella*, and *Klebsiella*). This pattern indicates that inducible control is not merely a precautionary choice, but a portable default strategy for managing Cas9 dosage across diverse Gram-negative hosts, while constitutive expression is selectively viable in organisms with demonstrated tolerance to sustained Cas9 activity.

Table IV.8: Cas9 expression strategies by host.

Genus	Promoter type(s)	Promoter(s)
Acidithiobacillus	constitutive (1/1)	Ptac (1/1)
Acinetobacter	inducible; IPTG (5/5)	Ptac (1/1)
Aeromonas	inducible; L-arabinose (1/1)	PBAD (1/1)
Agrobacterium	inducible; aTc (1/1)	Ptet (1/1)
Cupriavidus	inducible; L-arabinose (1/1)	PBAD (1/1)
	inducible; L-arabinose+theophylline (1/1)	PBAD/RBI riboswitch (1/1)
	constitutive (1/1)	PlacUV5 (1/1)
Edwardsiella	inducible; L-arabinose (1/1)	PBAD (1/1)
Enterobacter	constitutive (1/1)	native Spcas9 promoter (1/1)
Erwinia	inducible; L-arabinose (1/1)	PBAD (1/1)
Halomonas	constitutive (2/3)	native Spcas9 promoter (2/3)
	inducible; IPTG (1/3)	Ptrc (1/3)
Klebsiella	constitutive (6/7)	PrpsL (5/7)
	inducible; L-arabinose (1/7)	native Spcas9 promoter (1/7)
		PBAD (1/7)
Komagataeibacter	inducible; IPTG (1/1)	Ptrc (1/1)
Kosakonia	inducible; IPTG (1/1)	PLacO1 (1/1)
Leptospira	inducible; IPTG (1/1)	PlipL41–lacO–5'UTR_lipL41 (1/1)
Mycoplasma	inducible; aTc (1/1)	Pxyl/tetO2mod (1/1)
Photorhabdus	constitutive (1/1)	native Spcas9 promoter (1/1)
Pseudomonas	constitutive (8/18)	native Spcas9 promoter (5/18)
	inducible; L-arabinose (7/18)	PJ23105 (1/18)
	inducible; L-rhamnose (1/18)	Plac (1/18)
	inducible; cyclohexanone (1/18)	PrhaB (1/18)
	inducible; 3-MB (1/18)	PChnB (1/18)
		PPm (1/18)
Rhodobacter	constitutive (1/1)	Plac (1/1)
Salmonella	constitutive (5/7)	native Spcas9 promoter (5/7)
Schlegelella	inducible; L-arabinose (1/7)	PBAD (1/7)
Serratia	stationary-phase promoter (1/1)	P2 (1/1)

Genus	Promoter type(s)	Promoter(s)
Shewanella	constitutive (1/3)	Plac (1/3)
	inducible; L-arabinose (1/3)	PBAD (1/3)
	inducible; IPTG (1/3)	inducible; IPTG (1/3)
Synechocystis	inducible; theophylline (1/1)	PTrc-riboswitch (1/1)
Thermus	constitutive (1/1)	Pnqo (1/1)
Vibrio	inducible; aTc (1/2)	Ptet (1/2)
	inducible; L-arabinose (1/2)	PBAD (1/2)

In *P. aeruginosa*, successful editing has been achieved using both constitutive and inducible promoters for Cas9 expression [28, 31, 35, 41]. The pCasPA/pACRISPR system contains the Cas9 and λ-Red recombinase open reading frame (ORF) under control of the L-arabinose-inducible PBAD promoter, which allows for timed induction but can be leaky in *Pseudomonas* [41, 77]. When using this system, Chen et al. [41] highlight the lethality of Cas9 expression leakage and the importance of efficient HR for successful editing due to the small amount of antibiotic resistant colonies in non-induced transformation controls [41]. In *P. putida*, Wu et al. [43] used a broad-host-range RK2 replicon plasmid (pLS3819) where Cas9 is expressed from the tightly regulated, L-rhamnose-inducible, rhaRS-PrhaB system with up to 100% editing efficiency [43]. Aparicio, Lorenzo, and Martínez-García [7] employed the SEVA modular system in a three-plasmid configuration, where strains were first loaded with the constitutively expressed Cas9/tracrRNA, regulated by their native *S. pyogenes* promoters, and 3MB-inducible site-specific recombinase recombinase (SSR) in the pSEVA421-Cas9tr and pSEVA658-ssr plasmids, respectively. Only then *P. putida* is co-transformed with the pSEVA231-CRISPR, bearing the crRNA, and a ~100 nt ssDNA recombineering template. Interestingly, the authors explicitly mention the absence of deleterious effects associated with constitutive Cas9 expression [8]. By contrast, Wen et al. [49] noticed the consequences of constitutive expression still in the cloning host: Cas9 driven from a strong Plac promoter produced truncated or inactive variants and premature stop codons, confirming the toxicity of unregulated overexpression to *E. coli* DH5α. The authors redesigned the system by switching to a weaker RBS and eliminating spacer sequences upstream the Cas9 coding gene. The system was further used in *P. putida* with near 100 % editing efficiency [49]. Collectively, *Pseudomonas* systems show that Cas9 toxicity is fundamentally dose-dependent: while low-level constitutive expression can be tolerated, strong or poorly buffered expression rapidly becomes deleterious, making tightly controlled promoters—often sugar-inducible systems such as PBAD or PrhaB—preferable when high Cas9 levels are required [8, 41, 43, 49].

In *Salmonella*, Cas9 has been expressed mostly under constitutive, but also with inducible promoters [12, 14, 21, 22]. The original pCas/pTarget system is the most used CRISPR tool in *Salmonella*, where the λ-Red operon was placed under the L-arabinose–inducible ParaB promoter, while Cas9 itself was expressed from its native *Streptococcus pyogenes* promoter, as the authors explicitly state that pCB001—used to generate pCas—carried "the cas9 sequence and the native promoter from *S. pyogenes*" [20, 22–25]. Later, Basit et al. [21] tested the *S. aureus* pCasSA plasmid for *Salmonella gallinarum*, where

cas9 expression was driven by the strong constitutive rpsL promoter. In their comparative experiments, pCas9 outperformed pCasSA, achieving markedly higher deletion efficiency due to the compatibility of its Gram-negative promoters with the *Salmonella* transcriptional machinery [21, 78]. The authors reported no evidence of Cas9-associated toxicity, as transformation with empty pCas9 or pCasSA vectors yielded more than 300 colonies per plate, indicating the absence of off-target lethality [21].

The most used CRISPR editing tool in *Klebsiella* is the dual-plasmid pCasKP/pSGKP system [15, 26, 27, 71, 72, 79, 80]. The λ-Red recombinase genes are expressed under the L-arabinose-inducible ParaB promoter while Cas9 is constitutively expressed under the rpsL promoter, in the same thermosensitive plasmid, enabling scarless genome editing with efficiencies approaching 100% across multiple loci [26]. A recent study described a CRISPR–Cas9 construct based on the pSB1C3 backbone, in which Cas9 was expressed constitutively. Although the methodological details of plasmid assembly and regulatory control were not fully specified, the authors successfully generated targeted mutants, confirming the system's functionality [73]. Overall, current evidence indicates that *Klebsiella* can sustain constitutive Cas9 expression without lethality, enabling highly efficient and scarless genome editing across diverse strain backgrounds.

The pCasAb/pSGAb CRISPR system for *Acinetobacter baumannii* contains the Cas9 and the recombination module regulated through an IPTG-inducible tac promoter. Wang et al. [9] reports that while the expression of Cas9 alone was not problematic, the simultaneous expression of Cas9 and sgRNA is extremely lethal due to the inefficient nature of the native HR process. This justifies the authors' design choices regarding temporal expression control and the inclusion of an efficient HR system [9]. This system has been adapted in several studies to efficiently engineer *A. baumanii* strains and can be delivered through either electroporation or natural transformation [9, 11, 36].

Overall, the comparative analysis across the gathered literature demonstrates that Cas9 expression control is a primary determinant of genome-editing performance in Gram-negative bacteria. Hosts differ markedly in their tolerance to Cas9 dosage, and these physiological constraints dictate promoter choice, timing of induction, and the requirement for recombination support. Sugar-inducible promoters can partially or effectively mitigate toxicity when high Cas9 levels are needed, whereas some strains/species can accommodate low-to-moderate constitutive expression without penalty. Unregulated or excessive expression might select for truncated Cas9 variants or yield lethal double-strand break (DSB) burden, underscoring the dose-dependent nature of Cas9 toxicity. Notably, even seemingly minor architectural details, such as spacer sequences positioned upstream of Cas9, can influence expression outcomes, although this effect has so far been reported only in isolated cases. Collectively, these findings show that optimal system performance emerges from aligning promoter strength, regulation architecture, and recombination capacity with host-specific repair biology, making Cas9 expression strategy not an accessory tuning parameter, but a core engineering variable that defines feasibility, efficiency, and reliability of CRISPR–Cas9 editing in Gram-negative bacteria.

4.5.3 Recombinase Modules and Donor DNA

Repair of DSBs in Gram-negative bacteria generally requires recombinase-assisted homologous recombination, as endogenous end-joining pathways are weak or absent. For this reason, CRISPR–Cas9 toolkits integrate dedicated recombination modules and can rely on specific donor-template designs [81]. Yet the optimal combination is strongly host-dependent, and different genera require distinct regulatory and mechanistic solutions [12, 25, 41].

Table IV.9: Recombinase + donor compatibility.

Genus	Recombinase	Promoter type	Promoter	Donor format	Homology length range	Editing scope	Multiplex
Acidithiobacillus	not applicable (1/1)	not applicable (1/1)	not applicable (1/1)	plasmid (1/1)	500 bp (1/1)	KO (1/1) KI (1/1)	not applicable (1/1)
Acinetobacter	RecAb (5/5)	inducible; IPTG (5/5)	Ptac (5/5)	linear dsDNA (2/5) plasmid (1/5) ssDNA (4/5)	300-600 bp (linear dsDNA) (2/5) 250 bp (plasmid) (1/5) 40 nt (ssDNA) (4/5)	KI (2/5) KO (4/5) PM (2/5)	not applicable (5/5)
Aeromonas	not applicable (1/1)	not applicable (1/1)	not applicable (1/1)	plasmid (1/1)	500 bp (deletions) (1/1) 1000 bp (insertions) (1/1)	KO (1/1) KI (1/1)	not applicable (1/1)
Agrobacterium	λ-Red (1/1)	inducible; aTc (1/1)	Ptet (1/1)	linear dsDNA (1/1)	160 bp (1/1)	KO (1/1)	not applicable (1/1)

Genus	Recombinase	Promoter type	Promoter	Donor format	Homology length range	Editing scope	Multiplex
Cupriavidus	*λ*-Red (1/3) not applicable (2/3)	inducible; L-arabinose (1/3) not applicable (2/3)	PBAD (1/3) not applicable (2/3)	plasmid (3/3)	600 bp (1/3) 800 bp (1/3) 1000 bp (1/3)	KO (3/3) KI (1/3)	not applicable (3/3)
Edwardsiella	not applicable (1/1)	not applicable (1/1)	not applicable (1/1)	plasmid (1/1)	500 bp (deletions) (1/1) 1000 bp (insertions) (1/1)	KO (1/1) KI (1/1)	not applicable (1/1)
Enterobacter	*λ*-Red (1/1)	inducible; L-arabinose (1/1)	PBAD (1/1)	linear dsDNA (1/1)	not mentioned (1/1)	KO (1/1)	not applicable (1/1)
Erwinia	*λ*-Red (1/1)	inducible; L-arabinose (1/1)	PBAD (1/1)	linear dsDNA (1/1) ssDNA (1/1)	300 bp (1/1) 40 nt (1/1)	KO (1/1) KI (1/1)	yes (1/1)
Halomonas	*λ*-Red (1/3) not mentioned (2/3)	constitutive (1/3) not mentioned (2/3)	PMmp1	plasmid (3/3)	50-1000 bp (1/3) 500 bp (2/3) 1000 bp (1/3)	KO (3/3) KI (2/3)	not applicable (3/3)
Klebsiella	*λ*-Red (6/6)	inducible; L-arabinose (6/6)	PBAD (6/6)	plasmid (1/6) linear dsDNA (2/6) ssDNA (2/6)	500 bp (2/6) 45 nt (2/6)	KO (5/6) KI (1/6) PM (1/6)	not applicable (6/6)

Genus	Recombinase	Promoter type	Promoter	Donor format	Homology length range	Editing scope	Multiplex
Komagataeibacter	λ-Red (1/1)	inducible; L-arabinose (1/1)	PBAD (1/1)	plasmid (1/1)	500 bp (1/1)	KO (1/1) KI (1/1)	not applicable (1/1)
Kosakonia	*λ*-Red (1/1)	inducible; IPTG (1/1)	PLacO1 (1/1)	linear dsDNA (1/1)	421-628 bp (1/1)	KO (1/1)	not applicable (1/1)
Leptospira	NHEJ (1/1)	not applicable (1/1)	not applicable (1/1)	not applicable (1/1)	not applicable (1/1)	KO (1/1)	not applicable (1/1)
Mycoplasma	GP35 ssDNA recombinase (1/1)	constitutive (1/1)	P438 (1/1)	ssDNA (1/1)	40 nt (1/1)	PM (1/1) KO (1/1)	not applicable (1/1)
Photorhabdus	RecET (1/1)	inducible; L-arabinose (1/1)	PBAD (1/1)	plasmid (1/1)	400-700 bp (1/1)	KO (1/1)	not applicable (1/1)
Pseudomonas	SSR recombinase (2/14) Single-Stranded DNA-Binding protein NHEJ (1/14) Rec2/Bet (1/14) *λ*-Red (10/14)	PBAD (9/14) Pm (3/14) Prha (1/14) Pcl857/PL (1/14)	inducible; L-arabinose (9/14) inducible: L-rhamonse (1/14) inducible; 3-MB (3/14) thermoinducible (1/14)	plasmid (8/14) linear dsDNA (3/14) ssDNA (5/14)	500-1000 bp (6/14) 100-200 bp (2/14) 30-90 nt ssDNA (3/14)	KO (11/14) KI (2/14) PM (6/14)	yes (2/14)

Genus	Recombinase	Promoter type	Promoter	Donor format	Homology length range	Editing scope	Multiplex
Rhodobacter	not applicable (1/1)	not applicable (1/1)	not applicable (1/1)	plasmid (1/1)	500 bp (1/1)	KO (1/1) KI (1/1) PM (1/1)	not applicable (1/1)
Salmonella	*λ*-Red (6/7)	inducible; L-arabinose (6/7)	PBAD (6/7)	plasmid (3/7) ssDNA (1/7) short linear dsDNA (1/7) linear dsDNA (2/7)	35-1800 bp (5/7)	KO (5/7) KI (1/7) PM (1/7)	not applicable (7/7)
Schlegelella	*λ*-Red (1/1)	inducible; L-rhamnose (1/1)	Prha (1/1)	linear dsDNA (1/1)	100 bp (1/1)	R (1/1)	not applicable (1/1)
Serratia	*λ*-Red (1/1)	inducible; L-arabinose (1/1)	PBAD (1/1)	plasmid (1/1)	1000 bp (1/1)	KI (1/1) KO (1/1) PM (1/1)	not applicable (1/1)
Shewanella	phage recombinase W3 Beta 8 (1/3) not applicable (2/3)	constitutive (1/3) not applicable (2/3)	Plac (1/3) not applicable (2/3)	plasmid (2/3) ssDNA (1/3)	1000-1464 bp (2/3) 40 nt (1/3)	KO (2/3) FS (1/3) KI (2/3) KO (2/3)	yes (1/3)

Genus	Recombinase	Promoter type	Promoter	Donor format	Homology length range	Editing scope	Multiplex
Synechocystis	not applicable (1/1)	not applicable (1/1)	not applicable (1/1)	plasmid (1/1)	350 bp (1/1)	KO (1/1) KI (1/1)	yes (1/1)
Thermus	not applicable (1/1)	not applicable (1/1)	not applicable (1/1)	plasmid (1/1)	1000 bp (1/1)	KO (1/1) KI (1/1)	not applicable (1/1)
Vibrio	not applicable (2/2)	not applicable (2/2)	not applicable (2/2)	not applicable (2/2)	not applicable (2/2)	KI (1/2) KO (2/2) PM (121)	yes (1/2)

In the pCasPA/pACRISPR system for *Pseudomonas*, Cas9 is paired with the λ-Red recombination proteins (Exo, Gam, Bet), encoded on pCasPA plasmid under regulation of the araB promoter, which mediate homology-directed repair (HDR) after DSB formation [41]. In *P. aeruginosa* PAO1, the authors tested both short linear ssDNA and circular dsDNA and understood that donor format strongly influences both efficiency and flexibility. On one hand, short ssDNA (~90 bp) templates yielded very low recombination, while longer circular templates (>500 bp) achieved high repair rates. On the other, ssDNA can be synthesized easily and be used directly for editing [41]. The authors noted that expression the CRISPR/Cas9 and recombination machineries in the same plasmid may result in DSB-induced lethality due to late expression of the later, as also observed elsewhere [16, 41, 82]. Wu et al. [43] used a slightly different design using tightly regulated Redβ and Cas9 expression together with sgRNA transcription driven by inducible promoters whose regulatory machinery is endogenous to *P. putida* KT2440, reaching editing efficiencies of up to 100% [42, 43, 83, 84]. Although both studies use closely related designs, λ-Red/Cas9 regulation and the bacterial species being edited might be the main factors influencing editing efficiency.

In *P. aeruginosa PAO1*, Chen et al. [41] relied on co-expression of Cas9, Exo, Gam, and Bet under the single L-arabinose-inducible ParaB promoter. Despite inducing the pCasPA plasmid for two hours before electroporation of pACRISPR, the authors emphasize that λ-Red must already be present at sufficient levels before Cas9 introduces a genomic break. In their view, co-expression of Cas9 and the λ-Red proteins from the same promoter risks a situation where recombinase accumulation lags behind Cas9 activity, leaving double-strand breaks unrepaired [41]. This timing mismatch, together with the fact that even basal Cas9 expression is sufficient to trigger lethal double-strand breaks, severely compromises the

performance of short ssDNA donors in PAO1 [41, 85]. In addition, *P. aeruginosa* is well-recognized as a host with weak intrinsic HR capacity, further illustrating the demanding genetic background in which this system operates [41, 85]. By contrast, Wu et al. [43] worked in the more recombineering-permissive *P. putida* KT2440 and used Redβ alone, which they identified as "producing the highest recombineering efficiency" in this host. Furthermore, Cas9 and Redβ were placed under independent, tightly regulated promoters (PrhaB and Pm), allowing robust recombinase accumulation before sgRNA delivery [43]. These host- and regulation-dependent differences, in recombination machinery, expression timing, and intrinsic HR capacity, likely explain why ssDNA recombineering showed dramatically different efficiencies between both systems. Aparicio, Lorenzo, and Martínez-García [7] implemented ssDNA recombineering in *P. putida* KT2440 using the benzoate-inducible Ssr recombinase, achieving high efficiencies across single-gene edits—typically 50–93% and up to 97% for suitable base substitutions—while larger deletions showed a marked decline, from ~13% for 4.9 kb to ~1% for a 69 kb chromosomal segment, with multiplex deletion events occurring at ~3%. Edited alleles were recovered as those surviving Cas9–crRNA targeting of the wild-type sequence, illustrating that Ssr-mediated ssDNA incorporation can generate selectable edits spanning a wide range of sizes in this host [7]. These observations, together with the distinct recombination systems and strain backgrounds examined across studies, underscore how host- and recombinase-specific features shape ssDNA recombineering performance.

In *Salmonella*, recombineering is also built around λ-Red, mostly through the pCas/pTarget system but not exclusively [12, 14, 22–25]. In the widely applied pCas/pTarget system, Cas9 cleavage is paired with arabinose-induced λ-Red activation, after which the pTarget plasmid delivers sgRNA and donor DNA [20]. Donor arm length was found critical in *S. chollerasuis* and optimal length can be template specific since ~860 bp donors (360 bp upstream + 500 bp downstream) maximized the efficiency around 65% [25]. Tahir et al. [12] showed that coupling Cas9 with λ-Red yielded ~70% recombination efficiency, in *S. gallinarum*, using linear fragments, but plasmid-based donor templates failed to produce colonies, highlighting a limitation in donor delivery strategies [12]. These studies indicate that while λ-Red–assisted recombineering is broadly effective in *Salmonella*, editing outcomes remain highly dependent on donor-template architecture, with arm length, and format emerging as key variables that require empirical optimization [12, 25].

In *Klebsiella*, CRISPR–Cas9 editing has been performed using derivatives of the pCasKP/pSGKP system, which relies on λ-Red recombination [26, 71, 72, 79]. In this architecture, pCasKP expresses Cas9 together with the λ-Red proteins Gam, Bet, and Exo, while pSGKP plasmids express sgRNAs from the constitutive J23119 promoter; donor DNA can be supplied either as plasmid-borne repair arms, as linear dsDNA, or as ssDNA oligos, as originally demonstrated by Wang et al. in *K. pneumoniae* [26]. Liu et al. [72] reused this platform in a hypervirulent strain, co-transforming pSGKP-clpV-N20 with 300 μM ssDNA donor template and confirming precise *clpV* deletion by PCR and sequencing [72]. Sun et al. [79] similarly achieved gene editing by electroporating a gRNA cassette and an ssDNA template into cells preharboring pCas-apr [79]. This plasmid system was also adapted to engineer *K. oxytoca, K. michiganensis*, and *K. grimontii* with linear dsDNA donor with 500 bp homology arms. The study explicitly shows that

λ-Red induction strength is the dominant parameter governing editing efficiency since the initial induction at 0.2% L-arabinose gave efficient deletions for only one sgRNA, whereas 10-fold higher induction (2% L-arabinose) restored 65–95% deletion efficiency across four tested sgRNAs [71]. Altogether, these studies show that editing efficiency might be primarily limited by λ-Red expression levels and sgRNA performance rather than donor format in *Klebsiella* species.

Acinetobacter baumannii requires a species-specific recombinase. Wang et al. [9] demonstrated that RecAb from *A. baumannii* IS-123, but not λ-Red or RecET, supported repair of Cas9-induced double-strand breaks, noting that the intrinsic HR capacity of *A. baumannii* was weak and insufficient to repair the lethal DSB created by the sgRNA:Cas9 complex [9]. Wang, Wang, and Ji [11] states that donor format strongly influenced efficiency specifying that ssDNA is suitable for deletions and point mutations, while dsDNA donors enable insertions, with >200 bp homology arms improving insertion efficiency [11]. Yilmaz and Ozbek [36] further showed that *A. baumannii* accommodates multiple donor formats (80-nt ssDNA, 500-bp dsDNA, or plasmid-borne arms) all of which successfully mediated *ampC* gene disruption [36].

Across genera, editing outcomes are shaped primarily by the compatibility between the recombinase system, its regulation, and the host's intrinsic recombination capacity [9, 41, 43]. Across the analysed corpus (**Table IV.9**), recombinase-assisted homologous recombination is overwhelmingly implemented using λ-Red–type systems, which account for the majority of reported references (e.g. ~70–80% of all studies). This dominance is particularly pronounced in Enterobacterales, where λ-Red is reported in all *Klebsiella* (6/6), *Salmonella* (6/7), *Enterobacter* (1/1), *Erwinia* (1/1), *Kosakonia* (1/1), and *Serratia* (1/1) references. Outside Enterobacterales, λ-Red usage drops sharply and is frequently replaced by host-specific recombinases or omitted entirely, reflecting genus-dependent compatibility constraints (**Table IV.9**). λ-Red performs well in Enterobacterales but falters when Cas9 activity outpaces recombinase accumulation or when the host's native HR background is weak [26, 71, 72, 79]. Non-λ-Red recombinases are reported only sporadically, each appearing in one or a small number of references: RecAb in *Acinetobacter*, Ssr in *Pseudomonas putida*, RecET in *Photorhabdus*, W3 Beta-like recombinase in *Shewanella*, and NHEJ in *Leptospira*.

Donor DNA format shows a similarly conservative distribution across the dataset (**Table IV.9**). Plasmid-borne or linear dsDNA donors dominate, being reported in the majority of references across genera (e.g. >60% of all studies), whereas ssDNA donors are confined to a smaller subset of systems, primarily in Acinetobacter (4/5 references) and Pseudomonas (5/14 references). This skew reflects both delivery constraints and the dependence of ssDNA recombineering on highly optimized recombinase expression and host background. Donor architecture may be a critical determinant of efficiency, depending on the host, type of edit, and genomic context [7, 8, 11, 12, 25, 41, 43].

Across the analysed corpus, homology arm length emerges as a contextual tuning parameter rather than a universally optimizable variable. Short homology regions (typically around 45-60 nt) are predominantly associated with ssDNA donors used for point mutations and small deletions, whereas dsDNA donors for gene deletions or insertions generally employ arms in the 300–1000 bp range [9, 28, 36, 76]. However, the effective arm length depends strongly on host background and recombinase system. Lengths

that perform well in one genus may fail in other genera, specially without sufficient recombinase accumulation or intrinsic HR capacity. These observations indicate that homology arm length cannot be prescribed independently of donor format and recombinase context and instead requires empirical adjustment within each host–system combination.

Across all references reporting homology arm length (**Table IV.9**), dsDNA donors overwhelmingly employ extended homology regions in the 300–1000 bp range, which account for the majority of reported designs. In contrast, short homology arms (≤100 nt) are almost exclusively associated with ssDNA donors and are reported in a minority of studies. No genus shows systematic success with short arms in dsDNA-mediated deletions or insertions, reinforcing that homology length requirements are format- and recombinase-dependent rather than universally tunable.

Although alternative repair strategies such as non-homologous end joining (NHEJ) have been implemented in isolated systems (e.g. *Leptospira*), HR–based repair overwhelmingly dominates CRISPR–Cas9 editing in Gram-negative bacteria and remains the only broadly generalizable strategy across genera [8, 30, 38, 86–88].

Delivery constraints further condition viable recombination and donor strategies. In systems delivered by conjugation, donor DNA is most often supplied on plasmids rather than as linear fragments, reflecting the incompatibility of ssDNA or linear dsDNA with mating-based transfer [29, 89]. Conversely, electroporation-compatible hosts more readily support linear or ssDNA donors, enabling rapid recombineering workflows. As a result, the choice of delivery route indirectly shapes donor format, recombinase deployment, and achievable editing complexity [38]. Plasmid curing considerations further feed back into recombinase and donor design, particularly in iterative editing workflows [49]. Systems intended for repeated rounds of editing preferentially combine donor formats that do not require persistent plasmid maintenance with curing-compatible backbones or integrate programmed plasmid elimination via self-targeting or counter-selection [45, 76]. Consequently, recombinase choice and donor architecture are often optimized not only for single-edit efficiency, but also for compatibility with downstream curing and iteration strategies [45].

Donor assembly strategy also varies systematically with donor format and experimental workflow. Linear dsDNA donors are most commonly generated by PCR amplification, enabling rapid construction of deletion or insertion templates without cloning [13, 17, 28]. In contrast, plasmid-borne donors frequently rely on Gibson or other seamless assembly methods to integrate extended homology arms or complex inserts, supporting repeated use and iterative editing [16, 25]. Restriction cloning persists mainly in earlier or low-throughput systems, whereas modern CRISPR toolkits increasingly favor seamless assembly approaches to accelerate donor construction and reduce sequence constraints [37, 63]. Although donor assembly method does not directly influence recombination efficiency, it strongly affects experimental throughput and scalability, particularly in iterative genome engineering workflows [49, 76, 90, 91].

Taken together, **Table IV.9** shows that recombinase modules and donor DNA design are not freely interchangeable components but tightly coupled variables constrained by host biology. The numerical dominance of λ-Red–based systems, long dsDNA homology arms, and single-locus knock-outs reflects a

conservative but robust design space that prioritizes reliability over flexibility. Deviations from this space—such as ssDNA recombineering, alternative recombinases, or multiplex editing—remain exceptional and require precise alignment of recombinase choice, expression timing, and host recombination capacity. These data argue against one-size-fits-all CRISPR architectures and instead support host-specific optimization as the primary design principle for recombinase-assisted genome editing in Gram-negative bacteria.

4.5.4 sgRNA Architecture and Promoters

The engineering of sgRNA modules is central to CRISPR–Cas9 system performance, since promoter strength, modularity, and cloning strategy determine targeting efficiency and ease of reprogramming. While all systems rely on ~20-nt programmable spacers, the implementation varies widely across genera.

In *Pseudomonas*, sgRNA expression has been tailored for flexibility and modularity. Chen et al. [41] constructed pACRISPR, a plasmid with BsaI sites for Golden Gate spacer insertion and XbaI/XhoI sites for Gibson assembly of repair arms, in which sgRNAs were constitutively transcribed from the Ptrc promoter [41]. Wu et al. [43] diversified sgRNA promoters by developing modular pBBR1-based plasmids variants employing Pm, Pu, Prha, Ptac, or PmtlE. Even though the Pm promoter was the top performer in that specific application, the system still offers tunable sgRNA expression [43]. Aparicio, Lorenzo, and Martínez-García [7] reformatted the *S. pyogenes* CRISPR array (leader–DR–spacer–DR) into standardized SEVA backbones (e.g., pSEVA231-CRISPR and pSEVA231-C-spacer derivatives), and combined this with Cas9-mediated counterselection, which "boosted dramatically the appearance of the mutants" during recombineering in *Pseudomonas putida* [7]. Collectively, these systems demonstrate that *Pseudomonas* tolerates constitutive sgRNA expression and that modular plasmid architectures—whether pACRISPR, pBBR1-based variants, or SEVA-formatted CRISPR arrays—provide a robust and flexible framework for guide RNA delivery in this genus [7, 41, 43].

Multiple CRISPR–Cas9 platforms originally developed for *E. coli* or *S. aureus* have been repurposed for *Salmonella*. Jiang et al. [20] expressed genomic sgRNAs from the constitutive synthetic promoter pJ23119 within pTarget, introducing spacers by inverse PCR. The companion pCas plasmid carried an IPTG-inducible (Ptrc) sgRNA directed against the pMB1 replicon of pTarget, enabling Cas9-mediated curing of the sgRNA/donor plasmid after editing [20]. This system was used to edit *Salmonella* strains to systematically determine the functions of the three CitB-family two-component systems in pathogenicity, study antibiotic resistance, to produce detoxified outer membrane vesicles, and attenuated strains for vaccine use [22–25]. The two-plasmid tool, also for *E. coli*, developed by Jiang et al. [82] in Marraffini's lab, constitutively expresses the tracrRNA in the pCas9 plasmid and the array of CRISPR spacers in the pCRISPR plasmid, all under regulation of the respective native *S. pyogenes* promoters [82]. This system has been slightly adapted, by cloning the sgRNA cassette directly in the pCas9 plasmid, for assessing the role of the *ssaU* and *spvB* genes in *S. gallinarum* virulence, and was used with and without heterologous recombination machinery, respectively [12, 21]. Additionally, to pCas9, Basit et al. [21] also tested the pCasSA plasmid, initially developed for *Staphylococcus aureus*. This plasmid ensures constitutive Cas9 and sgRNA expression through the rpsL and cap1A promoters, respectively [21]. The two plasmid

no-SCAR (Scarless Cas9 Assisted Recombineering) system for *E. coli* has also been used in *Salmonella deglycase* [14, 30]. In contrast to the prementioned approaches in *Salmonella*, this system has the Cas9 and sgRNA transcription units under influence of the anhydrotetracycline-inducible pTet promoter while the λ-red genes are regulated by the L-arabinose inducible ParaB promoter [14]. Taken together, these systems show that *Salmonella* genome engineering has predominantly relied on constitutive sgRNA transcription from heterologous toolset.

Although fewer systems have been developed for *Klebsiella*, the overall logic of sgRNA expression closely mirrors the modular architectures established in *E. coli*. Wang et al. [26] described the pCasKP/pSGKP plasmid system, which not only relies on constitutive expression of Golden Gate cloned sgRNAs, under regulation of the J23119 promoter [26]. This system has effectively been used to evaluate the effectiveness of clpV, or the CrrAB two-component system, as targets to reduce virulence in hypervirulent *K. pneumoniae* strains [72, 79]. Overall, these examples indicate that *K. pneumoniae* tolerates straightforward, constitutive sgRNA expression, and that modular promoter–spacer architectures—originally optimized in *E. coli*—translate effectively to this genus without requiring additional regulatory tuning.

In *Acinetobacter baumannii*, sgRNA expression is generally constitutive. Wang et al. [9] engineered pSGAb-km, where sgRNAs were expressed under the synthetic constitutive J23119 promoter, with inverted BsaI sites for rapid Golden Gate insertion of spacers [9]. This strategy, combined with Cas9 and the endogenous RecAb from the companion plasmid, allowed high-efficiency scarless editing despite the genus' weak intrinsic HR.

A quantitative comparison across genera (**Table IV.10**) reveals that constitutive sgRNA expression overwhelmingly dominates CRISPR–Cas9 system design in Gram-negative bacteria. Across the analysed corpus, constitutive promoters account for the large majority of reported implementations, with all references in *Acinetobacter* (5/5), *Cupriavidus* (3/3), *Aeromonas* (1/1), and *Acidithiobacillus* (1/1) relying exclusively on constitutive sgRNA transcription. Even in genera with greater architectural diversity, such as *Pseudomonas*, inducible sgRNA expression appears only sporadically and is confined to single reports, whereas constitutive expression remains the default.

Table IV.10: sgRNA regulation and assembly.

Genus	Promoter type(s)	Promoter(s)	sgRNA cloning method
Acidithiobacillus	constitutive (1/1)	PJ23119 (1/1)	Restriction cloning; ClonExpress MultiS One Step Cloning Kit
Acinetobacter	constitutive (5/5)	PJ23119 (5/5)	Golden Gate (5/5)
Aeromonas	constitutive (1/1)	PJ23119 (1/1)	Gibson assembly (1/1)
Agrobacterium	inducible; aTc (1/1)	Ptet (1/1)	PCR (1/1)
Cupriavidus	constitutive (3/3)	PJ23119 (1/3) PTrc (1/3) PlacUV5 (1/3)	Gibson assembly (1/3) Golden Gate (2/3)

Genus	Promoter type(s)	Promoter(s)	sgRNA cloning method
Edwardsiella	constitutive (1/1)	PJ23119 (1/1)	Gibson assembly (1/1)
Enterobacter	constitutive (1/1)	PJ23119 (1/1)	Gibson assembly (1/1)
Erwinia	constitutive (1/1)	PJ23119 (1/1)	Golden Gate (1/1)
Halomonas	constitutive (3/3)	PJ23119 (3/3)	InFusion cloning (1/3)
			Golden Gate (1/3)
			Restriction cloning (1/3)
Klebsiella	constitutive (7/7)	PJ23119 (5/7)	Golden Gate (4/7)
		native S. pyogenes	Restriction cloning (2/7)
		CRISPR leader	Seamless Assembly cloning (1/7)
		promoter (1/7)	
		PTac (1/7)	
Komagataeibacter	inducible; IPTG	PTrc (1/1)	Golden Gate (1/1)
	(1/1)		
Kosakonia	constitutive (1/1)	PJ23119 (1/1)	Restriction cloning (1/1)
Leptospira	constitutive (1/1)	not mentioned (1/1)	Gibson assembly (1/1)
Mycoplasma	inducible; aTc	Pxyl/tetO2mod (1/1)	Gibson assembly (1/1)
	(1/1)		
Photorhabdus	constitutive (1/1)	P16S (1/1)	Golden Gate (1/1)
Pseudomonas	constitutive (14/17)	J23119 (3/17)	Golden Gate (12/17)
	inducible; IPTG	PTrc (7/17)	Restriction cloning (2/17)
	(1/17)	native S. pyogenes	PCR (1/17)
	inducible; 3-MB	CRISPR leader	Fast Mutagenesis System kit (1/17)
	(1/17)	promoter (3/17)	ClonExpress MultiS One Step
		Pm (1/17)	Cloning Kit / Uni Seamless Cloning
		PEM7 (1/17)	and Assembly Kit (1/17)
Rhodobacter	constitutive (1/1)	PJ95023 (1/1)	NEBuilder HiFi DNA Assembly (1/1)
Salmonella	constitutive (6/7)	native S. pyogenes	Golden Gate (3/7)
	inducible; IPTG	CRISPR leader	Restriction cloning (2/7)
	(1/7)	promoter (2/7)	InFusion cloning (1/7)
		PJ23119 (4/7)	PCR (1/7)
		Ptet (1/7)	
Schlegelella	constitutive (1/1)	PJ23119 (1/1)	not mentioned (1/1)
Serratia	constitutive (1/1)	PJ23119 (1/1)	PCR (1/1)
Shewanella	constitutive (2/3)	Plac (2/3)	Restriction cloning (1/3)
	inducible; IPTG	Ptac (1/3)	Gibson assembly (1/3)
	(1/3)		PCR (1/3)
Synechocystis	constitutive (1/1)	PJ23117 (1/1)	Golden Gate (1/1)

Genus	Promoter type(s)	Promoter(s)	sgRNA cloning method
Thermus	constitutive (1/1)	P16S (1/1)	NEBuilder HiFi DNA Assembly (1/1)
Vibrio	constitutive (1/2)	PJ23119 (1/2)	ClonExpress II One-Step Cloning
	inducible; aTc	Ptet (1/2)	(1/2)
	(1/2)		Golden Gate (1/2)

Promoter usage further reflects strong design convergence: the synthetic J-series promoter PJ23119 is the most frequently reused element across genera, accounting for the majority of sgRNA expression cassettes reported in Enterobacteriaceae and non-enteric Gram-negative hosts alike (**Table IV.10**). Native or conditionally inducible promoters (Ptrc, Ptac, Pm, Ptet) are used far less frequently and typically in exploratory or system-specific contexts rather than as broadly adopted solutions.

In contrast to promoter choice, sgRNA cloning strategy shows a clearer association with system scalability rather than host physiology. Golden Gate cloning dominates the dataset, representing the majority of references in genera with multiple independent reports (e.g., 5/5 in *Acinetobacter* and 2/3 in *Cupriavidus*), whereas Gibson assembly or restriction-based cloning appears mainly in low-count or early systems (**Table IV.10**). This numeric skew indicates that sgRNA transcription is generally non-limiting across hosts, whereas rapid and scarless spacer exchange is a key determinant of whether a CRISPR platform can support iterative or multiplex genome editing.

Collectively, these data indicate that sgRNA modules are treated as a largely solved design component in Gram-negative CRISPR toolkits: constitutive expression from strong synthetic promoters is broadly tolerated, and optimization efforts focus instead on cloning modularity and downstream recombination efficiency. As a result, sgRNA architecture encodes fewer host-specific constraints than Cas9 expression or plasmid backbone choice but remains a decisive factor for experimental throughput and extensibility rather than raw editing efficiency.

4.5.5 Multiplex editing

CRISPR-Cas9 multiplex editing refers to the simultaneous targeting of two or more genomic sites in a single engineering round [20, 54, 76, 90]. Multiplex editing can be useful for many applications, including the optimization of metabolic networks [17], functional genomics and genetic interaction mapping [92], genome reduction [93], and adaptive laboratory evolution [94].

Researchers have achieved the simultaneous modification of up to three loci in organisms like *Synechocystis sp.* PCC 6803 and *Pseudomonas putida* [54, 90]. In *P. putida*, the ReScribe system achieved nearly 100% efficiency in replacing TAG stop codons across three essential genes (*mraY*, *pvdJ*, and *bioD*) in one iteration [90]. ReScribe integrates multiplex recombineering using the Rec2 recombinase and 60-mer ssDNA oligonucleotides with a CRISPR-based counterselection module to achieve nearly 100% efficiency in genome recoding. The system's sgRNA (comprising crRNA and tracrRNA) is expressed from an all-in-one plasmid assembled through One-step Golden Gate-based cloning, which allows targeted spacers to be

inserted into a BsaI-flanked crRNA array. A critical design feature is the use of *Streptococcus canis* Cas9 (ScCas9), which recognizes a minimal 5'-NNG-3' protospacer-adjacent motif (PAM), enabling the direct counterselection of wild-type TAG stop codons even when the desired edit is a single base-pair change to a TAA codon [90]. The multiplex CRISPR-Cas9 technology for *Synechocystis sp.* PCC 6803 is an all-in-one single-vector system that utilizes a theophylline-responsive riboswitch to tightly control the translation of Cas9, effectively bypassing protein cytotoxicity to ensure high transformation and editing efficiencies. The system relies on the host's native HDR machinery rather than exogenous recombinases to repair double-strand breaks using linear double-stranded DNA (dsDNA) donor fragments, which are typically designed with 350 bp homology arms. Multiplexed editing of up to three targets is achieved by assembling a sgRNA array and separate donor pieces into the base vector via one-step Golden Gate assembly, and the final edited strains can be cleared of the plasmid using a nickel-inducible *mazF* curing system [54].

ReaL-MGE (Recombineering and Linear CRISPR/Cas9 assisted Multiplex Genome Engineering) integrates the λ-Red ($\gamma\beta\alpha$) recombinase system with CRISPR-Cas9 counterselection to enable precise, multiplexed manipulation of large genomic sequences in bacteria such as *E. coli*, *S. brevitalea*, and *P. putida*. The platform employs linear, PCR-generated dsDNA donor substrates protected by asymmetric 5' phosphorothioates and utilizes multiple linear gRNA gene cassettes assembled with the J23119 promoter and symmetrical 5' phosphorothioate protection. Key design features include the inactivation of host xseA and overexpression of xseB to boost recombination efficiency through ExoVII manipulation, as well as the use of linearized Cas9/sgRNA fragments in the ReaL-MGE 2.0 variant to overcome the severe cytotoxicity of plasmid-based Cas9 expression in non-model hosts. This tool enables the simultaneous insertion of multiple kilobase-scale sequences into the genomes of *E. coli*, *Schlegelella brevitalea*, and *P. putida* without off-target errors [17].

Co-expressing multiple gRNAs from a single plasmid can be challenging [17]. To bypass this, strategies such as utilizing multiple linear gRNA-expressing PCR fragments or constructing sgRNA arrays through Golden Gate assembly have been successfully deployed [17, 54]. Cengic et al. [54] reports a novel CRISPR-Cas9 tool with multiplex capability, for genome editing in *Synechocystis sp.* PCC 6803, in which three sgRNA transcription units are subcloned via Golden Gate in a pMD19 backbone, followed by a second Golden Gate assembly to generate the final target plasmid [54]. Similarly, the NT-CRISPR toolkit for *V. natrigens* also uses Golden Gate for the assembly of up to three gRNA transcription units, within the framework of a hierarchical cloning system, but does so directly in the NT-CRISPR plasmid [76]. These examples use distinct transcription units to express multiple gRNAs, with promoter repetition in both cases. Another option consists of integrating the gRNAs into an array, intercalated by tRNA linkers, enabling a single polycistronic transcript to produce multiple functional guides by leveraging the endogenous processing machinery. However, Zheng et al. [17] reports that this strategy was more laborious and did not result in significantly enhanced editing efficiency [17]. In the final design of the ReaL-MGE tool, the authors opted to simplify the editing process by providing the gRNA-expressing DNA as PCR-generated linear dsDNA fragments, stabilized by terminal phosphorothioates [17].

While effective, simultaneous editing often suffers from decreased transformation frequency as the

number of targets increases, on one hand due to increased DSB-caused lethality, and on the other due to the high metabolic burden caused by large editing plasmids [41, 54, 90]. The DSB-associated lethality can be circumvented by ensuring that the Cas9 expression is tightly regulated and properly timed. When Cas9 expression leakage from inducible promoters results in decreased or null transformation efficiency, theophylline-inducible riboswitches can be included downstream of a constitutive or an inducible promoter, the latter resulting in AND-gate logic, which may solve the toxicity issue [46, 54].

4.6 Design rules for new CRISPR systems

The following "design rules" were distilled from the literature research done in this chapter. Figure IV.3 was designed as a decision framework to guide the design of new CRISPR–Cas systems in non-model Gram-negative bacteria.

4.6.1 Rule 1 – Delivery feasibility defines everything downstream

In non-model Gram-negative bacteria, delivery feasibility is the primary and often decisive bottleneck in CRISPR–Cas9 genome editing. Before considering Cas9 variants, sgRNA architectures, or donor-template formats, researchers must establish how DNA can realistically enter and persist in the host cell [29, 89]. For example, in *Aeromonas hydrophila*, initial attempts to use electroporation were unsuccessful possibly due to restriction-modification defense systems. This forced a shift to conjugative transfer to ensure the integrity of the delivered DNA and consequently narrowed the set of useful plasmid backbones [89]. If genetic components cannot be introduced efficiently, any subsequent molecular optimization is irrelevant in practice. Platform choice must therefore be dictated by the host's intrinsic biological constraints rather than by abstract tool performance.

Various Gram-negative bacteria exhibit natural competence, which can be practical for intensive strain engineering [76, 95–98]. This strategy exploits endogenous DNA uptake systems and homologous recombination to introduce edits before Cas9 is activated as a counterselection inducer [76]. In some species, competence can be artificially induced through plasmid-encoded overexpression of the master regulator TfoX, bypassing the need for specific environmental cues such as chitin [76, 95]. The NT-CRISPR workflow, as an example, enables MuGENT-style multiplex editing, allowing multiple simultaneous genomic modifications without iterative antibiotic marker recycling [76, 99]. Critically, NT-CRISPR inverts the standard CRISPR logic: the edit is introduced first by natural transformation, followed by Cas9 induction to selectively eliminate wild-type alleles. The method yields markerless, scarless edits with single-base precision and reported killing efficiencies approaching 99.999% [76].

For bacteria that can be transformed by electroporation at moderate to high efficiencies (typically $>10^3$ CFU/μg DNA), plasmid or linear DNA delivery becomes feasible [91]. However, efficiency is highly host-dependent and often hinges on cell preparation protocols rather than on electrical parameters alone

[100]. Specific Gram-negative genera exhibit dramatic improvements when washed with non-standard buffers such as sorbitol, while others rely on classical mannitol or glycerol-based preparations [14, 38, 101]. Construct size imposes a hard constraint: streamlined protocols can accommodate "all-in-one" plasmids of ~7–9 kb, but transformation efficiency frequently collapses when plasmids exceed ~15 kb, effectively setting an upper bound on system complexity [29, 91]. When recombineering is used, ssDNA or dsDNA donor templates are commonly co-electroporated with a gRNA plasmid, and stabilization strategies such as phosphorothioate-protected ends are often required to mitigate nuclease degradation during recovery [9, 11, 13, 17, 90].

In non-model bacteria that are physically difficult to transform or that possess robust restriction–modification systems, conjugative transfer is the most reliable delivery route [29, 41, 89]. By transferring DNA directly from a donor strain into the recipient cytoplasm, conjugation frequently bypasses barriers that degrade DNA introduced by mechanical methods. This approach is particularly advantageous for large genetic payloads and has enabled CRISPR–Cas9 implementation in organisms otherwise considered genetically intractable, including slow-growing chemoautotrophs [29]. Successful conjugation-based systems depend on broad-host-range replicons such as pBBR1 or RK2, which can be mobilized efficiently and maintained across diverse Proteobacteria [43, 49, 89, 102].

A non-naive interpretation of failed transformations must account for Cas9-induced cytotoxicity. In many hosts, even basal (leaky) Cas9 expression is sufficient to cause lethal chromosomal damage, preventing plasmid establishment and masquerading as a delivery failure [49, 76]. Robust systems therefore implement tight, multi-layered repression of Cas9 until cells have fully recovered and segregated the incoming DNA [54, 91]. An interesting option is to include inducible promoters with post-transcriptional control elements such as theophylline-responsive riboswitches [54]. In extremely sensitive organisms, constitutive expression of anti-CRISPR proteins is required simply to permit survival after plasmid entry [76]. Finally, delivery strategy must be aligned with downstream workflow requirements: iterative editing demands replicons that can be reliably cured, as plasmid persistence can otherwise become the dominant bottleneck in sequential genome engineering [49, 76, 91].

As the bottom line, delivery feasibility is not a preliminary technical detail but the governing design constraint. All downstream CRISPR–Cas9 decisions, namely, system architecture, regulatory logic, and editing strategy—must be subordinated to the realities of how DNA enters, survives, and is tolerated by the host cell.

4.6.2 Rule 2 — Treat Cas9 as a Conditional Toxin: Inducibility, Timing, and Leakage Define Success

In non-model Gram-negative bacteria, CRISPR–Cas9 genome editing functions primarily through lethal counterselection, not through neutral DNA cleavage. When Cas9 is guided to a wild-type genomic locus, it generates a DSB that is typically fatal unless repaired by HR (HR) using an endogenous or supplied donor template [9]. As a result, editing efficiency often correlates directly with population death [9, 76,

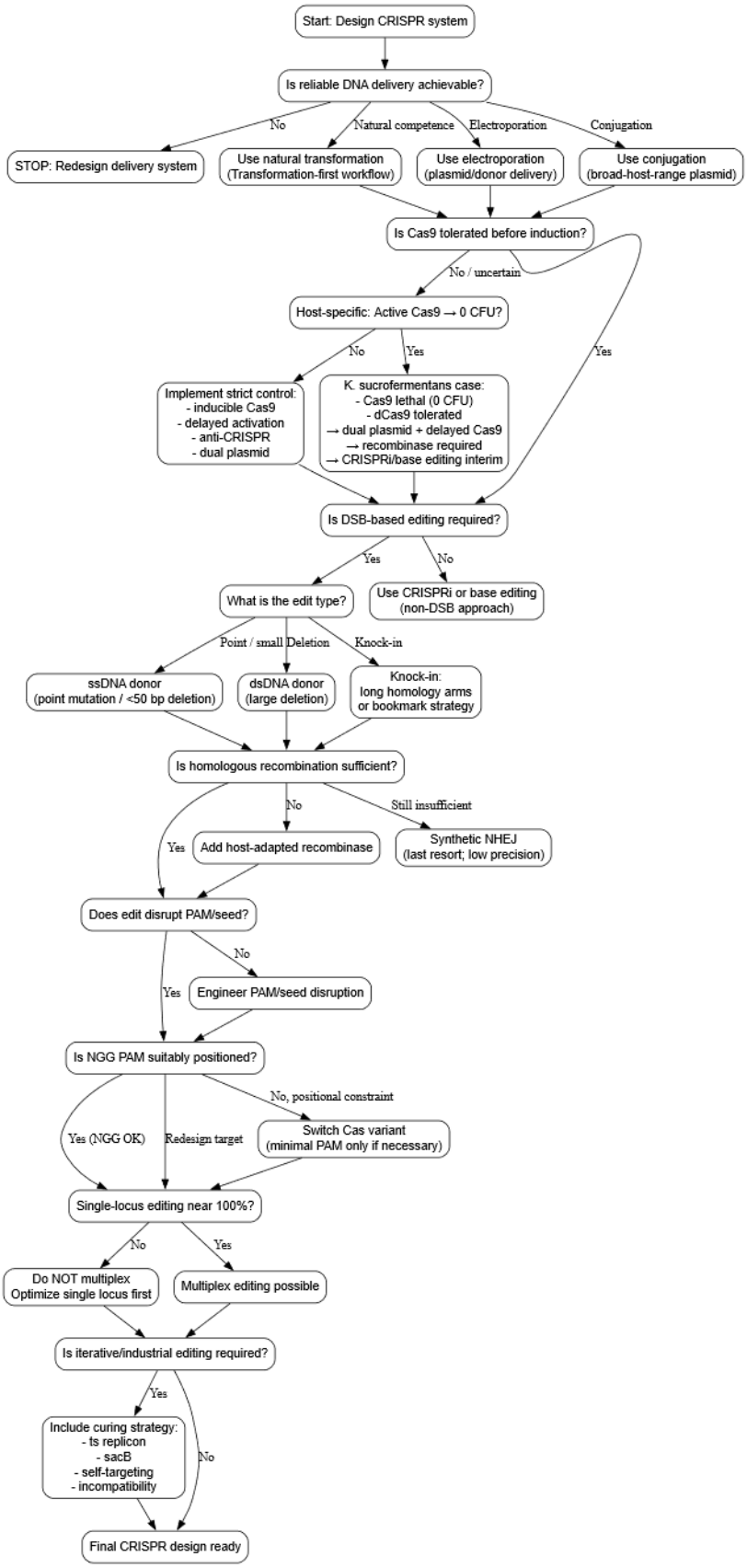


Figure IV.3: Decision framework for CRISPR–Cas system design in non-model Gram-negative bacteria.

91]. Constitutive Cas9 targeting has been shown to reduce viable colony counts by several orders of magnitude, demonstrating that Cas9 activity acts as a kill switch rather than a benign editing catalyst [76]. Consequently, Cas9 must be operationally conceptualized as a counterselection toxin whose role is to eliminate non-edited cells, not merely to introduce breaks [8, 33, 91].

Because unregulated Cas9 activity frequently yields zero transformants, tight inducible control is mandatory [54, 76]. Both transcriptional and translational strategies are used to suppress Cas9 during DNA entry and early recovery [38, 54, 76]. These include inducible promoters (e.g., arabinose- or IPTG-responsive systems), riboswitch-based translational control that keeps Cas9 expression non-lethal until induction, and constitutive expression of anti-CRISPR proteins to buffer basal leakage [4, 45, 54, 76, 91]. In some hosts, even minimal leaky expression from inducible systems is sufficient to cause lethality, requiring additional layers of repression simply to maintain Cas9-bearing plasmids [4, 54, 76].

Critically, timing outweighs expression strength as the dominant design variable [41]. High Cas9 activity is not beneficial if cleavage occurs before HR can take place [17, 38, 54]. Repair templates must be present and utilized before Cas9 is activated; otherwise, cells are eliminated before editing can occur [54, 91, 102]. Successful systems therefore delay Cas9 activation, using growth-phase-dependent promoters, or explicit two-step workflows, in which cells are first transformed, allowed to recover and grow, and only then exposed to Cas9-mediated cleavage to purge the remaining wild-type background [37, 76, 102].

Researchers must also account for the reality of basal leakage and escaper formation. Inducible systems are rarely fully OFF, and low-level Cas9 expression can still cause unintended killing or low-frequency editing [41, 54, 76, 86]. Moreover, because Cas9 imposes extreme selective pressure, surviving colonies frequently arise from mutations in cas9, the sgRNA scaffold, or the target PAM site rather than from successful genome editing [41, 73, 76, 88]. As a result, survival alone is not evidence of editing, and extensive downstream screening remains essential [21, 54, 71].

Operationally, Rule 2 mandates strict temporal separation: (i) maximize DNA delivery with no Cas9 activity, (ii) allow recovery and recombination to occur, and only then (iii) induce Cas9 to convert it into a selective toxin that eliminates non-edited cells. Failure to respect this timing logic is a primary cause of CRISPR–Cas9 failure in non-model Gram-negative bacteria.

4.6.3 Rule 3 — Match Donor DNA Architecture to Edit Type, Recombination Capacity, and Repair Pathways

Rule 3 is the point at which the biological objective of genome modification directly confronts the physical constraints of DNA delivery and the endogenous repair logic of non-model Gram-negative bacteria [38, 88]. Donor DNA design is not an implementation detail but a dominant determinant of success since the format, length, and sequence composition of the repair template must be selected as a calculated response to recombination burden, nuclease exposure, and competing repair pathways [17, 38, 76, 88, 90].

For single-nucleotide substitutions and deletions below ~50 bp, synthetic single-stranded DNA oligonucleotides constitute the most efficient donor format. These oligos act as recombination substrates rather than classical repair templates and must be designed accordingly [43, 88]. Efficiency is maximized when the oligo is complementary to the lagging-strand template at the replication fork, allowing it to mimic Okazaki fragments. This strand bias can increase recombination efficiency by up to two orders of magnitude compared to leading-strand designs [38, 88, 90].

Oligo length is not universal and must be empirically tuned. While 80–170 nt is often cited as a generic guideline, shorter designs can outperform longer ones for specific edits [90]. Conversely, insufficient homology severely limits deletion efficiency, as short arms fail to support stable annealing during replication-coupled recombination [38, 88, 90]. A further non-trivial constraint is methyl-directed mismatch repair (MMR), which can recognize and excise the desired edit before fixation. Effective evasion strategies include embedding multiple silent mutations adjacent to the target site or introducing mismatches, such as C–C pairs, that are poorly recognized by MMR systems in some species [38, 76]. Chemical stabilization of oligos via phosphorothioate bonds is not universally beneficial; while protective in some hosts, it provides little or no advantage in others and may be omitted when cost or simplicity is a concern [17, 43, 90].

Deletions spanning hundreds of base pairs to multiple kilobases require double-stranded DNA donors with extended homology arms. Editing efficiency decreases sharply as deletion size increases, reflecting the rising recombination burden imposed on the host [87, 102]. A baseline of ~500 bp homology per side is often sufficient for sub-kilobase deletions, but larger excisions demand longer arms to stabilize strand invasion and crossover events. Increasing homology arm length can partially offset size-related efficiency losses, particularly for multi-gene operons [41, 71, 87, 103].

A critical risk at this scale is repair by alternative end-joining pathways, including alternative end joining (A-EJ) and microhomology-mediated end joining (MMEJ) [29, 39]. These pathways can resolve Cas9-induced breaks without using the supplied donor, producing unpredictable deletions that nonetheless eliminate the PAM or protospacer and allow survival. Such escapers are especially problematic because they pass CRISPR counterselection while carrying incorrect genotypes [29, 39].

Gene knock-ins represent the most demanding application of CRISPR-assisted recombination in non-model Gram-negative bacteria. Effective insertion frequently requires homology arms of at least ~1 kb on each side, yet even with long arms, efficiencies are often orders of magnitude lower than for deletions. Large donor constructs substantially increase metabolic burden and are more susceptible to restriction–modification systems, further reducing recovery rates [17, 49, 57, 87, 104].

To mitigate these limitations, a two-step “bookmark” strategy is often employed. In the first step, the native locus is deleted and replaced with a short, orthogonal sequence that serves as a high-efficiency CRISPR target. Subsequent insertions are then directed to this bookmark rather than the original genomic context, decoupling knock-in efficiency from locus-specific constraints [71]. When plasmid size or restriction sensitivity becomes limiting, conjugative delivery of the CRISPR system and donor DNA can outperform electroporation by reducing acute toxicity and improving the recovery of rare recombinants [29, 89].

Independent of edit type, the edited genome must be rendered immune to further Cas9 cleavage. This requires explicit destruction of either the PAM or the seed region of the protospacer. Mutations within the seed sequence—typically the 8–12 nucleotides proximal to the PAM—are particularly effective, as single mismatches here frequently abolish cleavage. If the intended edit does not naturally disrupt the PAM, a silent mutation within the PAM must be engineered into the donor template [15, 35, 38, 41, 71, 73, 90].

In systems using Cas9 variants with minimal PAM requirements, this principle can be exploited directly. For example, when a stop codon itself fulfills the PAM requirement, a single synonymous recoding can simultaneously achieve the biological objective and eliminate Cas9 recognition [71, 90]. Failure to enforce PAM or seed destruction leads to re-cleavage and strong selection for escapers, which survive by inactivating the CRISPR machinery rather than repairing their genome [53, 88, 90]. At that point, counterselection collapses and the experiment fails, regardless of donor design quality.

In practice, Rule 3 demands that donor DNA architecture be treated as a primary design variable, not an afterthought. Edit size, repair pathway competition, and Cas9 immunity must be resolved simultaneously, or the system will preferentially select for survival without correctness.

4.6.4 Rule 4 — Assume Endogenous Repair Is Insufficient

In non-model Gram-negative bacteria, CRISPR–Cas9 genome editing must be designed under the assumption that endogenous DNA repair mechanisms are inadequate to resolve Cas9-induced DSBs unless the organism is known for high HR efficiency [9, 38]. Unlike a small set of model organisms, most bacteria lack robust native pathways that permit survival after targeted chromosomal cleavage. As a result, successful editing depends on explicitly engineering both the repair route and the selection logic [9, 12, 33, 48, 88].

In the absence of NHEJ system, a single unrepaired DSB is typically fatal [9, 38]. This lethality is deliberately exploited as a counter-selection mechanism: Cas9 cleavage eliminates wild-type alleles, while survival is restricted to cells that repair the break using a supplied homologous donor template. Editing efficiency is therefore inseparable from repair efficiency [9, 37, 88, 89].

Precise, scarless genome editing in bacteria relies on HDR mediated by an exogenous donor DNA template [28, 58, 88, 102]. Effective HDR requires (i) homology arms flanking the break site, typically on the order of 350–1000 bp, and (ii) disruption of Cas9 re-targeting through silent mutations in the PAM or protospacer sequence within the donor [9, 38, 63, 88, 102]. Even under optimal design, HDR efficiencies are often low and highly sensitive to homology length and the spatial relationship between the DSB and the intended edit [38, 102].

Although most Gram-negative bacteria encode RecA-dependent homologous recombination, intrinsic activity is often insufficient to repair Cas9-induced DSBs at usable frequencies [9, 41]. Consequently, phage-derived recombinases are commonly required [13, 25, 43]. The canonical λ-Red system functions reliably in *E. coli* but performs inconsistently across other genera and often requires strong induction to

overcome host restrictions [9, 71]. Successful editing in non-model organisms therefore depends on host-adapted recombination systems, such as Ssr/Rec2/RecAb variants in *Pseudomonas* [7, 8, 90, 105], the W3 Beta protein in *Shewanella* (reported to increase recombination rates by three orders of magnitude) [38], GP35 in *Mycoplasma pneumoniae* (enabling low but measurable point-mutation efficiencies) [88], or specialized RecET-derived systems in *Agrobacterium* where λ-Red fails [87].

A failed HDR experiment should not be expected to yield zero colonies [71]. Surviving "escapers" frequently arise through loss-of-function mutations in *cas9*, the sgRNA cassette, or the chromosomal target sequence itself [41, 71, 90]. In addition, some bacteria exhibit alternative end-joining activities, such as MMEJ or other alternative EJ pathways, which can generate unintended indels or rearrangements at the cut site [29, 36, 39]. Single-stranded DNA-binding proteins (SSBs) can further modulate outcomes by stabilizing linear DNA and facilitating low-fidelity repair, contributing additional biological noise [28].

When HDR remains impractically inefficient, synthetic NHEJ systems can be introduced as a last-resort survival strategy. Heterologous expression of Ku and LigD from *Mycobacterium smegmatis*, or phage-derived T4 DNA ligase, has enabled recovery of edited colonies in otherwise non-permissive hosts such as *Leptospira* [86]. However, these systems are inherently error-prone and typically produce heterogeneous deletions rather than defined edits. They should therefore be viewed as tools for enabling survival or gene disruption, not for precision genome engineering [28, 86].

CRISPR–Cas9 workflows in non-model Gram-negative bacteria must treat DNA repair as an engineered module, not a host-provided feature. Without deliberate provision of donor templates and appropriate recombination or ligation machinery, Cas9 functions primarily as a killing system rather than an editing tool.

4.6.5 Rule 5 — Treat the PAM as a Spatial Constraint, Not a Reason to Change the System

Rule 5 formalizes a pragmatic design principle: the protospacer adjacent motif (PAM) defines where a cut can be placed, not how efficiently genome editing will occur. In non-model Gram-negative bacteria, this translates into a clear default strategy: retain SpCas9 with its NGG PAM requirement unless the biological objective imposes a hard positional constraint that cannot be resolved otherwise. PAM flexibility expands the targetable sequence space, but it rarely improves editing outcomes.

SpCas9 from *Streptococcus pyogenes* remains the baseline nuclease across a wide range of non-model Gram-negative hosts, including *Salmonella*, *Pseudomonas aeruginosa*, *Acinetobacter baumannii*, *Aeromonas hydrophila*, and *Komagataeibacter* [4, 9, 12, 26, 89]. The NGG constraint becomes consequential only in high-precision use cases, such as genome recoding or single-nucleotide substitutions, where the edit must be positioned at a specific distance from the PAM to prevent re-cleavage of the edited allele [7, 8]. This situation arises when the mutation itself must disrupt the PAM or the protospacer to render the edited locus invisible to Cas9 [76, 90]. A canonical example is stop-codon recoding in *Pseudomonas putida*, where ScCas9 from *Streptococcus canis* was used because its minimal NNG PAM allowed the

native TAG stop codon to function directly as the PAM [90]. Conversion of TAG to TAA simultaneously introduced the desired mutation and abolished Cas9 recognition, enabling efficient and self-terminating editing [90]. Similar logic motivated the use of the near-PAM-less SpG Cas9 in *Vibrio natriegens*, where precise integrations and point mutations were required in regions lacking any suitable NGG sequence [76]. In these cases, the driver for switching nucleases was positional necessity, not superior performance.

A broader PAM should not be conflated with higher editing efficiency. Empirical data show that PAM flexibility increases the number of theoretically targetable sites but does not guarantee functional cutting or effective counterselection [76]. In *V. natriegens*, SpG Cas9 displayed extreme variability in killing efficiency across different NGN PAMs, with some motifs yielding near-complete lethality and others producing little or no effect [76]. This variability highlights that spacer sequence composition and seed-region compatibility dominate cutting efficiency, even within the same Cas variant [76]. More importantly, the final success of genome editing is usually constrained by host-dependent factors such as homologous recombination capacity, donor-template delivery, and recombinase support, rather than by PAM recognition itself [38, 76].

Several non-naive considerations further reinforce this rule. In high-GC organisms such as *Pseudomonas* species, NGG motifs are abundant, making SpCas9 almost universally adequate [90]. Alternative systems become relevant primarily in AT-rich regions or genomes, where NGG sites may be genuinely sparse [76, 90]. Moving away from SpCas9 also introduces substantial system-level changes, such as other guide RNA architectures, and different expression requirements [16, 91, 104]. While indirect workarounds such as introducing a secondary PAM site elsewhere in the genome can sometimes enable counterselection, these approaches are typically less efficient and more cumbersome than using a minimal-PAM variant when precise positioning is unavoidable [76].

In practical terms, Rule 5 is simple and restrictive by design. Researchers should not change Cas systems merely because a PAM is inconvenient. A switch is justified only when the required mutation is recalcitrant and cannot be achieved without targeting a specific nucleotide that does not lie near an NGG motif. In all other scenarios, SpCas9 provides the most robust and reliable killing mechanism for CRISPR-based counterselection in non-model Gram-negative bacteria.

4.6.6 Rule 6 — Multiplexing Scales Biological Risk Faster Than Technical Capability

In non-model Gram-negative bacteria, the ease of assembling multi-guide CRISPR constructs masks a fundamental constraint: biological pressure increases nonlinearly with each additional cut [16, 17, 90, 93, 99].

While adding guides is technically straightforward, multiplexing frequently collapses in hosts that have not been exhaustively optimized, converting an engineering exercise into a survival bottleneck [16, 76]. Simultaneous cuts can overwhelm endogenous recombination, particularly in strains with weak intrinsic HR, yielding partial edits, mixed populations, or outright lethality rather than clean multi-locus mutants

[29, 41]. Leaky expression at nominally repressed levels can be sufficient to kill cells before editing initiates. Multiplexing further increases toxicity by requiring expression of multiple gRNAs—often via repeated cassettes—raising cumulative metabolic load, reducing transformation efficiency, and slowing growth [17, 45].

Modern assembly methods (e.g., Golden Gate, tRNA linkers) lower the barrier to constructing multi-gRNA plasmids, but these constructs are frequently unstable [17, 76]. Repeated promoters or gRNA scaffolds predispose plasmids to recombination and deletion of CRISPR elements [17, 90]. High-intensity multiplex selection also accelerates the emergence of escapers—cells that survive by mutating Cas9, the sgRNA, or the chromosomal target [41, 90]. When combined editing efficiency is low, selection plates are dominated by such evaders rather than the desired mutants [71, 90].

If near-100% efficiency cannot be achieved at a single locus with a given guide and repair template, multiplexing that locus will likely yield zero correct clones. For complex objectives, researchers often adopt sequential edits to establish stability before attempting simultaneous targeting [49, 91]. Multiplexing is the reward for a perfected single-edit system—not a shortcut around a suboptimal one.

4.6.7 Rule 7 — Markerless strains are not optional in applied workflows

In applied synthetic biology, particularly in the construction of complex industrial strains, iterative genome editing is a functional requirement rather than an optimization [91]. In non-model Gram-negative bacteria, this necessity translates into a strict demand for *markerless* end states—strains devoid of residual antibiotic resistance genes, recombination cassettes, or plasmid backbones [9, 41, 58]. Without a defined strategy to remove editing machinery, each successful modification consumes scarce selection markers and progressively converts an otherwise viable chassis into a dead-end strain [9, 49]. From both biosafety and production-stability perspectives, failure to achieve a clean genetic background precludes further engineering and undermines industrial relevance [25, 90].

Applied workflows therefore prioritize explicit, robust mechanisms to ensure complete evacuation of CRISPR components after editing [22, 91]. Temperature-sensitive replicons remain a standard approach in Enterobacteriaceae: plasmids stable at permissive temperatures (e.g., 30 °C) cease replication upon upshift (typically 37–42 °C), enabling passive loss [25, 28, 71]. Chemical counterselection using *sacB* is also widely employed in Gram-negative systems. Upon exposure to sucrose, levansucrase activity generates lethal levan polymers, allowing straightforward selection of plasmid-free colonies [71, 105].

High-efficiency curing can also be achieved through self-targeting CRISPR logic. By inducing transcription of an sgRNA that targets the plasmid's own replicon, the editing system effectively destroys its backbone [14, 102]. Inducible Cas9-mediated double-strand breaks on the plasmid ensure irreparable damage and rapid loss, with reported cases achieving complete curing within a single day [45].

In iterative workflows, a pragmatic shortcut exploits plasmid incompatibility. Introduction of a new CRISPR vector carrying a different resistance marker can displace the resident plasmid at appreciable

frequency, accelerating turnover between editing rounds without dedicated curing steps [8].

In sum, plasmid exit must be treated as a core design element rather than a terminal cleanup step. Without a validated, host-appropriate curing mechanism, residual resistance, plasmid persistence, or genomic instability will block further manipulation and prevent the realization of complex, industrially relevant genotypes.

4.7 Chapter outlook

The experimental results obtained in *Komagataeibacter sucrofermentans* ATCC 700178 demonstrate a consistent and reproducible phenotype: nuclease-active Cas9 is not tolerated in this host. Independent of promoter strength (J23104 versus RAND14), regulatory logic (constitutive versus IPTG-inducible), or replication origin (pBBR1 versus RSF1010), all active Cas9 constructs yielded 0 CFU μg^{-1} DNA before and after electroporation optimization, whereas the corresponding dCas9 plasmid was transformed and maintained, although at compromised efficiency. Electroporation efficiency itself was not limiting, as statistical optimization increased transformation efficiency of a non-toxic plasmid to 1.24×10^6 CFU μg^{-1} DNA. The absence of colonies for all nuclease-active constructs therefore reflects intrinsic Cas9-associated lethality rather than failure of DNA delivery.

These data place *K. sucrofermentans* among the more Cas9-sensitive non-model Gram-negative bacteria. The literature synthesis presented in this chapter shows that Cas9 toxicity is fundamentally dose-dependent and tightly coupled to host recombination capacity and temporal regulation of cleavage [9, 59, 60]. In several genera, constitutive Cas9 expression is tolerated only when recombination support is robust or when expression levels remain below a critical threshold. In contrast, in hosts with weaker intrinsic repair capacity, even basal transcriptional leakage is sufficient to trigger lethal double-strand breaks. The complete absence of transformants in *K. sucrofermentans*, including under minimal constitutive promoters and non-induced inducible systems, strongly suggests that basal Cas9 expression exceeds the repair capacity of this strain at the stage of plasmid establishment.

The most immediate implication is that single-plasmid architectures expressing Cas9 upon replication are structurally incompatible with this host. Successful implementation will likely require strict temporal separation between DNA delivery, recombination, and Cas9 activation. In practical terms, this favors dual-plasmid systems in which Cas9 is carried on a tightly repressible helper plasmid, recombinase expression can be induced and accumulated before cleavage, and Cas9 is only activated after recovery and donor availability are ensured [9, 26]. Cross-genus comparisons indicate that recombinase–host compatibility is often the dominant determinant of editing efficiency. Although *Komagataeibacter* supports HR in sacB-based systems [1], this does not imply sufficient capacity to repair Cas9-induced double-strand breaks at usable frequencies. A viable CRISPR–Cas9 platform will likely require carefully timed recombinase induction and possibly evaluation of host-adapted recombination modules rather than direct transfer of λ-Red architectures optimized for Enterobacterales [30, 82].

The observed lethality further indicates that reducing effective Cas9 dosage might be necessary at multiple regulatory levels. Promoter exchange alone appears insufficient. Replicon copy number, ribosome-binding site strength, translational control elements, protein stability, and potentially anti-CRISPR buffering must all be considered as tunable variables. The failure of RAND14-driven Cas9 suggests that translational output and protein accumulation may be more decisive than nominal promoter classification. Architectures that minimize the window of active Cas9 presence—such as transient or suicide-based systems—may offer additional advantages by limiting intracellular exposure to nuclease activity during plasmid establishment [49, 62].

In parallel, the development of non-double-strand-break strategies provides a pragmatic short-term path forward. CRISPR interference and base editing approaches avoid the lethal burden associated with chromosomal cleavage and have already demonstrated functionality in *Komagataeibacter* species [2, 3]. These tools can enable functional genomics and pathway modulation while a DSB-based platform is rationally redesigned.

The broader comparative analysis across non-model Gram-negative bacteria shows that similar toxicity barriers were encountered in genera such as *Pseudomonas* and *Acinetobacter*, and were overcome not by abandoning CRISPR–Cas9 but by re-engineering system architecture around host-specific constraints [7, 9, 41]. The data presented here do not indicate that CRISPR–Cas9 is intrinsically incompatible with *Komagataeibacter*; they demonstrate that naïve transfer of architectures developed for Enterobacterales is non-viable in this context. The failure of constitutive single-plasmid systems should therefore be interpreted not as a negative result but as a boundary condition defining the design space.

In realistic terms, the outlook is conditional but constructive. In the short term, CRISPRi and base editors offer immediately deployable tools for functional studies. In the medium term, development should focus on tightly regulated dual-plasmid Cas9 systems with pre-induced recombination support and delayed nuclease activation. In the long term, a modular, host-optimized CRISPR platform capable of iterative, markerless genome engineering remains feasible, provided that Cas9 is treated not as a generic editing enzyme but as a conditional toxin whose dosage, timing, and repair context must be engineered with precision.

4.8 References

[1] Zhaojun Peng et al. “Utilizing the SacB-mediated gene editing system in Komagataeibacter xylinus to explore the function of bacterial cellulose synthase”. In: *Journal of Biotechnology* 407 (2025), pp. 48–58.

[2] Long-Hui Huang et al. “Tailoring bacterial cellulose structure through CRISPR interference-mediated downregulation of galU in Komagataeibacter xylinus CGMCC 2955”. In: *Biotechnology and Bioengineering* 117.7 (2020), pp. 2165–2176.

[3] Bo Xin et al. “CRISPR-guided base editor enables efficient and multiplex genome editing in bacterial cellulose-producing Komagataeibacter species”. In: *Applied and Environmental Microbiology* 91.2 (2025).

[4] Longhui Huang et al. “Tailoring Bacterial Cellulose through the CRISPR/Cas9-Mediated Gene Editing Tool in Komagataeibacter xylinus”. In: *ACS Synthetic Biology* 14.4 (2025), pp. 1161–1172.

[5] Ling-Pu Liu et al. “A Lambda Red and FLP/FRT-Mediated Site-Specific Recombination System in Komagataeibacter xylinus and Its Application to Enhance the Productivity of Bacterial Cellulose”. In: *ACS Synthetic Biology* 9.11 (2020), pp. 3171–3180.

[6] Vivianne J Goosens et al. “Komagataeibacter Tool Kit (KTK): A Modular Cloning System for Multigene Constructs and Programmed Protein Secretion from Cellulose Producing Bacteria”. In: *ACS Synthetic Biology* 10.12 (2021), pp. 3422–3434.

[7] Tomás Aparicio, Víctor Lorenzo, and Esteban Martínez-García. “CRISPR/Cas9-Based Counterselection Boosts Recombineering Efficiency in Pseudomonas putida”. In: *Biotechnology Journal* 13.5 (2018).

[8] Tomás Aparicio, Víctor Lorenzo, and Esteban Martínez-García. “CRISPR/Cas9-enhanced ssDNA recombineering for Pseudomonas putida”. In: *Microbial Biotechnology* 12.5 (2019), pp. 1076–1089.

[9] Yu Wang et al. “A Highly Efficient CRISPR-Cas9-Based Genome Engineering Platform in Acinetobacter baumannii to Understand the H2O2-Sensing Mechanism of OxyR”. In: *Cell Chemical Biology* 26.12 (2019), 1732–1742.e5.

[10] Yuzo Yamada, Ken-ichiro Hoshino, and Tetsuya Ishikawa. “The Phylogeny of Acetic Acid Bacteria Based on the Partial Sequences of 16S Ribosomal RNA: The Elevation of the Subgenus *Gluconoacetobacter* to the Generic Level”. In: *Bioscience, Biotechnology, and Biochemistry* 61.8 (1997), pp. 1244–1251.

[11] Yu Wang, Zhipeng Wang, and Quanjiang Ji. “CRISPR-Cas9-Based Genome Editing and Cytidine Base Editing in Acinetobacter baumannii”. In: *STAR Protocols* 1.1 (2020).

[12] Hamza Tahir et al. “Coupling CRISPR/Cas9 and Lambda Red Recombineering System for Genome Editing of Salmonella Gallinarum and the Effect of ssaU Knock-Out Mutant on the Virulence of Bacteria”. In: *Biomedicines* 10.12 (2022).

[13] Ping Lu et al. “Regulation of carbon flux and NADH/NAD+ supply to enhance 2,3-butanediol production in Enterobacter aerogenes”. In: *Journal of Biotechnology* 358 (2022), pp. 67–75.

[14] Anindita Sengupta et al. “Integrated Use of Biochemical, Native Mass Spectrometry, Computational, and Genome-Editing Methods to Elucidate the Mechanism of a Salmonella deglycase”. In: *Journal of Molecular Biology* 431.22 (2019), pp. 4497–4513.

[15] Peng Lan et al. “Emergence of High-Level Cefiderocol Resistance in Carbapenem-Resistant Klebsiella pneumoniae from Bloodstream Infections in Patients with Hematologic Malignancies in China”. In: *Microbiology Spectrum* 10.2 (2022).

[16] Jun Sun et al. “Genome editing and transcriptional repression in Pseudomonas putida KT2440 via the type II CRISPR system”. In: *Microbial Cell Factories* 17.1 (2018).

[17] Wentao Zheng et al. “ReaL-MGE is a tool for enhanced multiplex genome engineering and application to malonyl-CoA anabolism”. In: *Nature Communications* 15.1 (2024).

[18] Rafael Montenegro et al. “The putative phosphate transporter pitb (Pp1373) is involved in tellurite uptake in pseudomonas putida kt2440”. In: *Microbiology (United Kingdom)* 167.2 (2021).

[19] Yong Chen et al. “Chromosome engineering of the TCA cycle in Halomonas bluephagenesis for production of copolymers of 3-hydroxybutyrate and 3-hydroxyvalerate (PHBV)”. In: *Metabolic Engineering* 54 (2019), pp. 69–82.

[20] Yu Jiang et al. “Multigene editing in the Escherichia coli genome via the CRISPR-Cas9 system”. In: *Applied and Environmental Microbiology* 81.7 (2015), pp. 2506–2514.

[21] Abdul Basit et al. “CRISPR/Cas9-Based Deletion of SpvB Gene From Salmonella gallinarum Leads to Loss of Virulence in Chicken”. In: *Frontiers in Bioengineering and Biotechnology* 10 (2022).

[22] Lin Li et al. “Tigecycline-resistance mechanisms and biological characteristics of drug-resistant Salmonella Typhimurium strains in vitro”. In: *Veterinary Microbiology* 288 (2024).

[23] Xiamei Kang et al. “Characterization of Two-Component System CitB Family in Salmonella Pullorum”. In: *International Journal of Molecular Sciences* 23.17 (2022).

[24] Lu Lu et al. “Engineered Outer Membrane Vesicles for Antigen Delivery: Exploratory Study on Adjuvant Activity and Systemic Reactogenicity”. In: *Vaccines* 13.6 (2025).

[25] Xin Huang et al. “Generation and evaluation of Salmonella entericaserovar Choleraesuis mutant strains as a potential live-attenuated vaccine”. In: *Vaccine* 42.24 (2024).

[26] Yu Wang et al. “CRISPR-Cas9 and CRISPR-Assisted Cytidine Deaminase Enable Precise and Efficient Genome Editing in Klebsiella pneumoniae”. In: *Applied and Environmental Microbiology* 84.23 (2018), pp. 1834–1852.

[27] Jingnan Lv et al. “The Role of the Two-Component QseBC Signaling System in Biofilm Formation and Virulence of Hypervirulent Klebsiella pneumoniae ATCC43816”. In: *Frontiers in Microbiology* 13 (2022).

[28] Ran Chai et al. “Single-Stranded DNA-Binding Proteins Mediate DSB Repair and Effectively Improve CRISPR/Cas9 Genome Editing in Escherichia coli and Pseudomonas”. In: *Microorganisms* 11.4 (2023).

[29] Tingfeng Cheng et al. “Development of CRISPR-Cas9-based genome editing tools for non-model microorganism Erwinia persicina”. In: *Synthetic and Systems Biotechnology* 10.2 (2025), pp. 555–563.

[30] Chris R. Reisch and Kristala L.J. Prather. “The no-SCAR (Scarless Cas9 Assisted Recombineering) system for genome editing in Escherichia coli”. In: *Scientific Reports* 5 (2015).

[31] Si Liu et al. “CRISPR-Cas9 Editing of the Synthesis of Biodegradable Polyesters Polyhydroxyalkanaotes (PHA) in Pseudomonas putida KT2440”. In: *Methods in Molecular Biology*. Vol. 2397. Humana Press Inc., 2022, pp. 341–358.

[32] Yu Guo et al. “Identification and Characterization of a Metalloprotein Involved in Gallium Internalization in Pseudomonas aeruginosa”. In: *ACS Infectious Diseases* 5.10 (2019), pp. 1693–1697.

[33] Elena Velázquez, Yamal Al-Ramahi, and Víctor Lorenzo. “CRISPR/Cas9-enhanced Targetron Insertion for Delivery of Heterologous Sequences into the Genome of Gram-Negative Bacteria”. In: *Current Protocols* 2.9 (2022).

[34] Elena Velázquez et al. “Targetron-Assisted Delivery of Exogenous DNA Sequences into Pseudomonas putida through CRISPR-Aided Counterselection”. In: *ACS Synthetic Biology* 10.10 (2021), pp. 2552–2565.

[35] Nicolas T. Wirth, Ekaterina Kozaeva, and Pablo I. Nikel. “Accelerated genome engineering of Pseudomonas putida by I-SceI□mediated recombination and CRISPR-Cas9 counterselection”. In: *Microbial Biotechnology* 13.1 (2020), pp. 233–249.

[36] Ilknur Yilmaz and Tulin Ozbek. “Genome editing in Acinetobacter baumannii through enhanced natural transformation”. In: *Journal of Basic Microbiology* 64.6 (2024).

[37] Yusuke Suzuki, Atsushi Kouzuma, and Kazuya Watanabe. “CRISPR/Cas9-mediated genome editing of Shewanella oneidensis MR-1 using a broad host-range pBBR1-based plasmid”. In: *The Journal of General and Applied Microbiology* 66.1 (2020), pp. 41–45.

[38] Anna D. Corts et al. “Efficient and Precise Genome Editing in Shewanella with Recombineering and CRISPR/Cas9-Mediated Counter-Selection”. In: *ACS Synthetic Biology* 8.8 (2019), pp. 1877–1889.

[39] Ayaka Tsuji, Yasuko Takei, and Yoshinao Azuma. “Establishment of genetic tools for genomic DNA engineering of Halomonas sp. KM-1, a bacterium with potential for biochemical production”. In: *Microbial Cell Factories* 21.1 (2022).

[40] Lei Zhai et al. “Identifying the Alkaline Tolerance-Related Genes Through Transcriptome Analysis of Halomonas alkalicola CICC 11012 s”. In: *Current Microbiology* 82.7 (2025).

[41] Weizhong Chen et al. “CRISPR/Cas9-based Genome Editing in Pseudomonas aeruginosa and Cytidine Deaminase-Mediated Base Editing in Pseudomonas Species”. In: *iScience* 6 (2018), pp. 222–231.

[42] Taylor B. Cook et al. “Genetic tools for reliable gene expression and recombineering in Pseudomonas putida”. In: *Journal of Industrial Microbiology and Biotechnology* 45.7 (2018), pp. 517–527.

[43] Zhixin Wu et al. “Combination of ssDNA recombineering and CRISPR-Cas9 for Pseudomonas putida KT2440 genome editing”. In: *Applied Microbiology and Biotechnology* 103.6 (2019), pp. 2783–2795.

[44] Magdalena Popowska and Agata Krawczyk-Balska. “Broad-host-range IncP-1 plasmids and their resistance potential”. In: *Frontiers in Microbiology* 4.MAR (2013).

[45] Yang Yang Fan et al. “Enhanced Bioreduction of Radionuclides by Driving Microbial Extracellular Electron Pumping with an Engineered CRISPR Platform”. In: *Environmental Science and Technology* 55.17 (2021), pp. 11997–12008.

[46] Federico Turco et al. “Synthetic Biology Toolbox, Including a Single-Plasmid CRISPR-Cas9 System to Biologically Engineer the Electrogenic, Metal-Resistant Bacterium Cupriavidus metallidurans CH34”. In: *ACS Synthetic Biology* 11.11 (2022), pp. 3617–3628.

[47] Rafael Silva-Rocha et al. “The Standard European Vector Architecture (SEVA): A coherent platform for the analysis and deployment of complex prokaryotic phenotypes”. In: *Nucleic Acids Research* 41.D1 (2013).

[48] Esteban Martínez-García and Víctor Lorenzo. “Engineering multiple genomic deletions in Gram-negative bacteria: Analysis of the multi-resistant antibiotic profile of Pseudomonas putida KT2440”. In: *Environmental Microbiology* 13.10 (2011), pp. 2702–2716.

[49] Qifeng Wen et al. “A single-plasmid-based, easily curable CRISPR/Cas9 system for rapid, iterative genome editing in Pseudomonas putida KT2440”. In: *Microbial Cell Factories* 23.1 (2024).

[50] Daniel C. Volke et al. “Synthetic control of plasmid replication enables target- and self-curing of vectors and expedites genome engineering of Pseudomonas putida”. In: *Metabolic Engineering Communications* 10 (2020).

[51] Laura A. Silo-Suh et al. “Isolation, characterization, and utilization of a temperature-sensitive allele of a Pseudomonas replicon”. In: *Journal of Microbiological Methods* 78.3 (2009), pp. 319–324.

[52] E Maguin et al. “New thermosensitive plasmid for gram-positive bacteria”. In: *Journal of Bacteriology* 174.17 (1992), pp. 5633–5638.

[53] Yufei Zhang et al. “Efficient Knocking Out of the Organophosphorus Insecticides Degradation Gene opdB in Cupriavidus nantongensis X1T via CRISPR/Cas9 with Red System”. In: *International Journal of Molecular Sciences* 24.6 (2023).

[54] Ivana Cengic et al. “Inducible CRISPR/Cas9 Allows for Multiplexed and Rapidly Segregated Single-Target Genome Editing in Synechocystis Sp. PCC 6803”. In: *ACS Synthetic Biology* 11.9 (2022), pp. 3100–3113.

[55] Alessandro Lazdins et al. “Potentiation of curing by a broad-host-range self-transmissible vector for displacing resistance plasmids to tackle AMR”. In: *PLoS ONE* 15.1 (2020).

[56] Jing Ke et al. “CRAGE-CRISPR facilitates rapid activation of secondary metabolite biosynthetic gene clusters in bacteria”. In: *Cell Chemical Biology* 29.4 (2022), 696–710.e4.

[57] Ioannis Mougiakos et al. “Efficient Cas9-based genome editing of Rhodobacter sphaeroides for metabolic engineering”. In: *Microbial Cell Factories* 18.1 (2019).

[58] Liangtian Miao et al. “Construction of a synthetic biology toolkit for the genetic manipulation in the cellulose-producing strain Kosakonia oryzendophytica”. In: *Synthetic and Systems Biotechnology* 10.3 (2025), pp. 1050–1058.

[59] William Rostain et al. “Cas9 off-target binding to the promoter of bacterial genes leads to silencing and toxicity”. In: *Nucleic Acids Research* 51.7 (2023), pp. 3485–3496.

[60] Lun Cui and David Bikard. “Consequences of Cas9 cleavage in the chromosome of Escherichia coli”. In: *Nucleic Acids Research* 44.9 (2016), pp. 4243–4251.

[61] Esteban Martínez-García et al. “SEVA 3.0: An update of the Standard European Vector Architecture for enabling portability of genetic constructs among diverse bacterial hosts”. In: *Nucleic Acids Research* 48.D1 (2020), pp. D1164–D1170.

[62] Ida Lauritsen et al. “A versatile one-step CRISPR-Cas9 based approach to plasmid-curing”. In: *Microbial Cell Factories* 16.1 (2017).

[63] Jinjin Chen, Yilan Liu, and Radhakrishnan Mahadevan. “Genetic Engineering of Acidithiobacillus ferridurans Using CRISPR Systems To Mitigate Toxic Release in Biomining”. In: *Environmental Science and Technology* 57.33 (2023), pp. 12315–12324.

[64] Søren J. Sørensen et al. “Studying plasmid horizontal transfer in situ: A critical review”. In: *Nature Reviews Microbiology* 3.9 (2005), pp. 700–710.

[65] Brian H. Kvitko et al. “A simple method for construction of pir + Enterobacterial hosts for maintenance of R6K replicon plasmids”. In: *BMC Research Notes* 5 (2012).

[66] Richard Meyer. “Replication and conjugative mobilization of broad host-range IncQ plasmids”. In: *Plasmid* 62.2 (2009), pp. 57–70.

[67] Michael Jahn et al. “Copy number variability of expression plasmids determined by cell sorting and droplet digital PCR”. In: *Microbial Cell Factories* 15.1 (2016).

[68] Michael Weinstein, Richard C Roberts, and Donald R Helinski. *A Region of the Broad-Host-Range Plasmid RK2 Causes Stable In Planta Inheritance of Plasmids in Rhizobium meliloti Cells Isolated from Alfalfa Root Nodules*. Tech. rep. 22. 1992.

[69] Richard P Novick. *Plasmid Incompatibility*. Tech. rep. 4. 1987.

[70] Alvaro San Millan and R. Craig MacLean. “Fitness Costs of Plasmids: a Limit to Plasmid Transmission”. In: *Microbiology Spectrum* 5.5 (2017).

[71] Éva D.H. Almási et al. “An adapted method for Cas9-mediated editing reveals the species-specific role of -glucoside utilization driving competition between Klebsiella species”. In: *Journal of Bacteriology* 206.3 (2024).

[72] Wenke Liu et al. “A strategy for controlling Hypervirulent Klebsiella pneumoniae: inhibition of ClpV expression”. In: *BMC Microbiology* 25.1 (2025).

[73] Thaysa Leite Tagliaferri et al. “CRISPR-Cas9 targeting the blaKPC gene in a clinical isolate of Klebsiella michiganensis: Reduction of imipenem resistance and changes in genomic carbapenem resistance determinants”. In: *PLOS ONE* 20.8 August (2025).

[74] Jack James et al. “Protein over-expression in Escherichia coli triggers adaptation analogous to antimicrobial resistance”. In: *Microbial Cell Factories* 20.1 (2021).

[75] Qi Li et al. “Improving the Editing Efficiency of CRISPR-Cas9 by Reducing the Generation of Escapers Based on the Surviving Mechanism”. In: *ACS Synthetic Biology* 12.3 (2023), pp. 672–680.

[76] Daniel Stukenberg et al. “NT-CRISPR, combining natural transformation and CRISPR-Cas9 counterselection for markerless and scarless genome editing in Vibrio natriegens”. In: *Communications Biology* 5.1 (2022), p. 265.

[77] Jeffrey Meisner and Joanna B. Goldberg. “The Escherichia coli rhaSR-PrhaBAD inducible promoter system allows tightly controlled gene expression over a wide range in Pseudomonas aeruginosa”. In: *Applied and Environmental Microbiology* 82.22 (2016), pp. 6715–6727.

[78] Weizhong Chen et al. “Rapid and Efficient Genome Editing in Staphylococcus aureus by Using an Engineered CRISPR/Cas9 System”. In: *Journal of the American Chemical Society* 139.10 (2017), pp. 3790–3795.

[79] Lang Sun et al. “CrrAB regulates PagP-mediated glycerophosphoglycerol palmitoylation in the outer membrane of Klebsiella pneumoniae”. In: *Journal of Lipid Research* 63.9 (2022).

[80] Junyang Kuai et al. “Elucidating adaptive compensatory tigecycline resistance mechanisms of RamA, RarA and SoxS in Klebsiella pneumoniae”. In: *International Journal of Antimicrobial Agents* 66.4 (2025).

[81] Ruben D. Arroyo-Olarte, Ricardo Bravo Rodríguez, and Edgar Morales-Ríos. “Genome editing in bacteria: Crispr-cas and beyond”. In: *Microorganisms* 9.4 (2021).

[82] Wenyan Jiang et al. “RNA-guided editing of bacterial genomes using CRISPR-Cas systems”. In: *Nature Biotechnology* 31.3 (2013), pp. 233–239.

[83] Agnieszka Gawin, Svein Valla, and Trygve Brautaset. “The XylS/Pm regulator/promoter system and its use in fundamental studies of bacterial gene expression, recombinant protein production and metabolic engineering”. In: *Microbial Biotechnology* 10.4 (2017), pp. 702–718.

[84] Seong Keun Kim et al. “CRISPR interference-mediated gene regulation in Pseudomonas putida KT2440”. In: *Microbial Biotechnology* 13.1 (2020), pp. 210–221.

[85] Zhanglin Lin et al. “Efficient genome editing for Pseudomonas aeruginosa using CRISPR-Cas12a”. In: *Gene* 790 (2021).

[86] L. G.V. Fernandes, A. L.T.O. Nascimento, and J. E. Nally. “Induced protein expression in Leptospira spp. and its application to CRISPR/Cas9 mutant generation”. In: *Scientific Reports* 15.1 (2025).

[87] Shiqing Gao et al. “Efficient genome engineering in Agrobacterium tumefaciens C58 using recombineering assisted by CRISPR/Cas9”. In: *Journal of Biotechnology* 406 (2025), pp. 99–104.

[88] Carlos Piñero-Lambea et al. “Mycoplasma pneumoniae Genome Editing Based on Oligo Recombineering and Cas9-Mediated Counterselection”. In: *ACS Synthetic Biology* 9.7 (2020), pp. 1693–1704.

[89] Jun Feng et al. “High-Efficiency Genome Editing in Naturally Isolated Aeromonas hydrophila and Edwardsiella Piscicida Using the CRISPR-Cas9 System”. In: *Biotechnology and Bioengineering* 122.3 (2025), pp. 606–614.

[90] Enrique Asin-Garcia et al. “ReScribe: An Unrestrained Tool Combining Multiplex Recombineering and Minimal-PAM ScCas9 for Genome Recoding Pseudomonas putida”. In: *ACS Synthetic Biology* 10.10 (2021), pp. 2672–2688.

[91] Simona Valle et al. “Streamlined and efficient genome editing in Cupriavidus necator H16 using an optimised SIBR-Cas system”. In: *Trends in Biotechnology* 43.6 (2025), pp. 1470–1491.

[92] Lijun Guo et al. “Assembling the Streptococcus thermophilus clustered regularly interspaced short palindromic repeats (CRISPR) array for multiplex DNA targeting”. In: *Analytical Biochemistry* 478 (2015), pp. 131–133.

[93] Meliawati Meliawati, Christa Teckentrup, and Jochen Schmid. “CRISPR-Cas9-mediated Large Cluster Deletion and Multiplex Genome Editing in Paenibacillus polymyxa”. In: *ACS Synthetic Biology* 11.1 (2022), pp. 77–84.

[94] Yangyang Zheng et al. “Improving Furfural Tolerance of Escherichia coli by Integrating Adaptive Laboratory Evolution with CRISPR-Enabled Trackable Genome Engineering (CREATE)”. In: *ACS Sustainable Chemistry and Engineering* 10.7 (2022), pp. 2318–2330.

[95] Cameron J. Lloyd et al. “Natural Transformation in a Classical-Biotype Vibrio cholerae Strain”. In: *Applied and Environmental Microbiology* 87.10 (2021).

[96] Suvi Santala and Ville Santala. “*Acinetobacter baylyi* ADP1—naturally competent for synthetic biology”. In: *Essays in Biochemistry* 65.2 (2021), pp. 309–318.

[97] Dirk Hofreuter, Stefan Odenbreit, and Rainer Haas. “Natural transformation competence in *Helicobacter pylori* is mediated by the basic components of a type IV secretion system”. In: *Molecular Microbiology* 41.2 (2001), pp. 379–391.

[98] Inês Chen and Emil C. Gotschlich. “ComE, a Competence Protein from *Neisseria gonorrhoeae* with DNA-Binding Activity”. In: *Journal of Bacteriology* 183.10 (2001), pp. 3160–3168.

[99] Ankur B. Dalia, EmilyKate McDonough, and Andrew Camilli. “Multiplex genome editing by natural transformation”. In: *Proceedings of the National Academy of Sciences* 111.24 (2014), pp. 8937–8942.

[100] Thomas J. Piggot, Daniel A. Holdbrook, and Syma Khalid. “Electroporation of the E. coli and S. Aureus Membranes: Molecular Dynamics Simulations of Complex Bacterial Membranes”. In: *The Journal of Physical Chemistry B* 115.45 (2011), pp. 13381–13388.

[101] David J. Warren. “Preparation of highly efficient electrocompetent Escherichia coli using glycerol/mannitol density step centrifugation”. In: *Analytical Biochemistry* 413.2 (2011), pp. 206–207.

[102] Linbo Gou et al. “Construction of a CRISPR-Cas9-Based Genetic Editing Tool for Serratia marcescens Using a Stationary Phase Promoter and Its Application in Putrescine Production”. In: *Biotechnology and Bioengineering* 122.5 (2025), pp. 1233–1244.

[103] Anh Tran Thi Ngoc, Khanh Nguyen Van, and Yong Hoon Lee. “DnaJ, a heat shock protein 40 family member, is essential for the survival and virulence of plant pathogenic Pseudomonas cichorii JBC1”. In: *Research in Microbiology* 174.7 (2023).

[104] Giovanni Gallo et al. *A Hyperthermoactive-Cas9 Editing Tool Reveals the Role of a Unique Arsenite Methyltransferase in the Arsenic Resistance System of Thermus thermophilus HB27*. Tech. rep. 2021.

[105] Feng Song, Jinping Shu, and Shouke Zhang. “Gut bacterium Acinetobacter sp. assists Camellia weevil with host plant adaptation by degrading tea saponin via the benzoate pathway”. In: *Microbiome* 13.1 (2025).

5 General conclusions and future perspectives

Bacterial cellulose (BC) is a high-performance biopolymer whose unique physicochemical properties, including high crystallinity, water-holding capacity, mechanical strength, and chemical purity, make it attractive for a wide range of industrial, biomedical, and environmental applications. However, the commercial competitiveness of BC production remains constrained by the metabolic characteristics of its natural producers, chief among them inefficient carbon utilisation and limited tractability to genetic engineering. Throughout this thesis, we investigated the metabolic basis of BC production in *Komagataeibacter sucrofermentans* ATCC 700178, identified and characterised key enzymatic bottlenecks, and explored the capacity of genome editing tools to support rational strain improvement. Our work progressed from metabolic analysis and targeted knockout engineering, through the systematic evaluation of CRISPR–Cas9 implementation barriers, to the rational introduction of heterologous glucose assimilation modules, resulting in both a metabolically improved production strain and a conceptual framework for the next stage of strain development in this industrially relevant organism.

In **Chapter I** we reviewed the current state of BC biosynthesis, its regulation, and the synthetic biology tools available for engineering *Komagataeibacter*. The key metabolic liabilities of glucose utilisation in this organism were outlined, particularly the diversion of carbon towards gluconic acid via periplasmic oxidation, alongside the regulatory features of the cellulose synthase complex. The expanding KTK modular cloning system and early-stage CRISPR-based tools were presented as the foundations on which the experimental work of the following chapters rests, while the broader landscape of co-culture strategies and engineered living material (ELM) approaches illustrated the potential of synthetic biology to transform BC from a natural polymer into a programmable material platform.

In **Chapter II**, we established that periplasmic glucose oxidation by the membrane glucose dehydrogenase (mGDH) is the dominant metabolic bottleneck for BC production in glucose-grown cultures of *K. sucrofermentans*. Disruption of the gene encoding mGDH yielded the strain KS003, which abolished gluconic acid formation, maintained pH stability, and achieved a 5.77-fold increase in BC production relative to the wild type, with a glucose-to-BC conversion efficiency 5.6-fold higher than the parental strain. In parallel, we demonstrated that ethanol supplementation consistently enhances BC production through metabolic rerouting, specifically by modulating the diauxic acetate assimilation phase, independently of any direct contribution as a carbon source. An optimised combination of ethanol supplementation in wild-type cultures yielded a 2.26-fold improvement in BC production. These results established KS003 as a superior platform strain and provided two complementary, immediately implementable strategies for BC yield improvement.

In **Chapter III** we undertook a systematic evaluation of CRISPR–Cas9 architectures in *K. sucrofermentans*, motivated by the need for markerless, scarless genome editing tools to extend the metabolic

engineering strategy developed in Chapter II. All nuclease-active Cas9 constructs tested, spanning constitutive and inducible promoters, moderate and strong expression levels, and two distinct replication origins, failed to yield viable transformants, yielding zero colony-forming units per microgram of transforming DNA. Transformation efficiency was ruled out as the limiting factor; instead, we demonstrated that even basal, uninduced Cas9 expression is sufficient to cause lethal DNA damage in *K. sucrofermentans*, a host in which endogenous double-strand break (DSB) repair is evidently insufficient to cope with Cas9-mediated cleavage. In contrast, the catalytically dead dCas9 variant was stably maintained, validating CRISPRi as a functional gene repression tool. These findings were synthesised into a cross-species set of seven design principles for implementing CRISPR–Cas9 in non-model Gram-negative bacteria, centred on the imperative for strict temporal separation between DNA delivery, homologous recombination (HR), and nuclease activation.

In **Chapter IV** we asked whether strengthening cytoplasmic glucose assimilation in the KS003 background could further improve BC production once the dominant bottleneck of periplasmic oxidation had been removed. Two transporter–kinase modules were assembled with the KTK system: GLF-GLK, combining the *Zymomonas mobilis* glucose facilitator with glucokinase, and GALP3-GLK, combining a native galactose permease homologue with glucokinase. Both were introduced into wild-type and KS003 strains. KS003 alone already produced 1.45 ± 0.07 g L^{-1} BC versus 0.57 ± 0.32 g L^{-1} for the wild type; the addition of either transport module in the KS003 background resulted in modest and variable changes. This outcome was consistent with a picture of carbon allocation in which, with periplasmic oxidation eliminated, cytoplasmic glucose entry becomes a relevant but not solely rate-limiting step, and downstream metabolic capacity, together with plasmid maintenance burden, emerges as the next-order constraint.

Key contributions

Across the conclusions of this work, we wish to highlight the following contributions to the field:

First, the impact of mGDH disruption on BC production was in line with previous reports in the literature, confirming that periplasmic glucose oxidation is a major constraint on carbon availability for cellulose biosynthesis. A distinguishing aspect of our work was the systematic characterisation across a range of ethanol concentrations, which allowed us to capture the competition between all four PQQ-dependent membrane dehydrogenases for the shared ubiquinone pool. This competition means that blocking PQQ-GDH not only eliminates gluconic acid formation but also liberates ubiquinol capacity for the remaining dehydrogenases, potentiating the response to ethanol supplementation and explaining the additive gains observed in Chapter II.

Second, we demonstrated that ethanol supplementation is a practical, cost-effective, and readily scalable strategy for improving BC production, acting through modulation of intermediate metabolite pools rather than direct carbon supply. Given the simplicity of its implementation, this strategy is immediately translatable to existing fermentation processes and is compatible with the use of industrial by-product streams containing ethanol.

Third, we provided the most systematic characterisation to date of the barriers to CRISPR–Cas9 implementation in *Komagataeibacter*, and translated these into a generalisable design framework for non-model Gram-negative bacteria. A key conclusion is that Cas9 toxicity arises from basal expression even under nominally inducible architectures commonly used in model organisms, which has direct implications for any group attempting to introduce CRISPR editing into bacteria with limited characterised repair pathways.

Fourth, we validated the KTK modular cloning system as a functional platform for rapid construction and evaluation of multi-gene metabolic modules in both wild-type and engineered *K. sucrofermentans* backgrounds, extending its application to heterologous transporter–kinase combinations and reinforcing its utility for iterative design–build–test cycles.

Fifth, the results of Chapter IV demonstrate that, in the wild-type background, overexpression of heterologous glucose transporters does not improve BC production. This shows that periplasmic glucose oxidation by mGDH is so kinetically dominant that it effectively outcompetes cytoplasmic uptake routes, consuming the available glucose before it can be assimilated intracellularly. Consequently, mGDH disruption is a prerequisite for any cytoplasmic glucose assimilation strategy to have a meaningful impact on BC yields, and plasmid burden remains a constraint that will need to be addressed in subsequent work.

Limitations and future directions

Our work also presents several limitations that define the immediate priorities for future research:

First, functional CRISPR–Cas9 editing in *K. sucrofermentans* remains to be demonstrated. The design principles articulated in Chapter III point clearly towards tightly regulated dual-plasmid systems as the necessary next step, in which Cas9 is expressed from a stringently controlled, near-zero-background promoter and a tunable time window is enforced between transformation, recombination, and nuclease activation. In this regard, combining chemically inducible promoters with theophylline-inducible riboswitches at the translational level would provide a double-layered regulatory switch with negligible basal activity, offering a promising near-term strategy to achieve the temporal control required. Concurrently, CRISPRi, already shown here to function in *K. sucrofermentans*, provides a powerful and immediately available tool for systematic repression-based interrogation of metabolic genes, which can guide the prioritisation of future knockout targets.

Second, the strain improvements described in this thesis rely on plasmid-borne constructs, which confer metabolic burden and require ongoing antibiotic selection to be maintained. A key near-term priority will be the chromosomal integration of beneficial metabolic modules in a markerless manner. In this regard, the disrupted PQQ-GDH locus represents a natural landing pad for future metabolic engineering strategies: once CRISPR–Cas9 becomes functional in this host, it could be used to drive stable, scarless integration of targets such as GLF, GLK, and other relevant genes at that genomic location, combining the metabolic benefit of mGDH removal with the expression of cytoplasmic assimilation modules in a single, selection-marker-free construction.

Third, the glucose-to-BC conversion efficiency of KS003, while substantially improved over the wild type, remains well below theoretical yield, indicating that significant carbon flux is still directed towards biomass, CO_2, and other by-products. A genome-scale metabolic model (GEM) of *K. sucrofermentans* is currently under development within our group and, combined with transcriptomic data, will provide a principled basis for identifying additional rate-limiting steps and prioritising future engineering targets beyond those addressed in this thesis.

Fourth, the results presented in Chapters II and IV were obtained primarily in static, small-scale batch cultures using synthetic media. Future work should evaluate the improved strains and metabolic modules under conditions more representative of industrial processes, including agitated bioreactors, fed-batch operation, and complex low-cost carbon sources such as agricultural by-products. Understanding how the mGDH-deficient phenotype and the introduced transporter modules behave under oxygen-limited, agitated, or continuous fermentation regimes will be essential for translating the laboratory-scale improvements into economically relevant processes.

Taken together, this work advances our mechanistic understanding of the carbon allocation constraints governing BC production in *K. sucrofermentans* and establishes a set of complementary experimental and conceptual tools, including an improved platform strain, a modular cloning framework, and a principled approach to genome editing, for the next phase of rational strain development. The identification of mGDH as the primary metabolic target, the characterisation of the specific barriers to CRISPR–Cas9 implementation, and the evidence that periplasmic oxidation kinetically dominates over cytoplasmic transport collectively contribute to moving this industrially relevant organism towards the level of genetic tractability required for systematic, iterative improvement. As the genome editing toolkit matures and the insights from metabolic modelling accumulate, the combination of targeted gene disruptions, heterologous metabolic modules, and iterative design–build–test cycles represents a compelling route towards economically competitive BC production.